REMARKS

Reconsideration and withdrawal of the objection to and rejections of the claims, in view of the remarks herein, is respectfully requested. Claims 1-3 are amended. Claims 1-23 and 25-46 are now pending in this application.

Claim 17 was objected to because the claim includes non-elected subject matter, i.e., SEQ ID Nos:47, 48, 49, 66-71, and 73-80. As Applicant timely traversed the Restriction Requirement, Applicant retains the right to request that the Commissioner review the propriety of the Restriction Requirement. Therefore, no amendment to claim 17 is required at this time.

The 35 U.S.C. § 112, Second Paragraph, Rejection

Claims 1, 4-11, 17-19, 25, 30-31, 35-37, and 41-44 were rejected under 35 U.S.C. § 112, second paragraph, as being indefinite for failing to particularly point out and distinctly claim the subject matter which Applicant regards as the invention. The amendment to claim 1 obviates the § 112(2) rejection. Accordingly, withdrawal of the § 112(2) rejection is respectfully requested.

The 35 U.S.C. § 112, First Paragraph, Rejection

Claims 1-11, 15-16, 18-20, 25, 30-32, 34-37, and 41-44 were rejected under 35 U.S.C. § 112, first paragraph, as failing to comply with the written description requirement. This rejection, as it may be maintained with respect to the pending claims, is respectfully traversed.

The Office Action asserts that the recitation of "protein destabilization sequence", "mRNA destabilization sequence", "luciferase", and "reporter protein" fails to provide a sufficient description of the claimed genus of proteins, as it merely describes the functional features of the genus without providing any definition of the structural features of the species within the genus, citing for support Univ. Calif. v. Eli Lilly and Co., 119 F.3d 1559, 43 U.S.P.Q.2d 1398 (Fed. Cir. 1997).

The Office Action continues, asserting that the specification only describes the polynucleotide having the nucleic acid sequence of SEQ ID NO:72, which encodes a fusion polypeptide comprising a specific luciferase isolated from firefly, a specific PEST sequence, and a specific CL1, and that does not constitute a representative number of species to describe polynucleotides encoding a fusion polypeptide comprising a whole genus of variants,

recombinant and mutants of any or all reporter proteins or luciferases, any or all protein and/or mRNA destabilization sequences or any or all PEST sequences.

As amended, the claims recite particular reporter proteins (which have a particular function that is associated with a particular structure) or a mRNA destabilization (function) sequence structure. The claims also recite structure for the protein destabilization (function) sequence, e.g., SEQ ID NO:89, SEQ ID NO:90, SEQ ID NO:91, SEQ ID NO:92, SEQ ID NO:93, SEQ ID NO:94, SEQ ID NO:95, SEQ ID NO:96, SEQ ID NO:97, SEQ ID NO:98, or a PEST sequence, i.e., a sequence enriched in proline, glutamic acid, serine, and/or threonine residues. Thus, the properties (attributes) that identify the genus of nucleic acid molecules are that the sequences in the nucleic acid molecules are those for a particular reporter protein, and a particular protein destabilization sequence and/or RNA destabilization sequence, or combinations thereof. Underlying each of these properties is a structure. That is, not every nucleotide sequence encodes a reporter protein; not every nucleotide sequence present in a larger nucleotide sequence, once translated to a protein, confers a decreased half-life upon the translated protein; and not every nucleotide sequence present in a larger nucleotide sequence, once transcribed, confers a decreased stability to the resulting mRNA.

Applicant need not describe what is known to the art. Hybritech, Inc. v. Monoclonal Antibodies, Inc., 231 U.S.P.Q. 81, 94-95 (Fed. Cir. 1986). M.P.E.P. § 2163(II)(A)(3)(b) states that the description need only describe in detail that which is new or not conventional.

The documents submitted with the Amendment filed on March 29, 2007, as well as the references cited against the claims under 35 U.S.C. § 103(a), clearly evidence that sequences for reporter proteins, protein destabilization sequences and mRNA destabilization sequences were known to the art (see Andreatta et al., Biotechniques, 30:656 (2001), Leclerc et al., Biotechniques, 29:590 (2001), Gilon et al., EMBO J., 17:2759 (1998), King et al., Mol. Biol. Cell, 7:1343 (1996), Rechsteiner et al., Sem. Cell. Biol., 1:433 (1990), Fan et al., Genes and Devel., 11:2557 (1997), Balmer et al., Mol. Cell. Biol., 21:2070 (2001), and Belanger et al., Soc. Neurosci. Abs., 26:4117 (2000); all of record). An explanation as to why these documents and references are not sufficient to show that sequences for reporter proteins, protein destabilization sequences and mRNA destabilization sequences were known to the art has not been provided. See M.P.E.P. § 2163.04(II).

Further evidence that sequences for the recited reporter proteins were known to the art prior to Applicant's filing is provided by, e.g., Bouthors et al., (Protein Eng., 12:313 (1999); Lorenz et al. (Proc. Natl. Acad. Sci. USA, 88:4438 (1991); Matsumura et al. (Nat. Biotech., 17:696 (1999); Murray et al. (J. Mol. Biol., 254:993 (1995); Sirot et al. (Antimicr. Agents Chemo., 41:1322 (1997); Voladri et al. (J. Bacteriol., 178:7248 (1996)), Zhang et al. (Proc. Natl. Acad. Sci. USA, 94:4504 (1997); and Wood (Science, 244:700 (1989); a copy of each is enclosed herewith).

Moreover, the specification exemplifies three different firefly luciferase sequences (structure) (SEQ ID NOs: 48, 49, and 66), two different click beetle luciferase sequences (structure) (SEQ ID NOs: 77 and 79), a *Renilla* luciferase sequence (structure) (SEQ ID NO:47), a green fluorescent protein sequence (structure) (SEQ ID NO:68), as well as other reporters (see page 4 of the specification), numerous protein destabilization sequences and sources of other protein destabilization sequences (see pages 5 and 23 in the specification, e.g., a PEST sequence, for example, a PEST sequence from cyclin, e.g., mitotic cyclins, uracil permease or ODC, a sequence from the C-terminal region of a short-lived protein such as ODC, early response proteins such as cytokines, lymphokines, protooncogenes, e.g., c-myc or c-fos, MyoD, HMG CoA reductase, S-adenosyl methionine decarboxylase, CL sequences, a cyclin destruction box, N-degron, or a protein or a fragment thereof which is ubiquitinated *in vivo*), and numerous RNA destabilization sequences and sources for other such sequences (see page 6 of the specification, e.g., a sequence which likely forms a stem-loop, one or more AUUUA or UUAUUUAUU sequences, and including the 3' UTR of the bradykinin B1 receptor gene).

Therefore, more than one species of reporter protein, luciferase, protein destabilization sequence, and RNA destabilization sequence has been disclosed in the specification, contrary to the assertion in the Office Action that the specification only describes the polynucleotide having the nucleic acid sequence of SEQ ID NO:72, which encodes a fusion polypeptide comprising a specific luciferase isolated from firefly, a specific PEST sequence, and a specific CL1.

Thus, one of skill in the art can quite clearly envision the structure of the encoded fusion proteins in view of the species disclosed in Applicant's specification.

With regard to Univ. Calif. v. Eli Lilly and Co., 119 F.3d 1559, 43 U.S.P.Q.2d 1398 (Fed. Cir. 1997), the specification at issue *did not disclose a nucleotide sequence for the claimed*

human cDNA and disclosed only one rat cDNA sequence for the claimed vertebrate or mammalian cDNAs.

In contrast to the claims at issue in Eli Lilly, Applicant discloses numerous nucleotide sequences falling within the scope of the claimed genus, as discussed above.

In the Amendment mailed on November 15, 2007, Applicant pointed out that the terms at issue in the present application are not new or unknown biological material that the skilled artisan could easily miscomprehend. In Amgen v. Hoechst Marion Roussel, 314 F.3d 1313, 65 U.S.P.Q.2d at 1398 (Fed. Cir. 2003), the Federal Circuit pointed out that in Enzo Biochem. v. Gen-Probe, Inc., 296 F.3d at 1324, 63 U.S.P.Q.2d at 1613 (Fed. Cir. 2002), it was clarified that Eli Lilly did not hold that all functional descriptions of genetic material necessarily fail as a matter of law to meet the written description requirement; rather, the requirement may be satisfied if in the knowledge of the art the disclosed function is sufficiently correlated to a particular, known structure. The Federal Circuit continued stating that both Eli Lilly and Enzo Biochem. are inapposite to Amgen because the claim terms at issue ("vertebrate" and "mammalian") were not new or unknown biological materials that ordinarily skilled artisans would easily miscomprehend because they readily "convey distinguishing information concerning [their] identity" such that one of ordinary skill in the art could "visualize or recognize the identity of the members of the genus." Eli Lilly, 119 F.3d at 1567, 1568, 43 U.S.P.Q.2d at 1406.

The words or phrases "luciferase," "fluorescent protein," "chloramphenicol acetyltransferase," "beta-glucuronidase," "beta-galactosidase," "a PEST sequence" and "a mRNA destabilization sequence that is AU rich or forms a stem-loop" readily convey distinguishing information concerning their identity such that one of ordinary skill in the art can visualize or recognize the identity of the members of the genus.

Accordingly, withdrawal of the § 112(1) "written description" rejection is respectfully requested.

The 35 U.S.C. § 103 Rejection

Claims 1-11, 15-20, 25, 30-32, 34-37, and 41-44 were rejected under 35 U.S.C. § 103(a) as being unpatentable over Leclerc et al. (BioTechniques, 29:590 (2000)), Corish et al., Protein

Eng., 12:1035 (1999)), Gilon et al. (EMBO J., 17:2759 (1998)) and Kastelic et al. (WO 00/39314). This rejection is respectfully traversed.

Leclerc et al. prepared a construct in which a coding sequence for a firefly luciferase was linked to a C-terminal murine ornithine decarboxylase (mODC) coding sequence that includes a PEST sequence found near the C-terminus of wild-type mODC. It is disclosed that the PEST sequence in mODC corresponds to residues 423-450, and that residues 423-461 of mODC (modified by an amino acid substitution at two positions), i.e., the C-terminal residues of mODC, were fused to firefly luciferase sequences (see Figure 1).

Leclerc et al. reports that the half-life of the firefly luciferase with the PEST sequence was 0.84 hours. It is disclosed that the construct allows for detection of rapid increases or decreases in gene expression (abstract), such as those which are transient dynamic changes or in response to gene inhibiting or activating secretagogues (page 600). The authors note that other factors such as mRNA stability and processing influence reporter activity.

Corish et al. disclose constructs encoding green fluorescent protein (GFP) linked at the C-terminus to a 27 amino acid sequence from murine ODC that contains a PEST sequence or linked at the N-terminus to a 116 residue fragment from cyclin B1 that contains a destruction box (CDB), or both. Notably, the presence of both CDB and ODC sequences (at the N-terminus and at the C-terminus, respectively) resulted in a GFP protein having a half-life that was substantially the same (i.e., no additive or complementing effect) as the GFP protein with only the CDB sequence (see Figure 2) (at page 1037 in Corish et al., it is disclosed that "[t]he addition of the PEST motif to this CDB-GFP protein **marginally** reduced the average half-life further to 5.5 hours...Thus, addition of the PEST region does not appear to make a **significant** difference to fluorescence when protein levels are non-limiting" (emphasis added).

Therefore, it appears that the presence of the CDB sequence, which leads to ubiquitination at the N-terminus of GFP, dominates the half-life of the CDB-GFP-ODC fusion protein.

Gilon et al. report on the isolation of a set of protein degradation signals for ubiquitin based proteolysis in yeast.

Kastelic et al. disclose a construct having a coding region for luciferase linked to a mRNA instability sequence (clone # 63) and its use in a method to screen for compounds that promote the instability of mRNAs with mRNA instability sequences. The effect of the mRNA

instability sequence on luciferase expression in the results shown in Figure 4 is not particularly apparent until 24 hours after differentiation is induced, although the overall signal of clone # 63 is 3- to 5-fold less than the control clone (clone # 53, which has a luciferase construct but no mRNA instability sequence). With reference to this data, it is disclosed that one "would expect in the case of luciferase to see a weaker effect of mRNA destabilizing drugs since transcription remains high" (page 12).

Treatment of the clones with an agent known to promote the instability of mRNAs (a radicicol analog, i.e., SDZ 216-732) resulted in a decrease in activity in clone #63 over time (Figure 5 in Kastelic et al.). Treatment of the clones with actinomycin D (an agent that binds DNA at the transcription initiation complex and prevents elongation) resulted in a decrease in activity for both clones but relatively less of a reduction for clone # 63, while treatment of the clones with cycloheximide (an agent that inhibits protein synthesis) resulted in a decrease in activity clone # 53 and an increase in activity for clone # 63 (Figure 5).

If there are fewer luciferase mRNAs available for translation in clone # 63 cells as a result of the mRNA instability sequence, it is unclear why clone # 63 has more activity than clone # 53 in the presence of actinomycin D or cycloheximide at 8 hours. Moreover, the reduced activity for clone # 63 in the presence of SDZ 216-732 relative to clone # 53 at 8 hours in Figure 5 may be due to the reduced signal for clone # 63 (see Figure 4).

In view of the disclosure in Corish et al., it was unexpected that different protein destabilization sequences could have substantially cumulative effects.

Moreover, prior to Applicant's disclosure, it was unknown if two different protein destabilization sequences at the C-terminus of a reporter protein would result in a reporter protein with a half-life that was different than a reporter protein with one of the protein destabilization sequences, particularly in view of Corish et al., where the half life of the destabilized protein was almost exclusively due to a protein destabilization sequence at the N-terminus.

With regard to combining protein and mRNA destabilization sequences, the purpose of the two types of destabilization sequences is different. As transcription precedes RNA processing and RNA processing precedes translation, a mRNA destabilization sequence decreases the amount of translatable mRNA, which in turn decreases the amount of translated protein, but the half-life of the translated protein is unaffected. For constructs with a mRNA

destabilization sequence, this allows for screening of agents that promote mRNA destabilization (see Kastelic et al.). The presence of a protein destabilization sequence in a translated protein targets the protein for more rapid degradation than a corresponding protein without the protein destabilization sequence. A construct with a protein destabilization sequence would not be useful in screening for agents that promote mRNA destabilization.

Moreover, the signal for a construct with a mRNA destabilization sequence was 3- to 5-fold less than a construct without the mRNA destabilization sequence (see Figure 4 in Kastelic et al.). Thus, prior to Applicant's disclosure, one of skill in the art would not consider combining RNA and protein destabilization sequences with a reporter gene, as the reduction in available reporter protein mRNA transcripts that can be translated in conjunction with a reduction in reporter protein half-life may not yield sufficient reporter protein for any particular assay.

In this regard, the Examiner is requested to consider that the rapid and/or significantly larger increase in degradation in luciferase-CL-PEST or luciferase-protein destabilization sequence-mRNA destabilization sequence constructs was unexpected (Figures 9, 10B, 15 and 16 in Applicant's specification).

Accordingly, Applicant respectfully requests withdrawal of the § 103 rejection.

CONCLUSION

Applicant respectfully submits that the claims are in condition for allowance and notification to that effect is earnestly requested. The Examiner is invited to telephone Applicant's attorney ((612) 373-6959) to facilitate prosecution of this application.

If necessary, please charge any additional fees or credit overpayment to Deposit Account No. 19-0743.

Respectfully submitted,

SCHWEGMAN, LUNDBERG & WOESSNER, P.A.
Attorneys for Intel Corporation
P.O. Box 2938
Minneapolis, Minnesota 55402
(612) 373-6959

Date January 7, 2009 By _____
Janet E. Embretson
Reg. No. 39,665

CERTIFICATE UNDER 37 CFR 1.8: The undersigned hereby certifies that this correspondence is being deposited with the United States Postal Service with sufficient postage as first class mail, in an envelope addressed to: MS Amendment, Commissioner for Patents, P.O. Box 1450, Alexandria, VA 22313-1450 on this 7th day of January, 2009.

Dawn M. Fox
Name

Dawn M Fox
Signature

J. Mol. Biol. (1995) 254, 993–1005

JMB

Steroid Recognition by Chloramphenicol Acetyltransferase: Engineering and Structural Analysis of a High Affinity Fusidic Acid Binding Site

Iain A. Murray[1], Pauline A. Cann[1], Philip J. Day[1], Jeremy P. Derrick[1] Michael J. Sutcliffe[1], William V. Shaw[1]* and Andrew G. W. Leslie[2]

[1]*Department of Biochemistry University of Leicester Leicester, LE1 7RH, UK*

[2]*MRC Laboratory of Molecular Biology Cambridge, CB2 2QH, UK*

**Corresponding author*

The antibiotic fusidic acid and certain closely related steroidal compounds are potent competitive inhibitors of the type I variant of chloramphenicol acetyltransferase (CAT_I). In the absence of crystallographic data for CAT_I, the structural determinants of steroid binding were identified by (1) construction *in vitro* of genes encoding chimaeric enzymes containing segments of CAT_I and the related type III variant (CAT_{III}) and (2) site-directed mutagenesis of the gene encoding CAT_{III}, followed by kinetic characterisation of the substituted variants. Replacement of four residues of CAT_{III} (Gln92, Asn146, Tyr168 and Ile172) by their equivalents from CAT_I yields an enzyme variant that is susceptible to competitive inhibition by fusidate with respect to chloramphenicol (K_i = 5.4 μM). The structure of the complex of fusidate and the Q92C/N146F/Y168F/I172V variant, determined at 2.2 Å resolution by X-ray crystallography, reveals the inhibitor bound deep within the chloramphenicol binding site and in close proximity to the side-chain of His195, an essential catalytic residue. The aromatic side-chain of Phe146 provides a critical hydrophobic surface which interacts with non-polar substituents of the steroid. The remaining three substitutions act in concert both to maintain the appropriate orientation of Phe 146 and *via* additional interactions with the bound inhibitor. The substitution of Gln92 by Cys eliminates a critical hydrogen bond interaction which constrains a surface loop (residues 137 to 142) of wild-type CAT_{III} which must move in order for fusidate to bind to the enzyme. Only two hydrogen bonds are observed in the CAT-fusidate complex, involving the 3-α-hydroxyl of the A-ring and both hydroxyl of Tyr25 and NE2 of His195, both of which are also involved in hydrogen bonds with substrate in the CAT_{III}-chloramphenicol complex. In the acetyl transfer reaction catalysed by CAT, NE2, of His195 serves as a general base in the abstraction of a proton from the 3-hydroxyl of chloramphenicol as the first chemical step in catalysis. The structure of the CAT-inhibitor complex suggests that deprotonation of the 3-α-hydroxyl of bound fusidate by this mechanism could produce an oxyanion nucleophile analogous to that seen with chloramphenicol, but one which is incorrectly positioned to attack the thioester carbonyl of acetyl-CoA, accounting for the observed failure of CAT to acetylate fusidate.

Keywords: chloramphenicol acetyltransferase; steroid binding; competitive inhibition; chimaeric enzymes; protein engineering

Present addresses: I. A. Murray, Department of Pharmaceutical Chemistry, University of California San Francisco, 513 Parnassus Avenue, San Francisco, CA 94143-0446, U.S.A.; P. J. Day, Department of Chemistry and Biochemistry, University of Texas at Austin, Welch 5252, Austin, TX 78712, U.S.A.; J. P. Derrick, Department of Biochemistry and Applied Molecular Biology, University of Manchester Institute of Science and Technology, PO Box 88, Manchester M60 1QD, UK; M. J. Sutcliffe, Department of Chemistry, University of Leicester, Leicester, LE1 7RH, UK

Abbreviations used: CAT, chloramphenicol acetyltransferase; Cm, chloramphenicol; FA, fusidic acid.

0022-2836/95/500993-13 $12.00/0

Introduction

Steroid hormones and related steroidal molecules are known to bind to a range of macromolecular targets in eukaryotes including nuclear receptors, intracellular enzymes involved in steroid biosynthesis or metabolism, and sex-hormone and corticosteroid binding globulins present in plasma (Parker, 1993). Although the structure of the complex between progesterone and an anti-steroid Fab' fragment (Arevalo *et al.*, 1993), and unliganded structures of ketosteroid isomerase (Westbrook *et al.*, 1984), uteroglobin (Morize *et al.*, 1987), and a bacterial β-hydroxysteroid dehydrogenase (Ghosh *et al.*, 1991), have been determined by X-ray crystallography, the breadth of the spectrum of structural motifs for steroid binding by proteins remains unknown. In fact, the sole example of the structural determination of the complex of a steroidal ligand and an *in vivo* protein target is that recently determined for dehydroisoandrosterone bound to a bacterial cholesterol oxidase (Li *et al.*, 1993), a flavin-dependent enzyme believed to have a role in the degradation of 3-β-hydroxysteroids, permitting the bacterium to utilise cholesterol as a sole source of carbon and energy.

It is well documented that the type I variant (CAT_I) of the enzyme chloramphenicol acetyltransferase (CAT; EC 2.3.1.28), a common effector of bacterial resistance to the antibiotic chloramphenicol (Shaw, 1967), can also confer resistance to the steroidal antibiotic fusidic acid when expressed in an *Escherichia coli* mutant which, unusually for Gram-negative bacteria, is fusidate-sensitive (Bennett & Shaw, 1983). Resistance to chloramphenicol is achieved *via* the enzyme-catalysed transfer of an acetyl group from acetyl-CoA to the primary hydroxyl group of the substrate, yielding 3-acetylchloramphenicol which fails to bind to, and thus no longer inhibits, the peptidyl-transferase centre of prokaryotic ribosomes. Fusidic acid is also an inhibitor of bacterial protein synthesis but is known to act at the elongation phase *via* stabilisation of the complex of elongation factor G and GDP (reviewed by Cundliffe, 1981). As binding by CAT_I leads neither to acetylation nor to any other covalent modification of fusidate, it is likely that the resistance mechanism is simply one of sequestering the antibiotic from its target (Bennett & Shaw, 1983).

Genes encoding CAT have been isolated from many bacterial genera and nucleotide sequences of some 30 different natural variants are known, demonstrating 25 to 98% amino acid identity in pairwise comparisons. None are homologous in primary structure to known steroid-binding proteins, nor, with the exception of the acetyltransferase component of the pyruvate dehydrogenase complex which has the same tertiary fold as CAT (Mattevi *et al.*, 1992), are they known to be related structurally to other proteins of any type. All CAT variants are homotrimers (3 × 25 kDa) with three active sites located in the clefts at the subunit interfaces (Shaw & Leslie, 1991) and operate *via* a rapid-equilibrium ternary complex mechanism with random order of addition of substrates (Kleanthous & Shaw, 1984). The imidazole of His195 acts as a general base to abstract a proton from the primary hydroxyl of chloramphenicol, followed by attack of the resulting oxygen nucleophile at the carbonyl of the acetyl-CoA thioester. The resulting tetrahedral oxyanion intermediate, stabilised by hydrogen-bonding with the hydroxyl of Ser148, then collapses to yield the products 3-acetylchloramphenicol and CoA. Such a mechanism is supported by the results of chemical modification experiments (Kleanthous *et al.*, 1985) as well as X-ray crystallographic (Leslie, 1990) and site-directed mutagenesis (Lewendon *et al.*, 1990, 1994) studies of the type III variant of CAT (CAT_{III}) (Murray *et al.*, 1988). In contrast, fusidate resistance appears to be a unique property

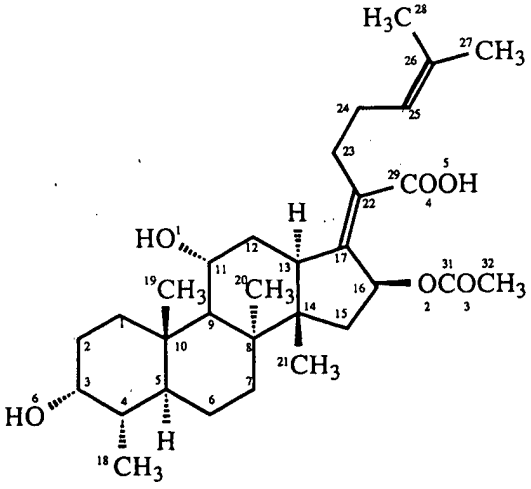

FUSIDIC ACID

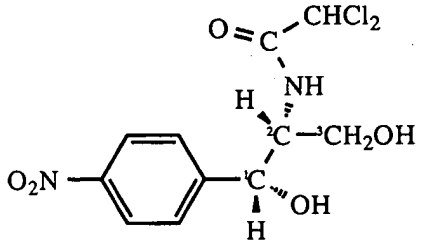

CHLORAMPHENICOL

Figure 1. Chemical structure of fusidic acid and chloramphenicol.

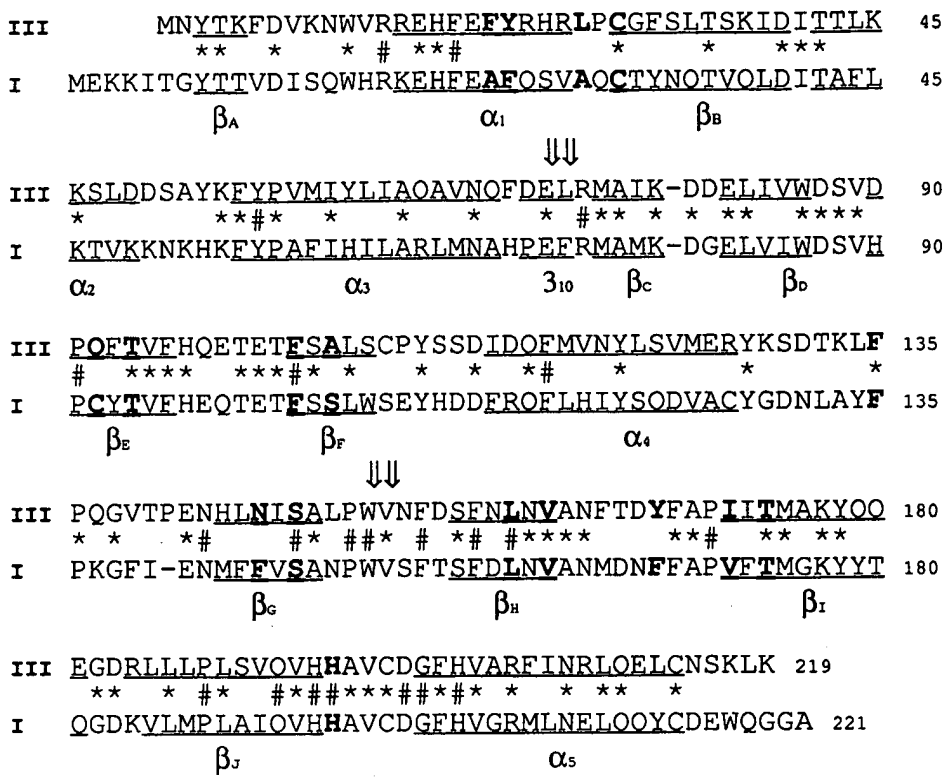

Figure 2. Sequence alignment of CAT_{III} and CAT_I. The primary sequences of CAT_{III} and CAT_I were optimally aligned and numbered as described by Shaw & Leslie (1991). Secondary structural motifs (helices and strands) observed in the crystal structure of CAT_{III} (Leslie, 1990), and the homologous regions of CAT_I, are underlined. The 17 residues which form the chloramphenicol binding site are shown in bold text. Positions of residue identity are indicated by * and those amino acids which are conserved in all known CAT variants by #. Double arrows above the sequence indicate the crossover points exploited in the construction of chimaeric CAT variants.

of the CAT_I enzyme, encoded by the transposon Tn*9* and many different enterobacterial R-plasmids. Fusidate binding to CAT_I is competitive with respect to chloramphenicol, despite the lack of obvious structural equivalence between the two ligands (Figure 1), and extends to various fusidate derivatives and related steroidal molecules (Bennett & Shaw, 1983).

An understanding of the determinants of binding of ligands which are not substrate analogues to proteins is a prerequisite to rational drug design and to the production of novel enzymes by protein engineering. In the case of steroid binding by CAT_I, such an objective could in principle be achieved by determination of the structure of the enzyme/fusidate complex by X-ray crystallography. However, a prolonged and exhaustive effort has failed to yield crystals of CAT_I with suitable diffraction properties. Efforts to model the binding of fusidate to CAT_I using the known structure of the complex of CAT_{III} and chloramphenicol (Leslie, 1990; M.J.S., unpublished experiments) have been frustrated by two obstacles; a lack of residue conservation between CAT_I and CAT_{III} (46% identity), even in the substrate binding sites, and the fact that a chloramphenicol site is located deep within each of the three inter-subunit clefts and could, in principle, be occluded (rather than occupied) by fusidate bound on the trimer surface. Random mutagenesis of the genes encoding either CAT_I or CAT_{III} was considered inappropriate due to the absence of a direct or facile selection for fusidate-sensitive mutants of the former, and the consideration that single point mutations were unlikely to confer fusidate resistance upon *E. coli* expressing CAT_{III}. However, starting with the assumption that the tertiary folds of CAT_I and CAT_{III} were likely to be essentially the same, and hence that steroid binding affinity is conferred primarily as a consequence of differences in amino acid side-chains, it seemed reasonable that site-directed mutagenesis of CAT_{III} could be useful in mapping the fusidate binding site. The desired result was achieved by the construction *in vitro* of recombinants expressing chimaeric CAT enzymes, followed by directed mutagenesis to produce variants of CAT_{III} which bind fusidic acid with high affinity and are amenable to crystallographic analysis.

Results and Discussion

Production and characterisation of CAT_I/CAT_{III} chimaeric enzymes

Steady state kinetic analysis of the inhibition of wild-type CAT_I and CAT_{III} by sodium fusidate

indicated that the steroidal inhibitor is bound ~200-fold more strongly by the former (K_i = 1.5 μM and 279 μM, respectively). In each case binding is competitive with respect to the substrate chloramphenicol. However, because chloramphenicol binds in each of three deep clefts on the enzyme surface of CAT_{III} (and presumably CAT_I also) it cannot be presumed *a priori* that fusidate binding is determined solely by the amino acid side-chains which form the substrate binding pocket. Calculations (using a sphere of radius 1.4 Å) indicated that in the CAT_{III}-chloramphenicol complex (Leslie, 1990) only one chlorine atom and the two oxygen atoms of the *p*-nitro substituent are solvent-accessible. Thus, binding of fusidate to non-conserved surface residues flanking the entrance to the chloramphenicol site (residues 26 to 30, 137 to 142 and 163 to 167; Figure 2) might in principle result in competitive inhibition by simply precluding access of substrate to the catalytic centre of CAT_I. Of the 17 amino acid side-chains which form the chloramphenicol binding site of CAT_{III}, only nine are retained in CAT_I of which four are conserved in all CAT variants (Figure 2; Zhao & Aoki, 1992). As a first step in delineating regions of CAT_I which contained determinants of high affinity steroid binding, we constructed a series of recombinant CAT genes encoding chimaeric enzymes.

Two crossover points were selected for construction of CAT_I/CAT_{III} chimaeras at locations which divide the CAT open reading frames approximately into thirds. The first crossover point, in a short 3_{10} helix on the enzyme surface between residues 72 and 73, was chosen because this site is known to tolerate insertions of additional amino acid residues while retaining activity (Betz & Sadler, 1981; I.A.M., unpublished experiments). The second was located between two highly conserved surface residues (Pro151 and Trp152) which form part of a reverse turn between β-strands G and H. The fact that the two CAT variants are 46% identical in sequence and readily form heterotrimers of CAT_I and CAT_{III} subunits that are catalytically competent (Packman & Shaw, 1981; Day *et al.*, 1995) raised the possibility that some of the chimaeric enzymes might be active, notwithstanding the potential for folding defects and/or inappropriate intra- and inter-monomer interactions. Of six possible chimaeric proteins encoded by crossovers at these positions, only five produced CAT protein, four of which were able to acetylate chloramphenicol and three were characterised in respect of inhibition by sodium fusidate. Enzymes in which residues 6 to 71 of CAT_{III} replaced residues 1 to 71 of CAT_I and in which residues 152 to 221 of CAT_I replaced residues 152 to 219 of CAT_{III} (the III-I-I and III-III-I chimaeras) were purified by standard affinity chromatography methods and their steady state kinetic parameters for acetyl transfer to chloramphenicol and inhibition by fusidate were determined (Table 1). The former is inhibited by fusidate (K_i = 2.0 μM) almost as effectively as is wild-type CAT_I (1.5 μM), whereas the latter is ~twofold less sensitive to fusidate (K_i = 505 μM) than wild-type CAT_{III}. A third chimaera (III-I-III) wherein residues 72 to 151 of CAT_{III} are replaced by their equivalents from CAT_I could only be assayed in crude cell-free extracts by means of a very sensitive radiometric assay (Gorman *et al.*, 1982) but did display fusidate sensitivity intermediate to that of the two wild-type enzymes assayed under similar conditions (data not shown). Taken together, such data suggest that the principal determinants of high affinity fusidate binding in CAT_I cannot reside in the N-terminal third of the protein and, additionally, that the C-terminal third of CAT_I is insufficient by itself to confer CAT_I-like affinity for fusidate, only binding the ligand in the context of residues 72 to 151 of that variant. It seemed likely therefore that differences in steroid affinity are most likely a consequence of substitutions of some of those residues (92, 105, 146, 168 and 172) known to be variable in the chloramphenicol binding site and/or in the surface loops 137 to 142 and 163 to 167. However, replacement of residues 139 to 143 (Val-Thr-Pro-Glu-Asn) of CAT_{III} by the shorter loop (Phe-Ile-Glu-Asn) from CAT_I yields an enzyme with kinetic parameters that are almost identical to those of wild-type CAT_{III} (Table 1). Therefore, site-directed mutagenesis of each of the eight non-conserved residues in the chloramphenicol binding site of CAT_{III} was used in an attempt to further define fusidate binding residues.

Table 1. Steady state kinetic parameters determined for wild-type and chimaeric CAT variants

Variant	k_{cat} (s^{-1})	K_m Cm (μM)	K_i FA (μM)
Wild-type CAT_I	97[a]	11[a]	1.5
Wild-type CAT_{III}	599[b]	11.6[b]	279
III-I-I	9.3	19	2.0
III-III-I	191	65	505
III ($I_{139-143}$)	534	17	193

III-I-I, Chimaeric CAT variant wherein residues 1 to 71 of CAT_I were replaced by residues 6 to 71 of CAT_{III}.

III-III-I, Chimaeric CAT variant wherein residues 152 to 219 of CAT_{III} were replaced by residues 152 to 221 of CAT_I.

III ($I_{139-143}$), Chimaeric CAT variant wherein loop 139 to 143 (VTPEN) of CAT_{III} is replaced by the equivalent loop (FIEN) of CAT_I.

Kinetic parameters were determined as described in Materials and Methods. Parameters are the mean of a minimum of three independent determinations, and standard error values are 15% (or less) of the quoted values. K_m values for the binding of the second substrate, acetyl-CoA, are within threefold of the values of the wild-type enzymes in the cases of all CAT variants analysed in the present study (data not shown).

[a] Data from Murray *et al.* (1991b).

[b] Data from Lewendon *et al.* (1988).

Site-directed mutagenesis of residues of the chloramphenicol binding site of CAT_{III}

Eight of the 17 amino acid side-chains which form the chloramphenicol binding site of CAT_{III} are substituted (Xaa) in CAT_I; Phe24(Ala), Tyr25(Phe), Leu29(Ala), Gln92(Cys), Ala105(Ser), Asn146(Phe), Tyr168(Phe) and Ile172(Val). The Y25F mutant was

Table 2. Steady state kinetic parameters determined for singly and multiply substituted CAT_{III} variants

Variant	k_{cat} (s^{-1})	K_m Cm (μM)	K_i FA (μM)
A.			
Wild-type CAT_{III}	599[a]	11.6[a]	279
F24A/L29A	500	33	133
Y25F	258[b]	15[b]	111
N146F	690	42	>2500
Y168F/I172V	358	38	255
B.			
Q92C/N146F	243	20	44
Q92C/N146F Y168F/I172V	377	20	5.4
F24A/L29A Q92C/N146F Y168F/I172V	112	48	3.8
Wild-type CAT_I	97[c]	11[c]	1.5

[a] Data from Lewendon *et al.* (1988).
[b] Data from Murray *et al.* (1991a).
[c] Data from Murray *et al.* (1991b).

prepared and analysed by steady state kinetic methods in an earlier study (Murray *et al.*, 1991a). The substitutions Q92C, A105S and N146F were each introduced into CAT_{III} as individual point mutations, whereas the F24A/L29A and Y168F/I172V double mutants were prepared using a single round of mutagenesis taking advantage of the close proximity of the codons of both pairs of residues in the CAT structural gene. The steady state kinetic parameters for chloramphenicol acetylation and inhibition by sodium fusidate for four such variants are presented in Table 2A. Data were not determined for the Cys92 and Ser105 enzymes because preliminary experiments were indicative of a fusidate sensitivity very similar to that of wild-type CAT_{III} in each case. With the exception of the N146F variant, each of the residue substitutions has only a minor influence on steroid binding. However, the substitution of Asn146 by phenylalanine effectively abolishes competitive binding of fusidate by CAT_{III}. Indeed, whereas inhibition of the N146F enzyme is seen at very high concentrations of inhibitor (>2.5 mM) it is impossible to distinguish between the effect of inhibitor binding to CAT and probable indirect effects of the detergent-like fusidate molecule on the partitioning of chloramphenicol between enzyme and solvent water (data not shown). Loss of affinity for the inhibitor accompanying the N146F mutation does not appear to be a consequence of any global changes in the integrity of the enzyme as judged by the near-wild-type kinetic properties of N146F in the acetyl transfer reaction. Therefore, and in spite of the fact that the N146F substitution has an effect opposite to that predicted, it seemed plausible that Phe146 might have an important role in binding of the inhibitor. In the structure of the binary complex of CAT_{III} and chloramphenicol, the side-chain of Asn146 is the centre of an extended hydrogen bond network which includes the amide side-chain of Gln92 and the phenolic hydroxyl of Tyr168 (Figure 3). As each of these hydrogen bond acceptors and donors is substituted by more hydrophobic amino acids (Cys92, Phe146, Phe168) in CAT_I it seemed likely that concerted substitution of all three residues might be necessary to produce a CAT_I-like fusidate binding phenotype. To that end we constructed and purified the Q92C/N146F double and Q92C/N146F/Y168F/I172V quadruple mutants of CAT_{III} and determined their kinetic parameters (Table 2B). Introduction of Cys92 in the context of Phe146 enhances binding >50-fold compared to N146F, yielding an enzyme with sixfold greater fusidate (K_i = 44 μM) affinity than that of wild-type CAT_{III}. When these two substitutions are combined with those of Y168F and I172V the fusidate inhibition constant (K_i) falls to 5.4 μM, a 50-fold enhancement in affinity over that of wild-type CAT_{III} and approaching that of the type I variant. Further modification *via* the F24A and L29A substitutions results in only a modest increase in binding affinity (K_i = 3.8 μM) supporting the conclusion of the chimaeric enzyme experiments that residues of the N-terminal segment of CAT_I play a limited role in steroid binding.

Crystal structure of the fusidate-CAT_{III}(Q92C/N146F/Y168F/I172V) complex

The structure of the Q92C/N146F/Y168F/I172V variant of CAT_{III} was determined at 2.2 Å resolution in the presence of bound fusidate (Table 3). With the exception of the substituted residues and the different bound ligands the structure is essentially

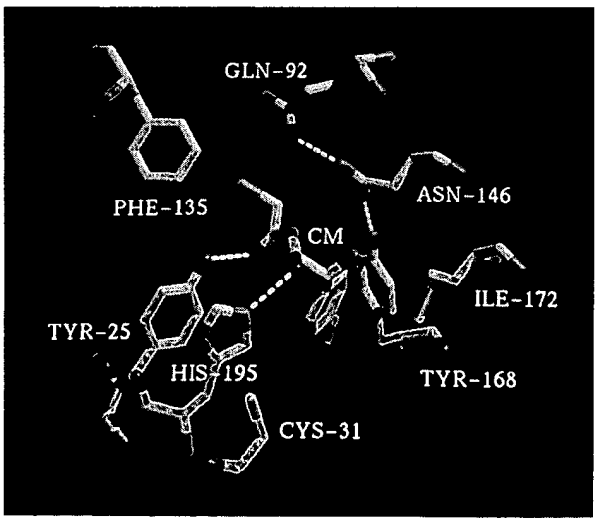

Figure 3. Hydrogen bond interactions in the complex of wild-type CAT_{III} and chloramphenicol. NE2 of His195, a critical catalytic residue, acts as a general base to abstract the hydroxyl proton of chloramphenicol as the initial chemical step of the acetyl-transfer reaction. Residues Gln92, Asn146 and Tyr168, which form an extended hydrogen bond network on one side of the substrate binding site (Leslie, 1990), are each replaced by hydrophobic amino acid side-chains in CAT_I.

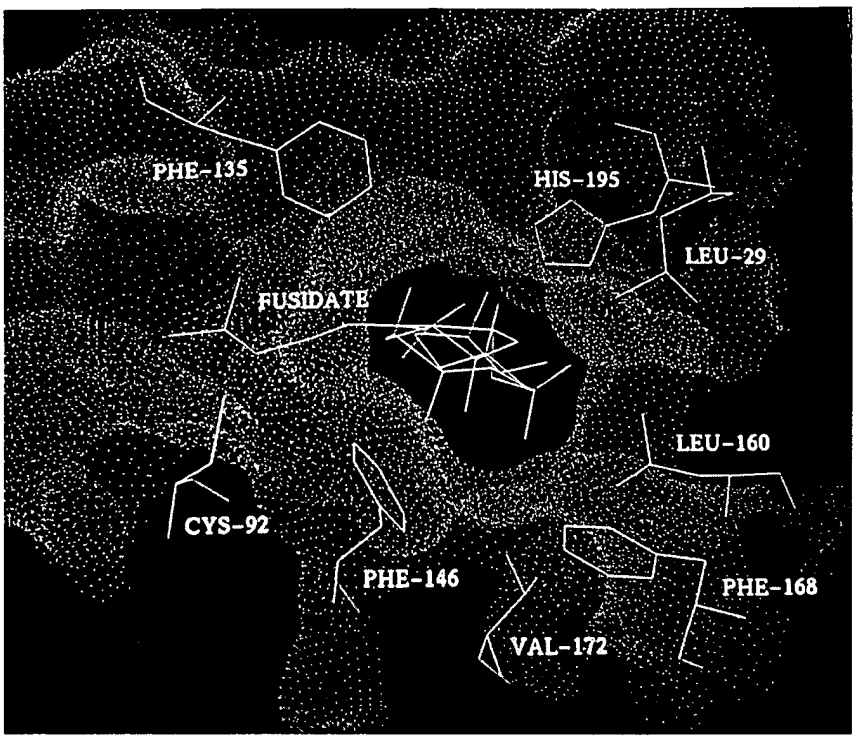

Figure 4. Fusidate bound in the chloramphenicol binding site of the Q92C/N146F/Y168F/I172V variant of CAT_{III}. The solvent-accessible surface (sphere radius 1.5 Å) was calculated for all amino acid side-chains which contained atoms positioned within 6 Å of atoms of the fusidate ligand. The four rings of the steroidal ligand are bound in a roughly cylindrical hydrophobic cavity with the A-ring at the base and D-ring closest to the surface of the trimer. The hydrophobic tail of the inhibitor projects out of the binding site onto the enzyme surface.

identical to that of wild-type CAT_{III} in complex with chloramphenicol (Leslie, 1990). The RMS differences between the structures of wild-type and quadruply substituted variants are 0.20 Å and 0.53 Å for main-chain and side-chain atoms, respectively. Two residues, Val139 and Thr140, are disordered in the structure and were deleted from the model. Such disorder reflects the loss of a stabilising hydrogen bond interaction between the side chains of Gln92 and Thr140 (which accompanies the Q92C substitution) and is also observed in the complex between the quadruple mutant and chloramphenicol (A.G.W.L., unpublished data). In addition the side-chain of His144 occupies two distinct positions due to alternate χ_1 angles of +60° (c.f. wild-type CAT_{III}) and −70°. As the peptide bond of His144 shows the highest deviation from planarity (12°) of any residue in wild-type CAT_{III}, the alternate conformer of this side-chain may reflect the loss of some conformational constraint following substitution of Asn146 by phenylalanine in the mutant.

The side-chains of Cys92, Phe146, Phe168 and Val172 and the atoms of the four ring systems of the fusidate molecule are well ordered in the CAT-inhibitor complex. The steroid A-ring is positioned at the base of the chloramphenicol binding pocket in close proximity to the imidazole side-chain of His195, an essential catalytic residue (Lewendon *et al.*, 1994). The B, C and D rings also occupy the chloramphenicol site whereas the remainder of the inhibitor projects onto the enzyme surface and is more accessible to solvent. Atoms of the hydrophobic "tail", the *O*-acetyl, and carboxylate substituents of the inhibitor (Figure 1) are disordered. In spite of the apparent mobility of the latter it may contribute to fusidate binding *via* electrostatic interaction with the guanidinium of Arg28, a side-chain which occupies clearly defined density in this structure but is disordered beyond CB in crystals of wild-type CAT_{III}.

As might be expected for a hydrophobic steroidal ligand, extensive non-polar interactions are observed in the CAT-fusidate complex (Figure 4). The C-14 methyl substituent (C-21) of the C-ring is in van der Waals contact (<3.6 Å) with all six carbon atoms of the side-chain of Phe146. CD2 and CE2 of the same residue also interact with the C-12 methylene group of the C-ring, supporting the earlier supposition that Phe146 is an important determinant of fusidate binding. CD2 of Leu160 contacts the C-4 methyl substituent (C-18) on the A-ring of fusidate and CD2 of Leu29 is involved in a similar interaction with the C-15 methylene group of the D-ring. In all, there are 57 contact distances of <4 Å between atoms of fusidate and the protein (Table 4) and a further nine to four ordered water molecules in the binding site. Perhaps surprisingly, none of the remaining three substituted residues (Cys92, Phe168 and Val172) make direct contact

Table 3. Refinement statistics for the CAT-fusidate complex

Diffraction data		
Reflections (6.0 to 2.2 Å)	13,517 (100% complete)	
R-value	17.4%	
Atomic model	No. of atoms	Mean isotropic thermal parameter (Å²)
Protein	1686	19.7
Fusidate	37	41.0
Solvent[a]	146	37.5
Stereochemical refinement parameter	RMS deviation from ideal values	Refinement restraint weighting values
Bond distances (Å)	0.018	0.020
Bond angles (Å)	0.049	0.040
Planar 1-4 distances (Å)	0.059	0.050
Planes (Å)	0.015	0.020
Chiral volumes (Å³)	0.166	0.150

[a] Includes 144 water atoms and two cobalt ions.

with the bound inhibitor. However the side-chains of Cys92 and Phe168 almost certainly contribute to the van der Waals binding energy via interactions with C-26/C-27 of the hydrophobic tail and atoms of the C-16 (*O*-acetyl) substituent, which are poorly ordered in the crystal. It is also probable that these substitutions are required to permit the appropriate orientation of Phe146 and to provide a more hydrophobic environment for binding of the apolar ring systems. The observed abolition of fusidate binding when the N146F substitution is made in isolation most likely reflects the inappropriateness of introducing a hydrophobic side-chain in the context of the relatively hydrophilic environment provided by Gln92 and Tyr168 of CAT_{III}. In wild-type CAT_{III} the amide nitrogen of Gln92 is involved in a hydrogen bond interaction with the side-chain hydroxyl of Thr140 stabilising the conformation of a surface loop (residues 137 to 142) adjacent to the chloramphenicol binding site. Elimination of this H-bond, *via* the Q92C substitution, facilitates a major re-orientation of the loop which would otherwise preclude binding of the hydrophobic tail of fusidate (Figure 5). The truncation of Tyr168 to phenyalanine is required to avoid a steric clash with the new position of residue 146 and is accompanied by movement of the entire side-chain of Phe168 towards residue 172. This in turn necessitates the substitution of Ile172 by the shorter valine side-chain.

The 3-α-hydroxyl group (O-6) of the A-ring is involved in hydrogen bonds with both NE2 of His195 (2.4 Å) and the phenolic-OH of Tyr25 (2.8 Å; Figure 6). Both Tyr25 and His195 are also involved in hydrogen bond interactions with chloramphenicol when it is bound to wild-type CAT_{III} (Leslie, 1990). As Tyr25 is replaced by phenylalanine in CAT_I it follows that the role of His195 is the more important in respect of both chloramphenicol and fusidate binding. Indeed, when Tyr25 of CAT_{III} is replaced by phenylalanine it results in only minor changes in the kinetic parameters of the acetyl transfer reaction (Murray *et al.*, 1991a). The observation that fusidate analogues wherein the 3-α-hydroxyl is replaced by a β-OH (3-epifusidate) or keto substituent (3-oxofusidate) bind weakly to wild-type CAT_I (Bennett & Shaw, 1983) serves to emphasise the importance of the hydrogen bond with His195. Pre-steady state kinetic analyses (Day *et al.*, 1995) show that the rate of fusidate dissociation from wild-type CAT_I increases when His195 is replaced by alanine but that the equivalent substitution in CAT_{III} has no effect on inhibitor dissociation, implying that the hydrogen bond interaction is absent in wild-type CAT_{III}. Indeed, one explanation of the requirement for the concerted substitution of four residues in the chloramphenicol binding site of CAT_{III} is that they are necessary to permit access of the inhibitor to the base of the substrate binding pocket to form the hydrogen bond with His195.

NE2 of His195 acts as a general base to abstract a proton from the primary (C-3) hydroxyl of chloramphenicol as the initial step in the acetyl transfer reaction. Although the 3-α-hydroxyl of bound fusidate could in principle also donate its proton to His195 it is ~1.6 Å removed from the position occupied by the primary (C-3) hydroxyl of chloramphenicol and in an entirely inappropriate orientation to attack the thioester carbonyl of acetyl-CoA and form a productive tetrahedral intermediate after proton abstraction (Figure 7). In addition, the C-2, C-3 and C-4 atoms of the A-ring of fusidate partly overlap with the positions of atoms of the tetrahedral intermediate (Lewendon *et al.*, 1990). This accounts for the inability of fusidate binding CAT variants to acetylate the steroidal inhibitor.

Using a sphere of radius 1.4 Å as probe we calculated that 575 Å² (or 81%) of the solvent-accessible area of fusidate becomes buried on binding to CAT. A similar proportion (89%, 1.7 Å probe radius) of progesterone is buried in its complex with the anti-progesterone monoclonal antibody DB3

Table 4. CAT-fusidate contacts less than 4 Å

Fusidate atom	CAT atom	Distance (Å)
C1	OH Tyr25	3.59
	CG2 Thr94	3.96
C2	OH Tyr25	3.84
	CG2 Thr94	3.50
	CE1 Phe103	3.77
	CZ Phe103	3.93
	O Wat448	3.84
C3	OH Tyr25	3.82
	NE2 His195	3.49
	O Wat436	3.96
	O Wat437	3.83
C4	O Wat437	3.66
C9	CD2 Phe146	3.91
C11	CD2 Phe146	3.89
C12	CE2 Phe135	3.78
	CE2 Phe146	3.14
	CD2 Phe146	3.37
C13	CE2 Phe146	3.77
C15	CD2 Leu29	3.07
C17	CE2 Phe146	3.89
	CZ Phe146	3.98
C18	CD2 Leu160	3.17
	NE2 His195	3.43
	CD2 His195	3.48
	O Wat437	3.87
C19	CB Phe146	3.89
C20	CE1 Phe24	3.85
	OH Tyr25	3.47
	CE1 Tyr25	3.68
	CD2 Leu29	3.69
C21	CZ Phe146	3.08
	CE2 Phe146	3.10
	CE1 Phe146	3.29
	CD2 Phe146	3.38
	CD1 Phe146	3.53
	CG Phe146	3.57
C22	CZ Phe146	3.86
	CE2 Phe146	3.93
C23	CE2 Phe135	3.94
	CE2 Phe146	3.67
	CZ Phe146	3.90
	O Wat314	3.66
C24	O Wat-314	3.68
C26	SG Cys92	3.88
C27	SG Cys92	3.66
	OG Ser107	3.69
C28	CD2 Phe135	3.04
	CE2 Phe135	3.50
	CG Phe135	3.82
	O Wat314	3.41
C31	CE2 Phe168	3.78
	CD2 Phe168	3.99
C32	CE2 Phe168	3.11
	CD2 Phe168	3.28
O1	OH Tyr25	3.54
	CE2 Phe135	3.86
	CZ Phe135	3.92
O2	CZ Phe146	3.90
O6	OH Tyr25	2.79[a]
	CZ Tyr25	3.41
	CE1 Tyr25	3.93
	CZ Phe103	3.59
	NE2 His195	2.42[a]
	CE1 His195	3.15
	CD2 His195	3.33
	O Wat436	3.73

[a] Hydrogen bond interactions.

(Arevalo *et al.*, 1993), whereas dehydroandosterone is completely enclosed and sequestered from bulk solvent when bound to cholesterol oxidase (Li *et al.*, 1993). However, in the latter case it is probable that the eight-carbon hydrophobic tail of the substrate cholesterol (which is replaced by a keto group in dehydroandrosterone) projects out of the binding pocket in a manner strictly analogous to that seen in the CAT-fusidate complex. In each structure the steroid binding site is primarily formed from the side-chains of hydrophobic amino acid residues but the precise spectrum of contacts is quite different in each case. All three proteins utilise hydrogen bonds to histidyl residues to stabilise the oxygen atom (keto or hydroxyl) of the C-3 substituent of the A-ring. In cholesterol oxidase His447, which is hydrogen bonded to the 3-keto substituent *via* a bridging water molecule, is implicated in each of several postulated mechanisms for the oxidation reaction (Li *et al.*, 1993).

Tight binding of steroidal and other highly apolar molecules to proteins requires not only a high degree of surface and steric complementarity between ligand and binding site but also a mechanism to address the energetic cost of a hydrophobic binding pocket which is accessible to bulk solvent in the unliganded state. In the cases of progesterone binding to the DB3 Fab' (Arevalo *et al.*, 1993), and of dehydroandrosterone to cholesterol oxidase (Li *et al.*, 1993), desolvation is achieved by conformational changes in the protein which accompany ligand binding. In the unliganded state the binding site of DB3 exists in a "closed" conformation, such that its hydrophobic amino acids are shielded from bulk solvent, which can convert to an open state to permit access of the progesterone. In cholesterol oxidase, the substrate binding site is completely isolated from bulk solvent both in the absence (when the site is occupied by ordered water molecules) and in the presence of the steroid. Thus, a model for steroid binding to cholesterol oxidase requires that the ligand binding cavity first open to permit binding then reclose around the substrate, with the concomitant displacement of the ordered water. In contrast to the above examples, the binding of fusidate to CAT does not appear to be accompanied by conformational changes of the protein to facilitate its access to the active site cleft at each subunit interface. This implies that CAT_{III} can tolerate the (presumably destabilising) effect of exposing three "new" hydrophobic residues to solvent in the unliganded state. In this respect it is perhaps significant that wild-type CAT_{III} is an extremely robust enzyme, being highly resistant to thermal denaturation (Lewendon *et al.*, 1988) and remaining folded and trimeric in 8 M urea (P.J.D., unpublished experiments). Although the stability of the Q92C/N146F/Y168F/I172V variant has not been studied, it should be noted that CAT_I, the chloramphenicol binding site of which is even more hydrophobic than that of the CAT_{III} quadruple mutant, is both less thermostable and less soluble than wild-type CAT_{III} (Day *et al.*, 1995).

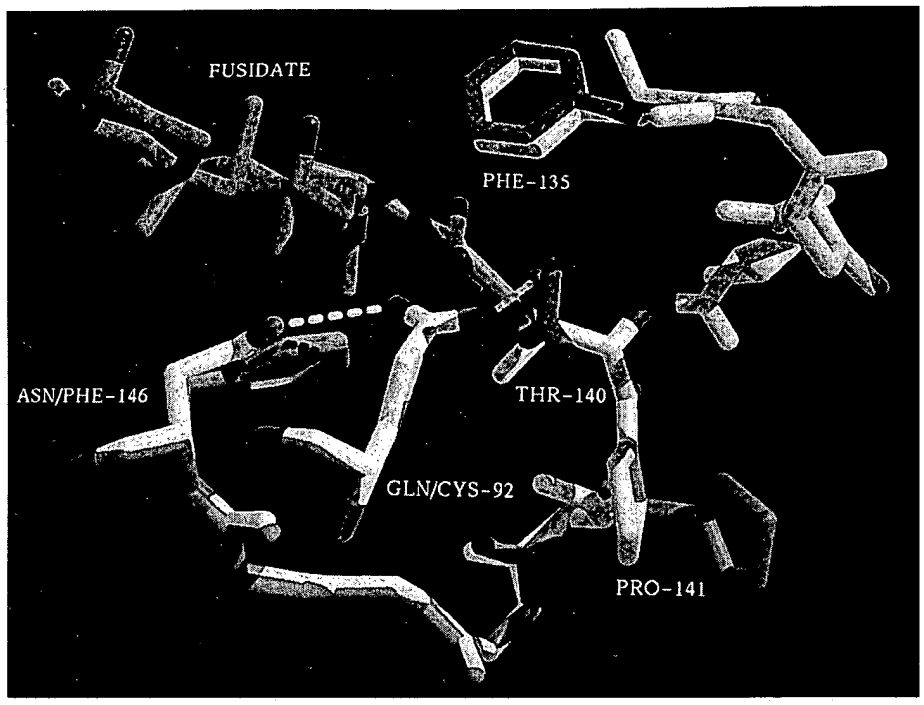

Figure 5. Surface loop movement accompanying the Q92C substitution. The structures of wild-type and the Q92C/N146F/Y168F/I172V variant of CAT_{III} were aligned by superposition of the main-chain atoms of residues 10 to 130 and 150 to 210. Residues 92 and 135 to 146 of the wild-type (white) and substituted (green) variants are shown in addition to the fusidate molecule bound to the latter. Note that the side-chains of residues 136–137 and 142–145 have been deleted from the image for the purpose of clarity. Replacement of Gln92 by cysteine eliminates the hydrogen bond to Thr140 permitting the movement of a surface loop (residues 137 to 142) which would otherwise preclude fusidate binding. Although Val139 and Thr140 are disordered in the CAT-fusidate complex and therefore not shown, the loop movement is revealed by a shift of several Å in the position occupied by Pro141.

Conclusions

We have used site-directed mutagenesis and X-ray crystallography to investigate the mechanism by which a single enzyme active site can bind two competing but chemically dissimilar ligands with approximately equal avidity. The structure of fusidate bound to the Q92C/N146F/Y168F/I172V variant of CAT_{III} reveals how a single protein can confer resistance *in vivo* to two entirely different classes of antimicrobial agent and is the third example (after β-lactamase and CAT itself) of an antibiotic resistance mechanism which is under stood at the atomic level. It has been suggested that

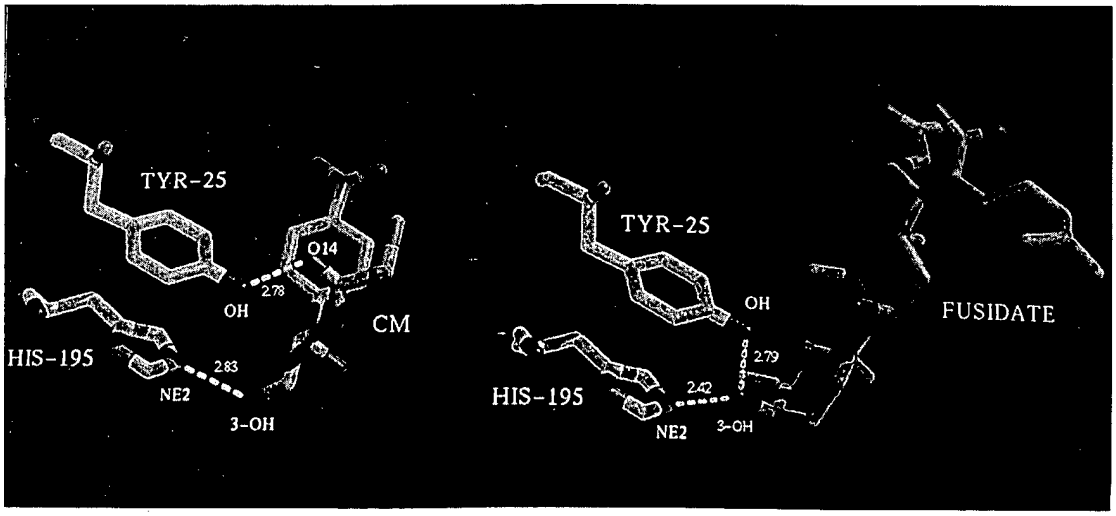

Figure 6. Intermolecular hydrogen bonds between bound ligand and the side-chains of Tyr25 and His195 occur in both CAT-chloramphenicol and CAT-fusidate complexes.

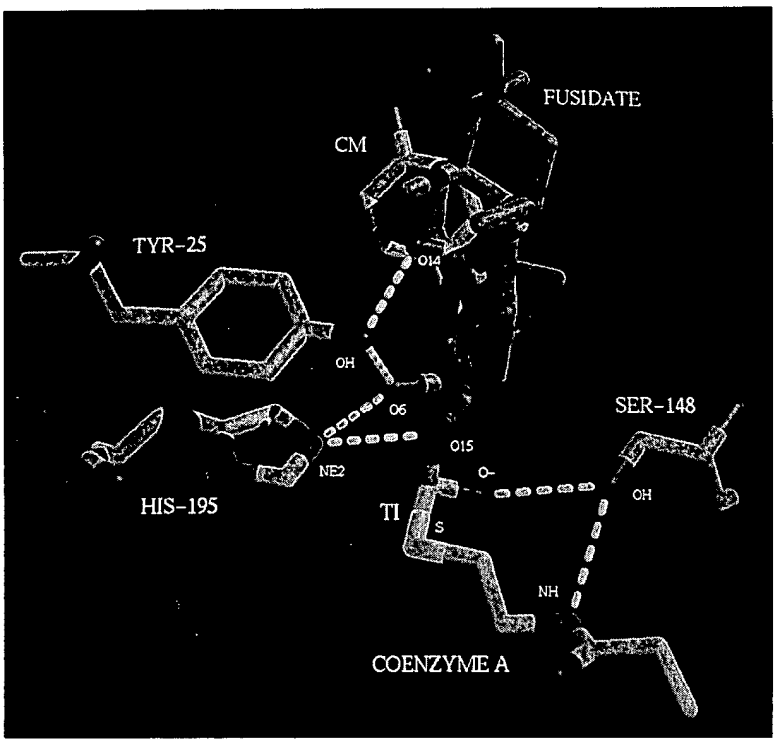

Figure 7. Superposition of bound fusidate inhibitor and the structure of the complex of wild-type CAT_{III} and the tetrahedral oxyanion intermediate of the acetyl-transfer reaction. In the acetyl-transfer reaction catalysed by CAT, abstraction (by NE2 of His195) of the 3-hydroxyl (O-15) proton of chloramphenicol facilitates nucleophilic attack at the carbonyl carbon of acetyl-CoA leading to the formation of an oxyanion tetrahedral intermediate (O-) which is stabilised by a hydrogen-bond interaction with the side-chain of Ser148 (Lewendon, *et al.*, 1990). While, in principle, proton abstraction from the 3-α-hydroxyl (O-6) substituent of fusidate may also occur, the position and orientation of this hydroxyl group (and steric hindrance due to overlap with the C-2 and C-3 carbon atoms of the A-ring) preclude formation of a productive tetrahedral intermediate, accounting for the observed failure of CAT to acetylate the steroidal inhibitor. For the purpose of clarity only the A, B and C rings of fusidate and those parts of CoA immediately proximal to the tetrahedral intermediate (TI) are shown.

co-administration of chloramphenicol and fusidate (or fusidate analogues) might offer a possible route to overcome CAT-mediated chloramphenicol resistance in clinical practice (Davies, 1994). Our structural data suggest that such a strategy may not be promising, since, of the diverse range of naturally occurring CAT variants, it is only CAT_I that carries the requisite motif of amino acid residues in the chloramphenicol binding site to generate a high affinity fusidate site. Conversely, it is apparent that mutations leading to the substitution of amino acids within the chloramphenicol binding site of a fusidate-binding CAT variant (c.f. CAT_I) might be expected to result in loss of inhibitor affinity without serious impairment of catalytic competence in the acetyl transfer reaction or consequent chloramphenicol resistance. It is not apparent whether CAT_I-mediated fusidate resistance is an evolved phenomenon or merely the result of a serendipitous arrangement of side-chains at the active site of this one variant. As only four of the 17 residues of the chloramphenicol binding site are conserved among known CAT variants it has not been possible to infer the evolutionary relationships between members of the family. Nonetheless, in the context of fusidate resistance, it is probably significant that CAT_I is of enterobacterial origin (including numerous genera that are relatively insensitive to fusidate due to limited outer membrane permeability) whereas naturally occurring CAT variants isolated from Gram-positive genera (commonly fusidate-sensitive) do not, to the best of our knowledge, confer resistance.

The CAT-fusidate complex is the third example of the determination of the structure of a protein bound to a steroidal ligand and one wherein the architecture of the binding site and the likely mechanism of ligand binding are both quite distinct from those observed in previously published structures. Because the Q92C/N146F/Y168F/I172V variant of CAT_{III} is only slightly compromised in the acetyl-transfer reaction (Table 2B) we believe that the active site of the protein is not significantly deformed in the absence of bound fusidate. This implies that the hydrophobic residues of the fusidate binding site are solvent-exposed in the unliganded enzyme and that, in contrast to cholesterol oxidase and the anti-progesterone Fab' DB3, significant conformational changes are not required to facilitate steroid binding. It is not known whether the determinants and dynamics of ligand binding to the effector recognition domains of

steroid receptors are analogous to those exemplified by the structures of the CAT-fusidate complex (binding at a preformed cleft), to that of DB3 and progesterone (opening of a closed binding site), or to the cholesterol oxidase-dehydroandrosterone complex (gating and reclosure of a preformed cavity). However, it is probable that the several discrete but linked functions of receptors of the steroid/vitaminD/thyroid hormone superfamily (Evans, 1988) will involve additional structural responses to ligand binding, favouring dimerisation and modulating the specificity and affinity of receptor interaction with DNA response elements.

Materials and Methods

Construction of recombinant genes and site-directed mutagenesis

Regions of the DNAs encoding CAT_I (Alton & Vapnek, 1979) and CAT_{III} (Murray *et al.*, 1988) were recombined *in vitro* using the technique of "sticky-feet" directed mutagenesis (Clackson & Winter, 1989). Single and multiple point mutations of CAT_{III} were introduced using oligonucleotide primers and single-stranded M13 DNA templates loaded with deoxyuridine by preparation in the *dut ung E. coli* strain RZ1032 (Künkel *et al.*, 1987). The presence of desired mutations and the absence of second site changes were confirmed by DNA sequence determination of both the complete coding and the 5' non-coding regions of the genes.

Expression and purification of CAT

Wild-type and mutant CAT proteins were expressed in *E. coli* JM101 after subcloning the coding sequences in pUC18. Enzymes were purified from cell-free extracts by affinity chromatography using chloramphenicol-Sepharose (Lewendon *et al.*, 1988) or by ion-exchange chromatography (DEAE-Sephacel) followed by affinity chromatography using Cibacron-blue Sepharose (Murray *et al.*, 1991a). Homogeneity of purified enzymes was confirmed by SDS-polyacrylamide gel electrophoresis and enzyme concentrations were determined by the method of Lowry *et al.* (1951).

Assay of CAT activity and kinetic determinations

CAT activity was assayed spectrophotometrically at 25°C as described previously (Lewendon *et al.*, 1990). Standard assays contained 0.4 mM acetyl-CoA (prepared from the lithium salt of CoA, Pharmacia, by the method of Simon & Shemin, 1953), 0.1 mM chloramphenicol and 1.0 mM 5,5'-dithiobis(2-nitrobenzoic acid) in TSE buffer (50 mM Tris-HCl (pH 7.5), 100 mM NaCl, 0.1 mM EDTA). One unit is defined as the amount of enzyme required to convert 1 μmol of chloramphenicol to 3-acetylchloramphenicol in one minute using the standard assay. Concentrations of acetyl-CoA and chloramphenicol were varied in the standard assay for determination of steady state kinetic parameters and all assays were carried out in triplicate. Initial rate values were used to construct double reciprocal plots and kinetic parameters were derived from slope and intercept replots (Kleanthous & Shaw, 1984). K_i values for competitive inhibition by sodium fusidate were determined by varying the concentrations of chloramphenicol and inhibitor in standard assays containing a fixed concentration of acetyl-CoA (routinely $\sim 5 \times K_m$), and were calculated from linear slope replots derived from double reciprocal plots. Crude extracts of chimaeric enzymes which appeared to be inactive in the standard assay were screened for low levels of CAT activity using a sensitive radiometric assay (Gorman *et al.*, 1982).

Crystallisation and structure determination

Single crystals of the Q92C/N146F/Y168F/I172V variant of CAT_{III} were prepared by microdialysis using small "Lucite" buttons as described previously (Leslie,1990). Each button contained 25 μl of protein (~ 5.7 mg ml^{-1}) in 10 mM MES buffer (pH 6.3), or the same buffer supplemented with 0.5 mM sodium fusidate, and were dialysed at 4°C against 10 ml of 10 mM MES (pH 6.3) containing 2 to 4% (v/v) 2-methyl-2,4-pentanediol, 1 mM hexamine cobalt (III) chloride, 0.1 mM dithiothreitol and either 1 mM chloramphenicol or 0.5 mM sodium fusidate. Crystals were isomorphous with those of the wild-type enzyme; space group *R*32 (equivalent hexagonal cell dimensions $a = 107.8$ Å, $c = 124.1$ Å). 80° of data were collected to 2.2 Å resolution from a single crystal (dimensions 260 μm × 240 μm × 120 μm) grown in the presence of fusidate using CuKα radiation from a GX13 rotating anode generator with double mirror collimation. Data were recorded on a prototype Hendrix-Lentfer image plate scanner with a diameter of 18 cm. The images were integrated with MOSFLM (Leslie, 1992) and programs from the CCP4 Suite (1994). A total of 68,511 observations were reduced to a unique dataset of 14,238 reflections with a crystallographic merging *R*-factor of 9.5% (24.9% in the highest resolution range). The dataset is 99% complete out to 2.2 Å resolution, with an overall $I/\sigma(I)$ ratio of 18.3 (7.6 at 2.2 Å resolution).

The refined structure of the CAT_{III}-chloramphenicol binary complex (Leslie, 1990) was used as a starting model for refinement. The chloramphenicol and all water molecules in the chloramphenicol binding pocket were removed from the model and the substitutions Q92C, N146F, Y168F and I172V made. This model was subjected to alternating rounds of refinement using the CCP4 programs SFALL, PROTIN and PROLSQ and manual rebuilding using the interactive graphics program O (Jones *et al.*, 1991). After one round of refinement there was very clear density compatible with a model of fusidate derived from the crystal structure of fusidic acid methyl ester *p*-bromobenzoate (Cooper & Hodgkin, 1968) and this was included in the model for all subsequent refinement. After four rounds of model building and refinement the final *R*-factor was 17.4% for all reflections in the resolution range 6.0 to 2.2 Å. Computer graphics images were produced using the *conic* option (Huang *et al.*, 1991) of the MidasPlus program (Ferrin *et al.*, 1988).

Acknowledgements

This work was supported by project grants from the Medical Research Council and Science and Engineering Research Council. M.J.S. is a Royal Society University Research Fellow. Molecular graphics images were produced using the MidasPlus program from the Computer Graphics Laboratory, University of California, San Francisco (supported by NIH RR-01081).

References

Alton, N. K. & Vapnek, D. (1979). Nucleotide sequence analysis of the chloramphenicol resistance transposon Tn9. *Nature*, **282**, 864–869.

Arevalo, J. H., Stura, E. A., Taussig, M. J. & Wilson, I. A. (1993). Three-dimension structure of an anti-steroid Fab' and progesterone-Fab' complex. *J. Mol. Biol.* **231**, 103–118.

Bennett, A. D. & Shaw, W. V. (1983). Resistance to fusidic acid in *Escherichia coli* mediated by the type I variant of chloramphenicol acetyltransferase. A plasmid-encoded mechanism involving antibiotic binding. *Biochem. J.* **215**, 29–38.

Betz, J. L. & Sadler, J. R. 1981. Variants of a cloned synthetic lactose operator. II. Chloramphenicol-resistant revertants retaining a lactose operator in the CAT gene of plasmid pBR325. *Gene*, **15**, 187–200.

Clackson, T. & Winter, G. (1989). 'Sticky-feet'-directed mutagenesis and its application to swapping antibody domains. *Nucl. Acid. Res.* **17**, 10163–10170.

Collaborative Computational Project, Number 4 (1994). *Acta Crystallog. sect. D*, **50**, 760–763.

Cooper, A. & Hodgkin, D. C. (1968). The crystal structure and absolute conformation of fusidic acid methyl ester 3-p-bromobenzoate. *Tetrahedron*, **24**, 909–922.

Cundliffe, E. (1981). In *Molecular Basis of Antibiotic Action* (Gale, E. F., Cundliffe, E., Reynolds, P. E., Richmond, M. & Waring, M. J., eds), pp. 405–547, Wiley Interscience, London.

Davies, J. (1994). Inactivation of antibiotics and the dissemination of resistance genes. *Science*, **264**, 375–382.

Day, P. J., Murray, I. A. & Shaw, W. V. (1995). Properties of hybrid active sites in oligomeric proteins: kinetic and ligand binding studies with chloramphenicol acetyltransferase trimers. *Biochemistry*, **34**, 6416–6422.

Evans, R. M. (1988). The steroid and thyroid hormone receptor superfamily. *Science*, **240**, 889–895.

Ferrin, T. E., Huang, C. C., Jarvis, L. E. & Langridge, R. (1988). The MIDAS display system. *J. Mol. Graphics*, **6**, 13–27.

Ghosh, D., Weeks, C. M., Grockhulski, P., Duax, W. L., Erman, M., Rimsay, R. L. & Orr, J. C. (1991). Three-dimensional structure of holo-3α,20β-hydroxysteroid dehydrogenase: a member of a short-chain dehydrogenase family. *Proc. Natl Acad Sci. USA*, **88**, 10064–10068.

Gorman, C. M., Moffat, L. & Howard, B. (1982). Recombinant genomes which express chloramphenicol acetyltransferase in mammalian cells. *Mol. Cell. Biol.* **2**, 1044–1051.

Huang, C. C., Pettersen, E. F., Klein, T. E., Ferrin, T. E. & Langridge, R. (1991). Conic: a fast renderer for space-filling molecules with shadows. *J. Mol. Graphics*, **9**, 230–236.

Jones, T. A., Zou, J. Y., Cowan, S. W. & Kjeldgard, M. (1991). Improved methods for building protein models in electron density maps and the location of errors in these models. *Acta Crystallog. sect A*, **47**, 110–119.

Kleanthous, C. & Shaw, W. V. (1984). Analysis of the mechanism of chloramphenicol acetyltransferase by steady-state kinetics. Evidence for a ternary complex mechanism. *Biochem. J.* **223**, 211–220.

Kleanthous, C., Cullis, P. M. & Shaw, W. V. (1985). 3-(Bromoacetyl) chloramphenicol, an active site directed inhibitor of chloramphenicol acetyltransferase. *Biochemistry*, **24**, 5307–5313.

Künkel, T. A., Roberts, J. D. & Zakour, R. A. (1987). Rapid and efficient site-specific mutagenesis without phenotypic selection. *Methods Enzymol.* **154**, 367–382.

Leslie, A. G. W. (1990). Refined crystal structure of chloramphenicol acetyltransferase at 1.75 Å resolution. *J. Mol. Biol.* **213**, 167–186.

Leslie, A. G. W. (1992). Recent changes to the MOSFLM package for processing films and image plate data. In CCP4 and ESF-EACMB Newsletter on Protein Crystallography, Number 26.

Lewendon, A., Murray, I. A., Kleanthous, C., Cullis, P. M. & Shaw, W. V. (1988). Substitutions in the active site of chloramphenicol acetyltransferase: role of a conserved aspartate. *Biochemistry*, **27**, 7385–7390.

Lewendon, A., Murray, I. A., Shaw, W. V., Gibbs, M. R. & Leslie, A. G. W. (1990). Evidence for transition-state stabilisation by serine-148 in the catalytic mechanism of chloramphenicol acetyltransferase. *Biochemistry*, **29**, 2075–2080.

Lewendon, A., Murray, I. A., Shaw, W. V., Gibbs, M. R. & Leslie, A. G. W. (1994). Replacement of catalytic histidine-195 of chloramphenicol acetyltransferase: evidence for a general base role for glutamate. *Biochemistry*, **33**, 1944–1950.

Li. J., Vrielink, A., Brick, P. & Blow, D. M. (1993). Crystal structure of cholesterol oxidase complexed with a steroid substrate: implications for flavin adenine dinucleotide dependent alcohol oxidases. *Biochemistry*, **32**, 11507–11515.

Lowry, O. H., Rosebrough, N. H., Farr, A. L. & Randall, R. J. (1951). Protein measurement with the folin phenol reagent. *J. Biol. Chem.* **193**, 265–275.

Mattevi, A., Obmolova, G., Schulze, E., Kalk, K. H., Westphal, A. H., de Kok, A. & Hol, W. G. (1992). Atomic structure of the cubic core of the pyruvate dehydrogenase multienzyme complex. *Science*, **255**, 1544–1550.

Morize, I., Surcouf, E., Vaney, M. C., Epelboin, Y., Buehner, M., Fridlansky, F., Milgrom, E. & Mornon, J. P. (1987). Refinement of the $C222_1$ crystal form of oxidised uteroglobin at 1.34 Å resolution. *J. Mol. Biol.* **194**, 725–739.

Murray, I. A., Hawkins, A. R., Keyte, J. W. & Shaw, W. V. (1988). Nucleotide sequence analysis and overexpression of the gene encoding a type III chloramphenicol acetyltransferase. *Biochem. J.* **252**, 173–179.

Murray, I. A., Lewendon, A. & Shaw, W. V. (1991a). Stabilisation of the imidazole ring of His-195 at the active site of chloramphenicol acetyltransferase. *J. Biol. Chem.* **266**, 11695–11698.

Murray, I. A., Lewendon, A., Williams, J. A., Cullis, P. M., Lashford, A. G. & Shaw, W. V. (1991b). A novel substrate for assays of gene expression using chloramphenicol acetyltransferase. *Nucl. Acids Res.* **19**, 6648.

Packman, L. C. & Shaw, W. V. (1981). The use of naturally occurring hybrid variants of chloramphenicol acetyltransferase to investigate subunit contacts. *Biochem. J.* **193**, 541–552.

Parker, M. G. (1993). *Steroid Hormone Action*, Oxford University Press, Oxford, U.K.

Shaw, W. V. (1967). The enzymatic acetylation of chloramphenicol by extracts of *R*-factor resistant *Escherichia coli*. *J. Biol. Chem.* **242**, 687–693.

Shaw, W. V. & Leslie, A. G. W. (1991). Chloramphenicol acetyltransferase. *Annu. Rev. Biophys. Biophys. Chem.* **20**, 363–386.

Simon, E. J. & Shemin, D. (1953). The preparation of S-succinyl coenzyme A. *J. Am. Chem. Soc.* **75**, 2520–2524.

Westbrook, E. M., Piro, O. E. & Sigler, P. B. (1984). The 6-Å crystal structure of Δ5-3-ketosteroid isomerase. Architecture and location of the active center. *J. Biol. Chem.* **259**, 9096–9103.

Zhao, J. & Aoki, T. (1992). Cloning and nucleotide sequence analysis of a chloramphenicol acetyltransferase gene from *Vibrio anguillarum*. *Microbiol. Immunol.* **36**, 695–705.

Edited by A. R. Fersht

(Received 31 July 1995; accepted 26 September 1995)

ANTIMICROBIAL AGENTS AND CHEMOTHERAPY, June 1997, p. 1322–1325 Vol. 41, No. 6
0066-4804/97/$04.00+0

A Complex Mutant of TEM-1 β-Lactamase with Mutations Encountered in Both IRT-4 and Extended-Spectrum TEM-15, Produced by an *Escherichia coli* Clinical Isolate

D. SIROT,[1]* C. RECULE,[2] E. B. CHAIBI,[3] L. BRET,[1] J. CROIZE,[2] C. CHANAL-CLARIS,[1] R. LABIA,[3] AND J. SIROT[1]

Laboratoire de Bactériologie-Virologie, Faculté de Médecine, 63001 Clermont-Ferrand Cedex,[1] Service de Bactériologie et Virologie, Centre Hospitalier Universitaire de Grenoble, 38043 Grenoble Cedex 9,[2] and UMR 175 Centre National de la Recherche Scientifique-MNHN, 29000 Quimper,[3] France

Received 28 October 1996/Returned for modification 3 February 1997/Accepted 6 April 1997

Escherichia coli* GR102 was isolated from feces of a leukemic patient. It expressed different levels of resistance to amoxicillin or ticarcillin plus clavulanate and to the various cephalosporins tested. The double-disk synergy test was weakly positive. Production of a β-lactamase with a pI of 5.6 was transferred to *E. coli* HB101 by conjugation. The nucleotide sequence was determined by direct sequencing of the amplification products obtained by PCR performed with TEM gene primers. This enzyme differed from TEM-1 (*blaT-1B* gene) by four amino acid substitutions: Met→Leu-69, Glu→Lys-104, Gly→Ser-238 and Asn→Asp-276. The amino acid susbstitutions Leu-69 and Asp-276 are known to be responsible for inhibitor resistance of the IRT-4 mutant, as are Lys-104 and Ser-238 substitutions for hydrolytic activity of the extended-spectrum β-lactamases TEM-15, TEM-4, and TEM-3. These combined mutations led to a mutant enzyme which conferred a level of resistance to coamoxiclav (MIC, 64 μg/ml) much lower than that conferred by IRT-4 (MIC, 2,048 μg/ml) but higher than that conferred by TEM-15 or TEM-1 (MIC, 16 μg/ml). In addition, the MIC of ceftazidime for *E. coli* transconjugant GR202 (1 μg/ml) was lower than that for *E. coli* TEM-15 (16 μg/ml) and higher than that for *E. coli* IRT-4 or TEM-1 (0.06 μg/ml). The MICs observed for this TEM-type enzyme were related to the kinetic constants K_m and k_{cat} and the 50% inhibitory concentration, which were intermediate between those observed for IRT-4 and TEM-15. In conclusion, this new type of complex mutant derived from TEM-1 (CMT-1) is able to confer resistance at a very low level to inhibitors and at a low level to extended-spectrum cephalosporins. CMT-1 received the designation TEM-50.

Overproduction of *Escherichia coli* chromosomal β-lactamase is one cause of resistance to β-lactam–β-lactamase inhibitor combinations such as amoxicillin (AMX)-clavulanate (CA) and also results in reduced susceptibility to all β-lactams except carbapenems (15).

In *E. coli*, resistance to all β-lactams except cephamycins and carbapenems may be caused by extended-spectrum β-lactamases. These enzymes are susceptible to β-lactamase inhibitors such as CA (10, 14, 15) and are therefore detected by synergy tests (10), and strains producing such mutants are often susceptible to β-lactam–β-lactamase inhibitor combinations.

In *E. coli* isolates, the most recently discovered mechanism of resistance to AMX-CA is production of inhibitor-resistant TEM β-lactamases (IRT) (8).

E. coli GR102, isolated from feces of a leukemic patient in the hematology unit of the teaching hospital of Grenoble, France, harbored an unusual β-lactam resistance phenotype with resistance to AMX and ticarcillin (TIC) alone and combined with CA and resistance to all cephalosporins, including cephamycins, at various levels. In addition, the double-disk synergy test used for extended-spectrum β-lactamase detection was weakly positive.

This complex phenotype suggested that the β-lactam resistance of the strain was due to the presence of several β-lactamases or a combination of different mechanisms of resistance to β-lactams.

* Corresponding author. Mailing address: Laboratoire de Bactériologie-Virologie, Faculté de Médecine, 28 Place Henri-Dunant, 63001 Clermont-Ferrand Cedex, France. Phone: 33 4 73 60 80 18. Fax: 33 4 73 27 74 94.

MATERIALS AND METHODS

Strains. The strains used included *E. coli* GR102, a clinical isolate producing a novel β-lactamase; *E. coli* HB101, used as a recipient strain for transfer; *E. coli* HB101/p111 (TEM-1 producing); *E. coli* CF0042 (IRT-4–TEM-35 producing) (8); and *E. coli* transformant DH5α (CF244), obtained by electroporation from *Klebsiella pneumoniae* Kp240 (TEM-15 producing) (16).

Susceptibility to β-lactams. The MICs of AMX, TIC, cephalothin (CF), cefotaxime (CTX), ceftazidime (CAZ), aztreonam (ATM), cefepime (FEP), and cefpirome (CPO) alone and combined with CA at a fixed concentration of 2 μg/ml were determined. A method of dilution with Mueller-Hinton agar (Sanofi Diagnostics Pasteur, Marnes-la-Coquette, France) and an inoculum of 10^4 CFU per spot were used. Antibiotics were provided as powders by SmithKline Beecham Pharmaceuticals (AMX, TIC, and CA), Roussel-Uclaf (CTX and CPO), Glaxo Wellcome Research and Development (CAZ), and Bristol-Myers-Squibb (ATM and FEP).

Detection of extended-spectrum β-lactamase was performed with the double-disk synergy test as described by Jarlier et al. (10).

Isoelectric focusing. Isoelectric focusing was performed with polyacrylamide gels containing ampholines with a pH range of 3.5 to 10.0 as previously described (19), and β-lactamases with known pIs (TEM-1 [pI 5.4], TEM-2 [pI 5.6], TEM-15 [pI 6.0], and IRT-4 [pI 5.2]) were used as standards.

Transfer experiment. A transfer experiment was performed with *E. coli* GR102 and the recipient *E. coli* HB101. Transconjugants were selected on agar containing rifampin (300 μg/ml) and gentamicin (8 μg/ml) or CAZ (0.5 μg/ml).

Sequencing of DNA amplified by PCR. On the assumption that the transconjugant strain contained bla_{TEM}, a single-stranded DNA template was generated for sequencing by PCR performed with an asymmetric ratio of amplification primers A and B, and the nucleotide sequence was determined as previously described (3), by direct sequencing of the amplified product obtained from the transconjugant *E. coli* GR202.

Determination of β-lactamase kinetic parameters k_{cat}, K_m, and k_{cat}/K_m. Affinity (K_m) and catalytic activity (k_{cat}) were determined with highly purified extracts (≥97% pure) by using a computerized microacidimetric method (13).

TABLE 1. Nucleotide and amino acid substitutions in bla_{TEM} genes

Nucleotide no.[a]	Nucleotide (amino acid)[b] in:			
	$bla_{TEM-1(Tn2)}$	bla_{TEM-15}	bla_{IRT-4}	bla_{CMT-1}
226	T (Phe)	C	T	T
317	C (Gln-39)	C	C	C
346	A (Glu)	A	G	A
407	A (Met-69)	A	C (Leu)	C (Leu)
436	T (Gly)	C	T	T
512	G (Glu-104)	A (Lys)	G	A (Lys)
604	T (Ala)	G	G	T
682	T (Thr)	T	T	T
914	G (Gly-238)	A (Ser)	G	A (Ser)
925	G (Gly)	G	G	G
1022	A (Asn-276)	A	G (Asp)	G (Asp)

[a] Nucleotide numbering is according to Sutcliffe (21).
[b] The amino acid is indicated when a point mutation leads to an amino acid substitution compared with the sequences of TEM-1(Tn2). Numbering is according to Ambler et al. (1).

All β-lactamases were purified from crude extracts by size exclusion chromatography on Sephadex G-100 (Pharmacia), preparative isoelectric focusing, and reverse-phase high-performance liquid chromatography on a C_{18} Nucleosil 500A column (Interchim) as described by Brun et al. (2). The homogeneity of the preparations was determined by analytical sodium dodecyl sulfate-polyacrylamide gel electrophoresis. The k_{cat}, K_m, and k_{cat}/K_m values of enzyme CMT-1 were compared with those of the β-lactamases TEM-1, TEM-15, and IRT-4. The kinetics of TEM-1 and its mutants toward penicillins and cephalosporins were compared. Inhibition studies of TEM-1 and the mutant enzymes with CA, sulbactam, and tazobactam were performed. The affinity of the enzyme for the inhibitor, expressed as the inhibition constant (K_i), was measured by using competition procedures with benzylpenicillin. It is determined from the extrapolated rate at the time when the inhibitor is added. The 50% inhibitory concentration (IC_{50}) was determined after incubation of the inhibitor and the enzyme for 10 min (completed inactivation) at 37°C before measurement of the remaining enzymatic activity. The IC_{50} is defined as the inhibitor concentration causing 50% inhibition of benzylpenicillin hydrolysis by the enzyme.

RESULTS

Resistance phenotype of *E. coli* GR102. *E. coli* GR102 expressed a complex β-lactam resistance phenotype with resistance to AMX and TIC alone and combined with CA and resistance to cephalosporins at various levels: high-level resistance to narrow-spectrum cephalosporins and low-level resistance to extended-spectrum cephalosporins (MICs, 1 to 32 μg/ml). A positive synergy test with CA suggested the presence of a mutant extended-spectrum β-lactamase of class A origin. In addition, this strain had reduced susceptibility to cefoxitin (MIC, 128 μg/ml) and, to a lesser extent, cefotetan and moxalactam (data not shown). This reduced susceptibility to cephamycins was probably related to decreased permeability of the strain for β-lactams, since *E. coli* GR102 had lost an outer membrane protein with a molecular mass of 40 kDa (data not shown). Overproduction of the chromosomal cephalosporinase was not detected.

This strain was also resistant to aminoglycosides (tobramycin, gentamicin, and netilmicin), probably owing to production of an AAC (3)-II enzyme, and to chloramphenicol, tetracyclines, and sulfonamides.

Conjugative transfer and isoelectric focusing. The gene encoding resistance to β-lactams, except cephamycins, was tranferred by conjugation from *E. coli* GR102 to rifampin-resistant *E. coli* HB101 (GR202). Selection for CAZ or gentamicin resistance revealed the transfer of an 85-kb plasmid conferring resistance to β-lactams, aminoglycosides (tobramycin, gentamicin, and netilmicin), tetracyclines, and sulfonamides.

By isoelectric focusing, two bands at pIs 5.4 and 5.6 were observed in *E. coli* GR102 and one band at pI 5.6 was observed in *E. coli* transconjugant GR202.

Nucleotide sequencing. As shown in Table 1, from the transconjugant GR202 producing a β-lactamase with a pI of 5.6, nucleotide sequencing revealed a bla_{TEM} gene identical to the *blaT-1B* gene (Tn-2) at positions 226, 317, 346, 436, 604, 682, and 925, which discriminate the bla_{TEM} genes (4, 7).

The bla_{TEM} gene from the *E. coli* transconjugant differed from the *blaT-1B* gene by four point mutations. These mutations consisted of the nucleotide change A→C at position 407, which leads to the amino acid substitution Met→Leu at position 69 (1); the nucleotide change G→A at positions 512 and 914, leading to the amino acid substitutions Glu→Lys at position 104 and Gly→Ser at position 238; and the nucleotide change A→G at position 1022, leading to the amino acid substitution Asn→Asp at position 276. The two amino acid substitutions at positions 69 and 276 are observed in the IRT-4–TEM-35 enzyme (2, 8, 22), and the two amino acid substitutions at positions 104 and 238 are observed in the extended-spectrum β-lactamase TEM-15 (16).

β-Lactam MICs for TEM mutants. Consequently, we compared the MICs of β-lactams for *E. coli* GR102 and its transconjugant GR202, producing a complex mutant form of TEM (CMT-1), with MICs for IRT-4-producing *E. coli* CF0042, TEM-15-producing *E. coli* CF244, and TEM-1-producing *E. coli* HB101 (Table 2).

For *E. coli* GR202 producing CMT-1, the MICs of AMX-CA (64 μg/ml) and TIC-CA (64 μg/ml) were much lower than

TABLE 2. MICs of β-lactams for *E. coli* CMT-1 (GR102 and its transconjugant, GR202), *E. coli* TEM-15 (CF244), *E. coli* IRT-4 (CF0042), and *E. coli* TEM-1 (HB101)

E. coli strain (enzyme)	MIC (μg/ml) of:															
	AMX		TIC		CF		CTX		CAZ		ATM		FEP		CPO	
	Alone	With CA[a]	Alone	With CA	Alone	With CA	Alone	With CA	Alone	With CA	Alone	With CA	Alone	With CA	Alone	With CA
GR102 (CMT-1)	4,096	256	>4,096	512	256	128	4	0.5	4	1	1	0.25	8	1	32	4
GR202[b] (CMT-1)	2,048	64	4,096	64	8	4	1	0.03	1	0.12	0.12	0.06	1	0.03	2	0.12
CF244[c] (TEM-15)	>4,096	16	>4,096	32	128	4	8	0.06	16	0.25	4	0.12	1	0.03	2	0.03
CF0042 (IRT-4)	4,096	2,048	1,024	512	8	4	≤0.06	≤0.06	≤0.06	≤0.06	≤0.06	≤0.06	≤0.06	≤0.06	≤0.06	≤0.06
HB101 (TEM-1)	4,096	16	4,096	32	8	2	≤0.06	≤0.06	≤0.06	≤0.06	≤0.06	≤0.06	≤0.06	≤0.06	≤0.06	≤0.06
HB101[d]	4	4	1	1	4	4	≤0.06	≤0.06	≤0.06	≤0.06	≤0.06	≤0.06	≤0.06	≤0.06	≤0.06	≤0.06

[a] CA was used at 2 μg/ml.
[b] *E. coli* HB101 transconjugant.
[c] *E. coli* DH5α transformant.
[d] *E. coli* recipient strain.

TABLE 3. Production of TEM-type β-lactamases in *E. coli*

Enzyme	pI	Producing organism	Activity in crude extract[a]	Sp act[b] of purified protein
TEM-1	5.4	HB101	2.2	2.48
TEM-35–IRT-4	5.2	CF0042	2.1	2.17
TEM-15	6.0	CF244	0.4	0.083
TEM-50–CMT-1	5.6	GR202	0.4	0.23

[a] Micromoles of benzylpenicillin per minute per milligram of protein.
[b] Micromoles of benzylpenicillin per minute per microgram of protein. Determined with highly purified preparations (≥97% pure).

those observed for IRT-4-producing strain CF0042 (2,048 and 512 μg/ml, respectively). Similarly, for strain GR202, MICs of CTX (1 μg/ml) and CAZ (1 μg/ml) were lower than those observed for TEM-15-producing strain CF244 (8 and 16 μg/ml, respectively) and higher than those for IRT-4 producing strain CF0042 (≤0.06 μg/ml). The same 1:8 ratio of MICs was observed for aztreonam (0.12 μg/ml for the CMT-1 producer and 4 μg/ml for the TEM-15 producer). The MICs of cefepime and cefpirome (1 and 2 μg/ml) were identical for the CMT-1 and TEM-15 producers.

E. coli GR202 (CMT-1) was 2 to 4 times less susceptible to AMX or TIC plus CA (64 μg/ml) and 16 times less susceptible to CTX, CAZ, FEP, and CPO (1 to 2 μg/ml) than was *E. coli* HB101 (TEM-1$^+$). MICs of β-lactam substrates in the presence of 2 and 4 μg of sulbactam or tazobactam per ml were about fourfold lower for the CMT-1-producing strain than for the TEM-1-producing strain (data not shown).

Enzymatic and kinetic parameters of β-lactamases. Enzymatic and kinetic parameters of the new complex mutant enzyme CMT-1 with regard to penicillins and cephalosporins were compared with those of the TEM-1, IRT-4, and TEM-15 β-lactamases (Tables 3 to 5). The specific activity of the highly purified CMT-1 protein was 10-fold lower than that of TEM-1 (Table 3).

For all penicillins, the k_{cat} values of CMT-1 were about 10-fold lower than those of TEM-1 and IRT-4 and about twice as high as those of TEM-15. The catalytic efficiencies (k_{cat}/K_m) of the three mutant enzymes were lower than those of the TEM-1 enzyme, and the values observed for CMT-1 and IRT-4 with carboxy- and ureidopenicillins were similar.

For cephalosporins, k_{cat} values of CMT-1 were slightly lower than or similar to those of TEM-15 for ceftriaxone, CTX, CAZ, and ATM; however, the catalytic efficiencies of the CMT-1 enzyme were only 5 to 11% of those of TEM-15 with ceftriaxone and CTX. No activity of TEM-1 or IRT-4 against expanded-spectrum cephalosporins and ATM (k_{cat}s of <1 s^{-1} associated with K_is of ≥500 μM) was detected.

The IC_{50} of CA for CMT-1 (Table 5) was higher (0.25 μM) than that for TEM-1 (0.08 μM) and TEM-15 (0.01 μM) but 100-fold lower than that for IRT-4 (28 μM). Sulbactam was the least efficient inhibitor of IRT-4 (IC_{50}, 304 μM), while its inhibitor efficiency was similar to that of CA for CMT-1 (IC_{50}, 0.5 μM). Tazobactam was the most efficient inhibitor of all of these β-lactamases. Moreover, CMT-1 (IC_{50}, 0.04 μM) and TEM-15 (IC_{50}, 0.01 μM) were more susceptible to inhibition by tazobactam than was TEM-1 (IC_{50}, 0.1 μM).

TABLE 4. Comparison of the kinetics[a] of TEM-1 and its mutant forms

Drug	k_{cat} (s^{-1}), K_m (μM), k_{cat}/K_m (μM^{-1}S^{-1})			
	TEM-1	TEM-35I–IRT-4	TEM-15	TEM-50–CMT-1
Benzylpenicillin	1,200, 25, 48.0	1,050, 140, 7.5	40, 6, 6.7	110, 17, 6.5
AMX	920, 26, 35.4	900, 245, 8.5	26, 5, 5.2	70, 33, 2.1
TIC	115, 10, 11.5	125, 320, 0.4	8, 2, 4.0	15, 30, 0.5
Carbenicillin	132, 13, 10.2	120, 360, 0.3	7, 3, 2.3	13, 60, 0.2
Piperacillin	987, 45, 21.9	945, 320, 2.9	64, 12, 5.3	111, 31, 3.6
CF	122, 250, 0.5	52, 1,200, 0.04	43, 23, 1.7	62, 324, 0.2
Cephaloridine	2,045, 800, 2.5	340, 1,420, 0.2	37, 30, 1.2	320, 310, 1.03
Cefoperazone	470, 260, 1.8	305, 1,325, 0.2	25, 22, 1.1	150, 118, 1.3
Cefuroxime	ND[b]	ND,	24, 91, 0.3	20, 260, 0.08
Ceftriaxone	ND	ND,	92, 50, 1.8	35, 385, 0.09
CTX	1.2, ND	ND,	180, 100, 1.8	150, 873, 0.2
CAZ	ND	ND,	7, 80, 0.1	3, ND
ATM	ND	ND,	0.2, ND	1, ND

[a] The standard deviation for analysis was ≤10%.
[b] ND, not detected; the rate was too small to determine k_{cat} and K_m reliably.

TABLE 5. Inhibition of TEM-1 and its mutant forms by CA, sulbactam, and tazobactam

Enzyme	IC_{50} (μM), K_i (μM)		
	CA	Sulbactam	Tazobactam
TEM-1	0.08, 0.1	6.1, 0.9	0.1, 0.01
TEM-35–IRT-4	28, 27	304, 49	1.8, 0.6
TEM-15	0.01, 0.02	0.03, 0.02	0.01, 0.008
TEM-50–CMT-1	0.25, 0.7	0.5, 0.4	0.04, 0.06

DISCUSSION

The TEM-1 derivative described in this report constitutes a new type of complex mutant, CMT-1, combining mutations responsible for inhibitor resistance (Leu-69 and Asp-276) and those responsible for extended-spectrum activity (Lys-104 and Ser-238). It is the first example of such a β-lactamase produced by a clinical isolate of *E. coli*.

Mutations conferring resistance to β-lactam inhibitors. Replacement of methionine 69, just adjacent to serine 70, by aliphatic amino acids such as leucine influences the positioning of residues (5, 17) because the buried side chain at position 69 lies behind β-strand B3, forming the back wall of the oxyanion pocket in which the β-lactam's carbonyl group is polarized (12). Moreover, crystallographic data indicate that residues in the C-terminal α helix, such as Asn-276, restrict the mobility of the Arg-244 side chain and so play a role in maintaining the integrity of the active site (11). Because small β-lactams such as CA must rely primarily on attractive interactions with the oxyanion hole and Arg-244, inhibitor resistance exists in the natural variant IRT-4, containing changes at residues 69 and 276 (12). This IRT-4 mutant enzyme is one of the most resistant to inhibition by CA among the IRT-type enzymes (2, 22), with a CA IC_{50} 350-fold higher than that for TEM-1. The CA resistance of this mutant is confirmed by high-level resistance to combinations of AMX and TIC with CA (MIC, 2,048 and 512 μg/ml, respectively). Inhibition studies showed that the CMT-1 enzyme was 100-fold less resistant than the IRT-4 mutant but only 3 times as resistant to inhibition by CA as the wild-type TEM-1 β-lactamase. These kinetic results were closely related to the moderate resistance level (64 μg/ml) of the CMT-1-producing strain to AMX-CA or TIC-CA. The inhibitor resistance usually caused by the Leu-69 mutation may be decreased by the close proximity of the Ser-238 mutation (see below).

Mutations conferring extended-spectrum activity. The Glu→Lys change at position 104 contributes to the precise positioning of residues 130 to 132 (SDN loop), which are involved in substrate binding, but seems insufficient alone to confer true resistance to expanded-spectrum cephalosporins (18, 20).

It is generally recognized that the substitution Gly→Ser-238 enlarges the active site, thereby creating an enzyme with increased affinity for the 7-oxyimino cephalosporins (6). All of the TEM variants reported to have Ser-238 contain methionine at position 69, and mutant enzyme CMT-1 is the first harboring both mutations Ser-238 and Leu-69. The affinity may be affected by a change at position 69, since the side chain at position 238, on the inner side of the B3 β-strand, lies very close to the side chain of residue 69 (12).

The TEM-1 variant, with the associated changes Glu→Lys-104 and Gly→Ser-238, is TEM-15 (16). Complex mutant CMT-1, with these last mutations, conferred a lower level of resistance to CTX and CAZ than did TEM-15, and this difference correlated with the kinetic constants. The kinetic comparison of substrate hydrolysis in extended-spectrum β-lactamases TEM-15 and CMT-1 revealed that the catalytic efficiency (k_{cat}/K_m) of CMT-1 was lower than that of TEM-15 for CTX (10-fold) and ceftriaxone (20-fold).

Overall, the hydrolytic properties of this complex TEM mutant enzyme were found to be closer to those of an extended-spectrum enzyme than to those of an inhibitor-resistant enzyme. However, the predominant effect of the mutations Lys-104 and Ser-238, which are responsible for extended-spectrum activity and inhibitor hypersusceptibility, was clearly attenuated by the mutations Leu-69 and Asp-276. In the strain producing CMT-1, complete reversal of CA resistance by mutations enhancing activity against 7-oxyimino cephalosporins was not observed as reported in a Ser-164–Ser-244 mutant obtained by site-specific mutagenesis (9).

E. coli GR102 was isolated from a patient treated with CPO (4 g/day) and amikacin (1 g/day) for 12 days. An *E. coli* strain with a typical β-lactam inhibitor resistance phenotype and the same resistances to other antibiotics had been isolated from the same sample (feces) from this patient a week before. This suggests that an inhibitor-resistant TEM mutant enzyme with the Leu-69 and Asp-276 mutations emerged first, and then, under antibiotic (CPO) and mutagenic agent (cytarabin and daunorubicin) pressure, this mutant underwent the two additional mutations, Lys-104 and Ser-238, responsible for extended-spectrum activity. Unfortunately, this hypothesis could not be confirmed since the initial *E. coli* IRT-producing strain was not kept.

In conclusion, the production of this complex TEM mutant cannot alone account for the high-level multiresistance to β-lactams of the *E. coli* GR102 isolate, in which several resistance mechanisms were involved (TEM-1 and, probably, decreased permeability). It would probably be more beneficial for an *E. coli* strain to produce two different TEM mutants (an extended-spectrum mutant and an inhibitor-resistant mutant) simultaneously than to produce one double mutant. If each mutant conferred its own resistance phenotype, high-level resistance to both CA combinations and extended-spectrum cephalosporins could then be expected.

ACKNOWLEDGMENTS

We thank J. M. Frère for the gift of highly purified TEM-15 extract and P. Courvalin for the gift of *K. pneumoniae* Kp240 producing the TEM-15 enzyme. We thank Rolande Perroux, Marlène Jan, and Dominique Rubio for technical assistance.

This work was supported in part by a grant from the Direction de la Recherche et des Etudes doctorales, Ministère de l'Education Nationale, Paris, France.

REFERENCES

1. **Ambler, R. P., A. F. N. Coulson, J. M. Frère, J. M. Ghuysen, B. Joris, M. Forsman, R. C. Levesque, G. Tiraby, and S. G. Waley.** 1991. A standard numbering scheme for the class A β-lactamases. Biochem. J. **276**:269–272.
2. **Brun, T., J. Péduzzi, M. M. Caniça, G. Paul, P. Névot, M. Barthélémy, and R. Labia.** 1994. Characterization and amino acid sequence of IRT-4, a novel TEM-type enzyme with a decreased susceptibility to β-lactamase inhibitors. FEMS Microbiol. Lett. **120**:111–118.
3. **Chanal, C., M. C. Poupart, D. Sirot, R. Labia, J. Sirot, and R. Cluzel.** 1992. Nucleotide sequences of CAZ-2, CAZ-6, and CAZ-7 β-lactamase genes. Antimicrob. Agents Chemother. **36**:1817–1820.
4. **Chen, S. T., and R. C. Clowes.** 1987. Variations between the nucleotide sequences of Tn*1*, Tn2, and Tn*3* and expression of β-lactamase in *Pseudomonas aeruginosa* and *Escherichia coli*. J. Bacteriol. **169**:913–916.
5. **Delaire, M., R. Labia, J. P. Samama, and J. M. Masson.** 1992. Site-directed mutagenesis at the active site of *Escherichia coli* TEM-1 β-lactamase. J. Biol. Chem. **267**:20600–20606.
6. **Du Bois, S. K., M. S. Marriott, and S. G. B. Amyes.** 1995. TEM- and SHV-derived extended-spectrum β-lactamases: relationship between selection, structure and function. J. Antimicrob. Chemother. **35**:7–22.
7. **Goussard, S., and P. Courvalin.** 1991. Sequence of the genes *blaT-1B* and *blaT-2*. Gene **102**:71–73.
8. **Henquell, C., C. Chanal, D. Sirot, R. Labia, and J. Sirot.** 1995. Molecular characterization of nine different types of mutants among 107 inhibitor-resistant TEM β-lactamases from clinical isolates of *Escherichia coli*. Antimicrob. Agents Chemother. **39**:427–430.
9. **Imtiaz, U., E. K. Manavathu, S. Mobashery, and S. A. Lerner.** 1994. Reversal of clavulanate resistance conferred by a Ser-244 mutant of TEM-1 β-lactamase as a result of a second mutation (Arg to Ser at position 164) that enhances activity against ceftazidime. Antimicrob. Agents Chemother. **38**: 1134–1139.
10. **Jarlier, V., M. H. Nicolas, G. Fournier, and A. Philippon.** 1988. Extended broad-spectrum β-lactamases conferring transferable resistance to newer β-lactam agents in *Enterobacteriaceae*: hospital prevalence and susceptibility patterns. Rev. Infect. Dis. **10**:867–878.
11. **Jelsch, C., F. Lenfant, J. M. Masson, and J. P. Samama.** 1992. β-Lactamase TEM-1 of *E. coli*. Crystal structure determination at 2.5 A resolution. FEBS Lett. **299**:135–142.
12. **Knox, J. R.** 1995. Extended-spectrum and inhibitor-resistant TEM-type β-lactamases: mutations, specificity, and three-dimensional structure. Antimicrob. Agents Chemother. **39**:2593–2601.
13. **Labia, R., J. Andrillon, and F. Le Goffic.** 1973. Computerized microacidimetric determination of β-lactamase Michaelis-Menten constants. FEBS Lett. **33**:42–44.
14. **Labia, R., A. Morand, K. Tiwari, J. S. Pitton, D. Sirot, and J. Sirot.** 1988. Kinetic properties of two plasmid-mediated β-lactamases from *Klebsiella pneumoniae* with strong activity against third-generation cephalosporins. J. Antimicrob. Chemother. **21**:301–307.
15. **Livermore, D. M.** 1995. β-Lactamases in laboratory and clinical resistance. Clin. Microbiol. Rev. **8**:557–584.
16. **Mabilat, C., and P. Courvalin.** 1990. Development of "oligotyping" for characterization and molecular epidemiology of TEM β-lactamases in members of the family *Enterobacteriaceae*. Antimicrob. Agents Chemother. **34**: 2210–2216.
17. **Oliphant, A. R., and K. Struhl.** 1989. An efficient method for generating proteins with enzymatic properties: application to β-lactamase. Proc. Natl. Acad. Sci. USA **86**:9094–9098.
18. **Petit, A., L. Maveyraud, F. Lenfant, J. P. Samama, R. Labia, and J. M. Masson.** 1995. Multiple substitutions at position 104 of β-lactamase TEM-1: assessing the role of this residue in substrate specificity. Biochem. J. **305**:33–40.
19. **Sirot, D., C. Chanal, C. Henquell, R. Labia, J. Sirot, and R. Cluzel.** 1994. Clinical isolates of *Escherichia coli* producing multiple TEM-mutants resistant to β-lactamase inhibitors. J. Antimicrob. Chemother. **33**:1117–1126.
20. **Sowek, J. A., B. Singer, S. Ohringer, M. F. Mally, T. J. Dougherty, J. Z. Gougoutas, and K. Bush.** 1991. Substitution of lysine at position 104 or 240 of TEM β-lactamase enhances the effect of serine-164 substitution on hydrolysis or affinity for cephalosporins and the monobactam aztreonam. Biochemistry **30**:3179–3188.
21. **Sutcliffe, G.** 1978. Nucleotide sequence of the ampicillin resistance gene of *Escherichia coli* plasmid pBR322. Proc. Natl. Acad. Sci. USA **75**:3737–3741.
22. **Zhou, X. Y., F. Bordon, D. Sirot, M. D. Kitzis, and L. Gutmann.** 1994. Emergence of clinical isolates of *Escherichia coli* producing TEM-1 derivatives or an OXA-1 β-lactamase conferring resistance to β-lactamase inhibitors. Antimicrob. Agents Chemother. **38**:1085–1089.

JOURNAL OF BACTERIOLOGY, Dec. 1996, p. 7248–7253
0021-9193/96/$04.00+0

Vol. 178, No. 24

Structure-Function Relationships among Wild-Type Variants of *Staphylococcus aureus* β-Lactamase: Importance of Amino Acids 128 and 216

RAMA KISHAN R. VOLADRI,[1]* MURALI K. R. TUMMURU,[1] AND DOUGLAS S. KERNODLE[1,2]

Division of Infectious Diseases, Department of Medicine, Vanderbilt University, Nashville, Tennessee 37232-2605,[1] and Department of Veterans Affairs Medical Center, Nashville, Tennessee 37232[2]

Received 30 May 1996/Accepted 10 October 1996

β-Lactamases inactivate penicillin and cephalosporin antibiotics by hydrolysis of the β-lactam ring and are an important mechanism of resistance for many bacterial pathogens. Four wild-type variants of *Staphylococcus aureus* β-lactamase, designated A, B, C, and D, have been identified. Although distinguishable kinetically, they differ in primary structure by only a few amino acids. Using the reported sequences of the A, C, and D enzymes along with crystallographic data about the structure of the type A enzyme to identify amino acid differences located close to the active site, we hypothesized that these differences might explain the kinetic heterogeneity of the wild-type β-lactamases. To test this hypothesis, genes encoding the type A, C, and D β-lactamases were modified by site-directed mutagenesis, yielding mutant enzymes with single amino acid substitutions. The substitution of asparagine for serine at residue 216 of type A β-lactamase resulted in a kinetic profile indistinguishable from that of type C β-lactamase, whereas the substitution of serine for asparagine at the same site in the type C enzyme produced a kinetic type A mutant. Similar bidirectional substitutions identified the threonine-to-alanine difference at residue 128 as being responsible for the kinetic differences between the type A and D enzymes. Neither residue 216 nor 128 has previously been shown to be kinetically important among serine-active-site β-lactamases.

β-Lactam antibiotics, including the penicillins and cephalosporins, are important agents in the therapy of bacterial infections. However, in some clinical settings the usefulness of these agents has been diminished by the emergence and spread of bacterial strains that produce β-lactamase, which hydrolyzes the β-lactam ring and inactivates the drug's antimicrobial effect (27). This problem has been demonstrated most dramatically with *Staphylococcus aureus*. Whereas the vast majority of clinical isolates of *S. aureus* were highly susceptible to penicillin G at the time of its introduction into clinical use in the early 1940s, the spread of β-lactamase-producing, penicillin-resistant strains was so widespread by the late 1940s that penicillin G was no longer a reliable antistaphylococcal agent. Most clinical isolates of *S. aureus* produce β-lactamase (36).

Four types of *S. aureus* β-lactamase have been identified by serologic (34, 35) and kinetic (19, 20) methods. These variants originally were designated types A, B, C, and D by Richmond (34) and Rosdahl (35). This nomenclature should not be confused with that of the different classes of β-lactamases, A through D, that has been used more recently to group the β-lactamases of all bacterial species on the basis of active site (serine versus zinc), size, and kinetic characteristics (4). Each of the four recognized types of *S. aureus* β-lactamase (A, B, C, and D) is a class A β-lactamase with a serine active site. The mature form of the enzyme has a molecular mass of 30 kDa, contains 257 amino acids, and is excreted extracellularly (1).

The type A and C staphylococcal β-lactamases are easily distinguished kinetically, either by substrate profile (18) or by K_m and catalytic constant (k_{cat}) determinations (43). Whereas the kinetics of hydrolysis exhibited by the type A and D staphylococcal β-lactamases are similar (20), they can be rapidly and reproducibly distinguished by a fivefold difference in the ratio of the rates of the initial velocity of hydrolysis of penicillin G and cefazolin (43). The lower penicillin G/cefazolin hydrolysis ratio of the type D β-lactamase appears to be related to a lower k_{cat} for the hydrolysis of penicillin G by purified type D enzyme than the other staphylococcal β-lactamases (43).

The genes encoding the type A, C, and D β-lactamases of *S. aureus* are located on plasmids and have been cloned and sequenced (5, 8, 9, 40). The deduced amino acid sequences identify six amino acid differences in the primary sequence of the prototypic type A β-lactamase from strains PC1 and S1 compared with the type C sequence from strain 3804, including amino acids 116, 202, 205, 206, 212, and 216. In addition, there are five differences, at amino acids 93, 121, 128, 226, and 229, between the prototypic type A β-lactamase and the type D β-lactamase produced by strain FAR4. The type C and D enzymes differ by 11 amino acids.

The molecular basis for the kinetic heterogeneity exhibited by the staphylococcal β-lactamases has not been determined. However, the structure of the type A variant of *S. aureus* β-lactamase is known from X-ray crystallographic analysis (11, 12), and several of the amino acids which are different between the type A, C, and D β-lactamases are located close to the active-site cleft. To test the hypothesis that single amino acid differences at sites close to the active site are responsible for the kinetic heterogeneity exhibited by naturally occurring variants of *S. aureus* β-lactamase, we constructed mutant β-lactamases with single amino acid substitutions at sites where the wild-type enzymes differ and evaluated the kinetics of the mutant enzyme.

* Corresponding author. Mailing address: Division of Infectious Diseases, Department of Medicine, Vanderbilt University Medical Center, Nashville, TN 37232. Phone: (615) 327-4751, ext. 5486. Fax: (615) 343-6160. Electronic mail address: voladrrr@ctrvax.vanderbilt.edu.

TABLE 1. Plasmids and phagemids used in this study

Plasmid	Host	Resistance[a]	Description	Source or reference
pS1	*S. aureus*	Amp	From strain S1, carries *blaZ* encoding type A β-lactamase	18
pII3804	*S. aureus*	Amp	From strain 3804, carries *blaZ* encoding type C β-lactamase	9
pUB101	*S. aureus*	Amp	From strain FAR4, carries *blaZ* encoding type D β-lactamase	25
pE194	*S. aureus*	Em	From strain RN2442, carries gene encoding Em^r	13
pBC SK+	*E. coli*	Cm	Phagemid vector	Stratagene
pTZ18R	*E. coli*	Amp	Phagemid vector	Bio-Rad
pVK100	*S. aureus-E. coli*	Em, Cm	*E. coli-S. aureus* shuttle plasmid constructed by cloning 3.7-kb pE194 on a *Sac*I site into *Sal*I of pBC SK+	This study
pVK101	*S. aureus-E. coli*	Em, Cm	pVK100 with a 4-kb *Eco*RI-*Hin*dIII fragment carrying β-lactamase regulatory genes from pI3796 but lacks *blaZ*	This study
pVK102	*E. coli*	Amp	pTZ18R with 4-kb *Hin*cII fragment with type A *blaZ* from pS1	This study
pVK103	*E. coli-S. aureus*	Amp, Em	pVK101 with 1.1-kb *Hin*dIII fragment with type A *blaZ* from pVK102	This study
pVK104	*E. coli*	Amp	pBC SK+ with 8-kb *Eco*RI fragment with type C *blaZ* from pII3804	This study
pVK105	*E. coli-S. aureus*	Amp, Em	pVK101 with 1.8-kb *Hin*dIII fragment with type C *blaZ* from pVK104	This study
pVK106	*E. coli-S. aureus*	Amp, Em	pVK101 with 1.3-kb *Hin*dIII fragment with type D *blaZ* from pUB101	This study
pVK107	*E. coli-S. aureus*	Amp, Em	pVK101 with 1.1-kb *Hin*dIII type A *blaZ* fragment except a single nucleotide substitution leading to S216N change	This study
pVK108	*E. coli-S. aureus*	Amp, Em	pVK101 with 1.1-kb *Hin*dIII type A *blaZ* fragment except a single nucleotide substitution leading to T128A change	This study
pVK109	*E. coli-S. aureus*	Amp, Em	pVK101 with 1.8-kb *Hin*dIII type C *blaZ* fragment except a single nucleotide substitution leading to N216S change	This study
pVK110	*E. coli-S. aureus*	Amp, Em	pVK101 with 1.3-kb *Hin*dIII type D *blaZ* fragment except a single nucleotide substitution leading to A128T change	This study

[a] Amp, ampicillin; Cm, chloramphenicol; Em, erythromycin.

MATERIALS AND METHODS

Chemicals and media. Standard powders of nitrocefin (BBL Microbiology Systems, Cockeysville, Md.); cephaloridine (Sigma Chemical Co., St. Louis, Mo.); methicillin, ampicillin, and cephapirin (Bristol Laboratories, Syracuse, N.Y.); and cefazolin and penicillin G (Eli Lilly & Co., Indianapolis, Ind.) were used to prepare antibiotic solutions for kinetic studies. Cation-exchange resin P11 (Whatman Laboratories, Kent, England) and *meta*-aminophenyl boronic acid hemisulfate and succinamide-activated sepharose (Sigma) were used for preparing columns for β-lactamase purification. Restriction endonucleases, T4 DNA ligase, and Sequenase were purchased from United States Biochemical Corp., Cleveland, Ohio. A Muta Gene Phagemid kit (Bio-Rad Laboratories, Fullerton, Calif.) was used for site-directed mutagenesis. The oligonucleotides required for site-directed mutagenesis and sequencing of the β-lactamase gene were synthesized on a Cyclone Plus Automatic DNA synthesizer (Millipore, Bedford, Mass.) by the DNA Core Facility, Department of Molecular Physiology and Biophysics, Vanderbilt University. Modified 1% CY broth was prepared as described by Novick (29). LB and 2× YT media were prepared according to the methods of Maniatis et al. (26). Tryptic soy broth was purchased from BBL.

Bacterial strains, plasmids, and cultivation. The plasmids and phagemids used and constructed during this study are listed in Table 1. *S. aureus* RN4220 (R. P. Novick, Public Health Research Institute, New York, N.Y.) was used as a recipient for protoplast transformation. *Escherichia coli* DH5α was used for the transformation and propagation of *E. coli* plasmids and *S. aureus-E. coli* shuttle plasmids except when indicated otherwise.

Construction of *S. aureus* β-lactamase expression vector. An *E. coli-S. aureus* shuttle vector, pVK101, was constructed with erythromycin as a selectable marker in *S. aureus*, by using a strategy similar to that employed by East et al. (8) to construct *S. aureus* β-lactamase expression vector pAE706. First *S. aureus* plasmid pE194 was digested with *Sal*I and cloned into the *Sac*I site of pBC SK+ (Stratagene, La Jolla, Calif.) to create pVK100. Next *blaR* (β-lactamase regulatory gene) from *S. aureus* plasmid pI3796 was cloned on a 4-kb *Hin*dIII-*Eco*RI fragment into pVK100 to produce pVK101.

Cloning of type A, C, and D *blaZ*. Large-scale isolation of plasmid DNA from *S. aureus* by ultracentrifugation in a cesium chloride gradient (Var lac oid Chemical Co., Inc., Bergenfield, N.J.) was performed by methods described by Galetto et al. (10). A 4-kb *Hin*cII fragment carrying the *blaZ* (β-lactamase structural gene) from pS1 was cloned into pTZ18R to create pVK102. *Hin*dIII digestion of pVK102 enabled the type A *blaZ* to be mobilized on a 1.1-kb fragment which was cloned into pVK101. This produced pVK103 in which *blaZ* and *blaR* are transcribed divergently from the same intracistronic region. A similar strategy was used to clone the type C *blaZ* from pII3804 into pVK101 via a pBC SK+ intermediate (pVK104) to produce pVK105. The plasmid DNA from pUB101 was digested with *Hin*dIII, and a 1.3-kb fragment carrying type D *blaZ* was cloned in the desired orientation into pVK101 to produce pVK106.

Site-directed mutagenesis of β-lactamase. Oligonucleotide-directed mutagenesis was performed by the method of Kunkel et al. (23, 24). *Hin*dIII fragments containing the type A, C, and D *blaZ* genes were cloned individually into the phage vector M13mp18 (42). Two oligonucleotides, each with a single mismatch (underlined), were used to introduce specific mutations at amino acids 128 (5′TCACTATATGCCATTGAAGCC3′; Thr to Ala) and 216 (5′AGTATCTC CGTTTTTATTATT3′; Ser to Asn) of the type A *blaZ*. Additional primers were constructed to produce the reverse mutation in the type C and D *blaZ* genes (i.e., 5′AGTGTCTCCGCTTTTATTATT, Asn to Ser, type C *blaZ* and 5′ATCACT ATATGTCATTGAAGC, Ala to Thr, type D *blaZ*). Single-stranded DNA from the six randomly picked plaques was sequenced by the dideoxy chain termination method (38) using Sequenase enzyme to confirm the desired mutation. The complete open reading frame was sequenced in order to rule out the presence of any spurious mutations.

Expression of wild-type and mutant β-lactamases in *S. aureus* RN4220. Wild-type *blaZ* encoding type A, C, and D β-lactamases and mutant *blaZ* genes from M13mp18 recombinants were cloned as 1.1- to 1.8-kb *Hin*dIII fragments into the *Hin*dIII site of *S. aureus-E. coli* shuttle plasmid pVK101. Recombinants were selected on LB medium containing ampicillin (100 μg/ml) and chloramphenicol (30 μg/ml). The desired orientation of the insert was verified either by restriction with *Eco*RV, which has a single site within type A and D *blaZ* and one just upstream of the *blaZ* promoter within *blaR*, or by PCR. Protoplast transformation was used to transfer the recombinant shuttle plasmids into *S. aureus* RN4220 (6).

β-Lactamase purification from *S. aureus*. The wild-type β-lactamase-producing strains and the RN4220 transformants were grown in 5 liters of modified 1% CY medium containing methicillin (0.5 μg/ml) or 2-(2′-carboxyphenyl)benzoyl-6-aminopenicillanic acid (7.5 μM, to induce β-lactamase production) at 37°C and 150 rpm for 18 h. The extracellular β-lactamases were purified by sequential cation-exchange and affinity chromatography (21).

Enzyme kinetics. Initial velocities of hydrolysis were monitored at a wavelength corresponding to the maximal change in absorbance between the unhydrolyzed substrate and the hydrolyzed product, which included the following: cephaloridine, 254 nm; cefazolin, 272 nm; nitrocefin, 482 nm; cephapirin, 258 nm; ampicillin, 235 nm; and penicillin G, 232 nm (37, 39). β-Lactamase assays were performed in 0.1 M sodium phosphate buffer, pH 6.0, in 1-cm cuvettes at 37°C with a DU-70 recording spectrophotometer (Beckman Instruments, Fullerton, Calif.). For K_m and k_{cat} determinations, assays of the initial velocity of hydrolysis were performed using 100, 50, 33.3, 20, 14.2, and 11.1 μM solutions of each cephalosporin antibiotic. Penicillin hydrolysis assays were performed at initial substrate concentrations of 1,000, 500, 333, 200, 142, and 111 μM. The maximal rate of hydrolysis, V_{max}, and the Michaelis constant, K_m, for each substrate-enzyme combination were determined from $[s]/v$-against-$[s]$ plots (where $[s]$ is substrate concentration and v is velocity) (41) with computerized software (Hyper; Department of Biochemistry, University of Liverpool, Liverpool, United Kingdom). The turnover number, k_{cat}, was calculated from the V_{max} by using a molecular mass of the purified β-lactamase of 30,000 g/mol. Mean values and standard error of the mean values were calculated from the results of

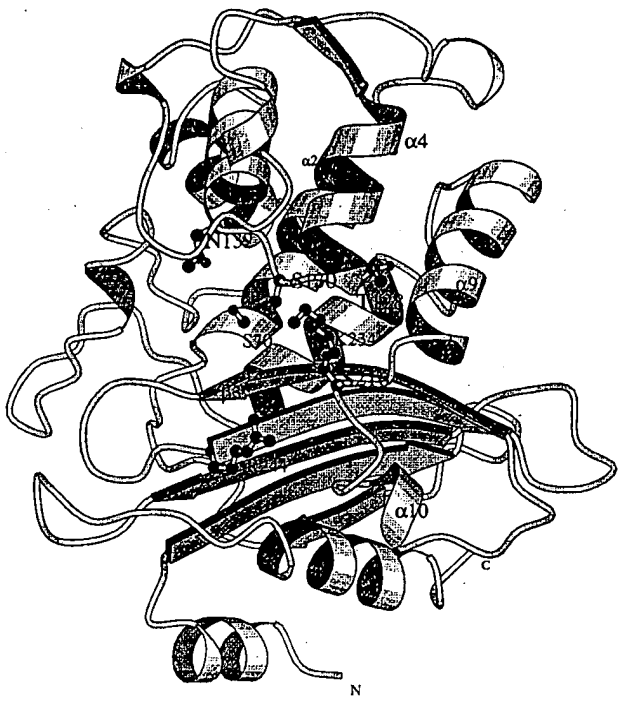

FIG. 1. Tertiary structure of *S. aureus* PC1 β-lactamase. The active-site cleft of the β-lactamase is located at the left side of the β3 strand. The active-site amino acids are S-70, S-130, N-132, K-234, and R-244. Amino acids T-128 and S-216 were substituted by site-directed mutagenesis of the cloned structural gene. The diagram was generated by the computer software MOLSCRIPT (22) using X-ray crystallographic coordinates stored in the Brookhaven Protein Database (accession no. 3BLM).

8 to 12 [*s*]/*v*-against-[*s*] plots for each enzyme-substrate combination by using computer software (Minitab Data Analysis Software, release 10.2; Minitab, Inc., State College, Pa.).

RESULTS

Construction and expression of mutant β-lactamases. The primary goal of this study was to determine the functional domains, particularly the specific amino acid(s), responsible for the kinetic heterogeneity observed among naturally occurring variants of *S. aureus* β-lactamase. Mutant β-lactamases with single amino acid substitutions at residues 128 (Thr to Ala) and 216 (Ser to Asn) were constructed by using oligonucleotide-directed mutagenesis and the type A β-lactamase gene (*blaZ*) as a template. In addition, the reverse mutations were introduced by using the type D (Ala to Thr, residue 128) and type C (Asn to Ser, residue 216) *blaZ* genes as template DNA. These residues were selected primarily because of the amino acids which differed among the type A, C, and D β-lactamases, 128 and 216 were closest to the active-site cleft (Fig. 1). Each *blaZ* was cloned into *E. coli-S. aureus* shuttle plasmid pVK101, which was then transformed into *S. aureus* RN4220. β-Lactamase production was induced, and the wild-type β-lactamases expressed by the reference strains and the mutant enzymes expressed in RN4220 were purified to homogeneity.

Effect of substitution at amino acid 216 on the kinetics of type A and C β-lactamases. β-Lactams which have been shown previously to be useful in distinguishing between the wild-type *S. aureus* β-lactamases (20) were used to compare the kinetics of hydrolysis of the reference and mutant enzymes (Tables 2 and 3). Between the type A and type C β-lactamases there were a 10-fold difference in the K_m values of cefazolin, a 5-fold difference in the K_m values of cephapirin, and a 5-fold difference in the k_{cat} values of nitrocefin. These differences appear to be due to whether Ser or Asn was present at residue 216. Replacement of Ser by Asn in the type A β-lactamase yielded a mutant (A, S216N) that was closer kinetically to the type C than the type A enzyme (e.g., cefazolin K_m values: 167 μM, mutant; 145 μM, type C; 13.1 μM, type A). The reverse mutation using type C *blaZ* DNA for site-directed mutagenesis yielded a mutant (C, N216S) that was similar to the type A enzyme (cefazolin K_m value, 15.3 μM). Also, the differences between the kinetic type A and type C *S. aureus* β-lactamases are clearly shown by comparing relative efficiency of hydrolysis values (Table 4). The k_{cat} values of most substrates other than nitrocefin did not clearly distinguish between the type A and type C enzymes (Table 3).

Effect of substitution at amino acid 128 on the kinetics of type A and D β-lactamases. The reference type A β-lactamase had a cefazolin K_m value that was threefold lower than and an ampicillin K_m value that was twofold greater than the respective K_m values of the type D enzyme. In addition, the k_{cat} values of ampicillin and penicillin G were three- to fourfold higher with the type A compared to the type D β-lactamase. These differences were related to whether Ala or Thr was present at residue 128. Replacement of Thr by Ala in the type A β-lactamase yielded a mutant (A, T128A) that was closer kinetically to the type D than the type A enzyme (e.g., penicillin k_{cat} values: 47 s^{-1}, mutant; 254 s^{-1}, type A; 66 s^{-1}, type

TABLE 2. K_m values of β-lactam antibiotics for purified wild-type and mutant β-lactamases of *S. aureus*[a]

Antibiotic	Mean K_m [μM (SEM)] for β-lactamase						
	Wild type			Altered by site-directed mutagenesis			
	pS1, type A	pII3804, type C	pUB101, type D	pVK107 (A, S216N)	pVK108 (A, T128A)	pVK109 (C, N216S)	pVK110 (D, A128T)
Cephaloridine	4.3 (1.0)	6.3 (1.8)	4.6 (1.2)	6.5 (1.7)	5.3 (1.3)	4.5 (0.7)	4.8 (1.1)
Cefazolin	**13.1** (2.8)	**145** (18.7)	**38.3** (9.3)	**167** (35)	**43.9** (6.6)	**15.3** (2.7)	**13.3** (1.8)
Cephapirin	**4.5** (1.2)	**24.9** (1.7)	7.1 (1.7)	**27.3** (3.9)	7.0 (0.8)	**5.5** (1.5)	4.5 (1.0)
Nitrocefin	**5.1** (1.3)	**10.5** (2.3)	7.1 (1.6)	**11.6** (2.3)	6.8 (1.5)	**6.7** (1.5)	6.6 (1.7)
Ampicillin	**195** (35)	128 (22)	**119** (22)	153 (14)	**118** (15)	208 (31)	**219** (43)
Penicillin G	29.2 (6.5)	25.5 (6.9)	26.0 (8.2)	29.0 (9.1)	34.3 (9.4)	31.3 (8.6)	19.7 (6.5)

[a] The initial velocities of hydrolysis of 100, 50, 33.3, 20, 14.2, and 11.1 μM solutions of the cephalosporins and 1,000, 500, 333, 200, 142, and 111 μM solutions of ampicillin and penicillin G were monitored with a recording spectrophotometer. K_m values were determined by the use of [*s*]/*v*-against-[*s*] plots. Each value represents the mean from 8 to 12 determinations. K_m values that are altered by amino acid replacements are in boldface.

TABLE 3. k_{cat} values of β-lactam antibiotics for purified wild-type and mutant β-lactamases of *S. aureus*

Antibiotic	Mean k_{cat} value [s^{-1} (SEM)]" for β-lactamase						
	Wild type			Altered by site-directed mutagenesis			
	pS1, type A	pII3804, type C	pUB101, type D	pVK107 (A, S216N)	pVK108 (A, T128A)	pVK109 (C, N216S)	pVK110 (D, A128T)
Cephaloridine	1.5 (0.3)	2.6 (0.2)	0.97 (0.2)	3.4 (0.4)	0.83 (0.1)	0.74 (0.17)	1.37 (0.1)
Cefazolin	1.4 (0.1)	1.8 (0.1)	2.1 (0.1)	2.51 (0.3)	2.24 (0.1)	0.86 (0.1)	0.92 (0.1)
Cephapirin	0.37 (0.01)	0.6 (0.01)	0.21 (0.02)	0.75 (0.1)	0.19 (0.03)	0.27 (0.02)	0.36 (0.01)
Nitrocefin	**33.7** (4.6)	**6.9** (0.4)	**16.3** (2.0)	**8.0** (0.9)	**15.3** (3.4)	**33.1** (4.1)	**37.0** (4.4)
Ampicillin	**560** (49)	249 (14)	**133** (23)	353 (28)	**91** (10)	392 (33)	**423** (46)
Penicillin G	**254** (17)	140 (5)	**65.6** (6)	162 (14)	**47.3** (6.8)	173 (16)	**192** (12)

" Mean value in molecules of antibiotic hydrolyzed per second per molecule of enzyme, as determined from [*s*]/*v*-against-[*s*] plots and assuming a molecular mass of the purified β-lactamase of 30,000 g/mol. Each value is derived from 8 to 12 determinations. k_{cat} values that are altered by amino acid replacements are in boldface.

D). The reverse mutation using type D *blaZ* DNA for site-directed mutagenesis yielded a mutant (D, A128T) that was similar to the type A enzyme (penicillin G k_{cat} value, 192 s^{-1}). The type A and D enzymes are easily distinguished by the ratio of the rates of hydrolysis of penicillin G and cefazolin (Table 5).

DISCUSSION

Naturally occurring variants of *S. aureus* β-lactamase can be distinguished on the basis of the kinetics of hydrolysis of selected penicillin and cephalosporin antibiotics (20, 43). In this study we have shown that these kinetic differences are determined by single amino acid substitutions at positions close to the active site of the enzyme. Specifically, the presence of an Asn instead of Ser at residue 216 determines a type C kinetic profile, and the presence of an Ala instead of Thr at residue 128 determines a type D kinetic profile. Enzymes exhibiting the type A kinetic profile have Ser and Thr at these two sites, respectively. We also found that substitutions at some positions other than 128 and 216 where the type A, C, and D enzymes have different amino acids did not alter the kinetic profile of the enzyme (e.g., amino acid 121 [data not shown]).

This situation is reminiscent of what has been reported for the newer TEM-type β-lactamases and SHV β-lactamase variants among gram-negative bacterial species (17). Broad-spectrum TEM and SHV variant β-lactamases capable of hydrolyzing ceftazidime, cefotaxime, and/or other newer cephalosporins have become problematic in many medical centers in recent years, especially among isolates of *Klebsiella pneumoniae* and *E. coli* (14, 17, 31). As with the *S. aureus* enzymes, the altered kinetic profile of the broad-spectrum TEM-type β-lactamases is based on modest changes in primary structure, generally one to three amino acid substitutions at sites close to the active site (32). In addition, single mutations that result in TEM and SHV variant β-lactamases exhibiting resistance to commercially available β-lactamase inhibitors such as clavulanic acid have been described (7, 15).

A major difference between the histories of the variant TEM and staphylococcal enzymes, however, is that whereas the former appear to be a consequence of selective antibiotic pressure in the clinical setting, the *S. aureus* enzymes appear to have remained remarkably stable over time. Although β-lactamase-producing strains of *S. aureus* spread widely during the first few years following the clinical introduction of penicillin, some clinical isolates collected and saved prior to penicillin use have been shown to produce the A and C variants of *S. aureus* β-lactamase. Furthermore, the prevalence of the various types of staphylococcal β-lactamases among clinical isolates in the United States in the 1980s (19, 20) are similar to what was reported in England by Richmond in the mid-1960s when he first described the existence of different staphylococcal β-lactamase serotypes (34). Despite the widespread use since the early 1960s of antistaphylococcal penicillins such as methicillin, oxacillin, and nafcillin, new staphylococcal β-lactamases capable of hydrolyzing these agents efficiently have not been observed.

Both of the amino acid positions that we have shown to be responsible for the kinetic differences among the wild-type *S. aureus* enzymes have not previously been cited as contributing to β-lactamase function. The major kinetic difference between the type A and C enzymes is the K_m values of certain cepha-

TABLE 4. Relative efficiencies of hydrolysis for β-lactam antibiotics of purified wild-type and mutant β-lactamases of *S. aureus*

Antibiotic	REH" (%) of β-lactamase						
	Wild type			Altered by site-directed mutagenesis			
	pS1, type A	pII3804, type C	pUB101, type D	pVK107 (A, S216N)	pVK108 (A, T128A)	pVK109 (C, N216S)	pVK110 (D, A128T)
Cephaloridine	100	100	100	100	100	100	100
Cefazolin	**32**	**3**	24	**3**	28	**24**	25
Cephapirin	**24**	**6**	14	**5**	17	**30**	29
Nitrocefin	**1,943**	**159**	1,095	**133**	1,406	**1,980**	2,004
Ampicillin	**820**	**473**	562	**449**	481	**868**	690
Penicillin G	**2,565**	**1,336**	**1,200**	**1,071**	**863**	**2,208**	**3,578**

" Relative efficiency of hydrolysis (REH) is a relative value of k_{cat}/K_m. These values are expressed as a percentage of the REH for cephaloridine by the same β-lactamase (i.e., the cephaloridine REH was calculated in liters per mole per second and assigned a value of 100), determined from the mean k_{cat} and K_m values for each enzyme-substrate combination. REH values that are altered by amino acid replacements are in boldface.

TABLE 5. Ratios of the rates of hydrolysis of penicillin G and cefazolin by kinetic type A and D β-lactamases

β-Lactamase (type)	Relative k_{cat} ratio[a]	Fixed-concn ratio[b]
Wild type		
pS1 (A)	178.7	183.5
pUB101 (D)	32.5	36.6
Altered by site-directed mutagenesis		
pVK108 (A, T128A)	23.6	45.7
pVK110 (D, A128T)	208.5	162.5

[a] Ratio of the k_{cat} values of penicillin G and cefazolin.
[b] Determined from the initial velocities of hydrolysis using a 500 μM concentration of penicillin G and 100 μM concentration of cefazolin.

losporins, particularly cefazolin and cephapirin (Table 2). These enzymes differ not only in hydrolysis of certain cephalosporin substrates but also in the inhibition profile of some β-lactamase inhibitors, including sulbactam (unpublished observations) and tazobactam (3), with the type A enzyme being more susceptible to inhibition.

The substitution at residue 216 might affect β-lactamase structure and function in several ways. First, the side chain of Asn is bulkier (the accessible surface area of Asn is 158 Å [15.8 nm] [28]) than that of Ser (122 Å [12.2 nm]) and may be hindering the substrate binding into the active-site cleft. Modelling studies with cefazolin docked into the PC1 β-lactamase active-site cleft show that the side chain C_3 substituent in cefazolin is positioned close to side chain of Ser-216 (unpublished observations) and substitution of Asn for Ser at this position would result in steric hindrance. Second, the refined crystal structure of PC1 β-lactamase at 2 Å (0.2 nm) indicated that the amino acid 216 is located on a short 3_{10} helix comprising amino acids 215 to 217 and this helix is stabilized through a helix N capping (33) between Asn-214, which is highly conserved among class A β-lactamases (2), and Ser-216 (O-N, 2.9 Å [0.29 nm]). In addition to this, the side chain OH of Ser-216 is also involved in a hydrogen bond with Asn-214 side chain carbonyl (O-O, 3.3 Å [0.33 nm]). Substitution of Asn for Ser at 216 may alter the topology of this short helix. The crystal structure of a type C enzyme could help to clarify the structure of this loop, and attempts are under way to crystallize the type C enzyme. Third, amino acid 216 is located close to the β3 strand, and changes at this residue might alter the relative positioning of other active-site amino acids such as the K-T-G triad.

The reason why the replacement of Thr by Ala at residue 128 should affect enzyme function is less clear. The effect of the substitution was primarily a reduction in the k_{cat} of the penicillins and nitrocefin along with modest effects on the K_m values of cefazolin and ampicillin (Table 2). The crystal structure of PC1 indicates that amino acid 128 is located at the C terminus of α-helix 4 close to the active-site cleft. It is two residues away from the highly conserved S-D-N loop (amino acids 130 to 132) of the class A β-lactamases. The catalytic function of the S-D-N loop has been verified by site-directed mutagenesis of *Streptomyces albus* G β-lactamase (16) and *E. coli* TEM β-lactamase (30). The proximity of amino acid 128 to the catalytically important S-D-N loop might explain the kinetic differences between the type A and type D *S. aureus* β-lactamases. Preliminary experiments in which residue 128 has been replaced by other amino acids also have been shown to affect the kinetics of hydrolysis (unpublished observations).

In conclusion, naturally occurring type A, C, and D variants of *S. aureus* β-lactamase exhibit kinetic differences due to single amino acid differences at positions close to the active site which have not previously been shown to be involved in enzymatic activity. It is likely that the substitution at the amino acid 128 affects enzyme function by altering the structure of catalytically important S-D-N loop. The differences between the type A and type C enzyme could be due to steric hindrance to substrate binding and/or some structural stabilization effects. This has to be verified by kinetic studies with mutant enzymes in which amino acids 128 and 216 are substituted with different amino acids as well as molecular modelling studies with different β-lactam substrates.

ACKNOWLEDGMENTS

This work was supported by National Institutes of Health grant AI32126.

We are thankful to K. V. Radha Kishan for providing a ribbon diagram figure (Fig. 1) of *S. aureus* β-lactamase.

REFERENCES

1. **Ambler, R. P.** 1980. The structure of beta-lactamases. Philos. Trans. R. Soc. London B **289**:321–331.
2. **Ambler, R. P., A. F. W. Coulson, J. M. Frère, J. M. Ghuysen, B. Joris, M. Forsman, R. C. Levesque, G. Tiraby, and S. G. Waley.** 1991. A standard numbering scheme for the class A beta-lactamases. Biochem. J. **276**:269–270.
3. **Bonfiglio, G., and D. M. Livermore.** 1994. Beta-lactamase types amongst *Staphylococcus aureus* isolates in relation to susceptibility to beta-lactamase inhibitor combinations. J. Antimicrob. Chemother. **33**:465–481.
4. **Bush, K., G. A. Jacoby, and A. A. Medeiros.** 1995. A functional classification scheme for β-lactamases and its correlation with molecular structure. Antimicrob. Agents Chemother. **39**:1211–1233.
5. **Chan, P. T.** 1986. Nucleotide sequence of the *Staphylococcus aureus* PC1 beta-lactamase gene. Nucleic Acids Res. **14**:5940.
6. **Chang, S., and S. N. Cohen.** 1979. High frequency transformation of *Bacillus subtilis* protoplasts by plasmid DNA. Mol. Gen. Genet. **168**:111–115.
7. **Delaire, M., R. Labia, J. P. Samama, and J. M. Masson.** 1992. Site-directed mutagenesis at the active site of *Escherichia coli* TEM-1 beta-lactamase. Suicide inhibitor-resistant mutants reveal the role of arginine 244 and methionine 69 in catalysis. J. Biol. Chem. **267**:20600–20606.
8. **East, A. K., S. P. Curnock, and K. G. H. Dyke.** 1990. Change of a single amino acid in the leader peptide of a staphylococcal beta-lactamase prevents the appearance of the enzyme in the medium. FEMS Microbiol. Lett. **69**: 249–254.
9. **East, A. K., and K. G. H. Dyke.** 1989. Cloning and sequence determination of six *Staphylococcus aureus* beta-lactamases and their expression in *Escherichia coli* and *Staphylococcus aureus*. J. Gen. Microbiol. **135**:1001–1015.
10. **Galletto, D. W., J. L. Johnston, and G. L. Archer.** 1987. Molecular epidemiology of trimethoprim resistance among coagulase-negative staphylococci. Antimicrob. Agents Chemother. **31**:1683–1688.
11. **Herzberg, O.** 1991. Refined crystal structure of beta-lactamase from *Staphylococcus aureus* PC1 at 2.0 Å resolution. J. Mol. Biol. **217**:701–719.
12. **Herzberg, O., and J. Moult.** 1987. Bacterial resistance to beta-lactam antibiotics: crystal structure of beta-lactamase from *Staphylococcus aureus* PC1 at 2.5 Å resolution. Science **236**:694–701.
13. **Horinouchi, S., and B. Weisblum.** 1982. Nucleotide sequence and functional map of pE194, a plasmid that specifies inducible resistance to macrolide, lincosamide, and streptogramin type B antibodies. J. Bacteriol. **150**:804–814.
14. **Huletskly, A., J. R. Knox, and R. C. Levesque.** 1993. Role of Ser-238 and Lys-240 in the hydrolysis of third-generation cephalosporins by SHV-type beta-lactamases probed by site-directed mutagenesis and three-dimensional modeling. J. Biol. Chem. **268**:3690–3697.
15. **Imitiaz, U., E. Billings, J. R. Knox, E. K. Manavanthu, S. A. Lerner, and S. Mobashery.** 1993. Inactivation of class A β-lactamases by clavulanic acid: the role of arginine-244 in a proposed nonconcerted sequence of events. J. Am. Chem. Soc. **115**:4435–4442.
16. **Jacob, F., B. Joris, S. Lepage, J. Dusart, and J. M. Frère.** 1990. Role of the conserved amino acids of the "SDN' loop (Ser130, Asp131 and Asn132) in a class A beta-lactamase studied by site-directed mutagenesis. Biochem J. **271**:399–406.
17. **Jacoby, G. A., and A. A. Medeiros.** 1991. More extended-spectrum β-lactamases. Antimicrob. Agents Chemother. **35**:1697–1704.
18. **Johnston, L. H., and K. G. H. Dyke.** 1971. Stability of penicillinase plasmids in *Staphylococcus aureus*. J. Bacteriol. **107**:68–73.
19. **Kernodle, D. S., P. A. McGraw, C. W. Stratton, and A. B. Kaiser.** 1990. Use of extracts versus whole-cell bacterial suspensions in the identification of *Staphylococcus aureus* β-lactamase variants. Antimicrob. Agents Chemother. **34**:420–425.
20. **Kernodle, D. S., C. W. Stratton, L. W. McMurray, J. R. Chipley, and P. A.**

McGraw. 1989. Differentiation of beta-lactamase variants of *Staphylococcus aureus* by substrate hydrolysis profiles. J. Infect. Dis. **159**:103–108.
21. **Kernodle, D. S., D. J. Zygmunt, P. A. McGraw, and J. R. Chipley.** 1990. Purification of *Staphylococcus aureus* β-lactamases by using sequential cation-exchange and affinity chromatography. Antimicrob. Agents Chemother. **34**:2177–2183.
22. **Kraulis, P. J.** 1991. MOLSCRIPT: a program to produce both detailed and schematic plots of protein structure. J. Appl. Crystallogr. **24**:946–950.
23. **Kunkel, T. A.** 1985. Rapid and efficient site-specific mutagenesis without phenotypic selection. Proc. Natl. Acad. Sci. USA **82**:488–492.
24. **Kunkel, T. A., J. D. Roberts, and R. A. Zakour.** 1987. Rapid and efficient site-specific mutagenesis without phenotypic selection. Methods Enzymol. **154**:367–382.
25. **Lacey, R. W., and J. Grinsted.** 1972. Linkage of fusidic acid resistance to the penicillinase plasmid in *Staphylococcus aureus*. J. Gen. Microbiol. **73**:501–508.
26. **Maniatis, T., E. F. Fritsch, and J. Sambrook.** 1989. Molecular cloning: a laboratory manual, 2nd ed. Cold Spring Harbor Laboratory, Cold Spring Harbor, N.Y.
27. **Medeiros, A. A.** 1984. Beta-lactamases. Br. Med. Bull. **40**:18–27.
28. **Miller, S., J. Janin, A. M. Lesk, and C. Chotia.** 1987. Interior and surface of monomeric proteins. J. Mol. Biol. **196**:641–656.
29. **Novick, R. P.** 1963. Analysis by transduction of mutations affecting penicillinase formation in *Staphylococcus aureus*. J. Gen. Microbiol. **33**:121–136.
30. **Osuna, J., H. Viadiu, A. L. Fink, and X. Soberón.** 1995. Substitution of Asp for Asn at position 132 in the active site of TEM beta-lactamase. Activity toward different substrates and effects of neighboring residues. J. Biol. Chem. **270**:775–780.
31. **Paul, G. C., A. B. Gerbaud, A. M. Philippon, B. Pangon, and P. Courvalin.** 1989. TEM-4, a new plasmid-mediated β-lactamase that hydrolyzes broad-spectrum cephalosporins in a clinical isolate of *Escherichia coli*. Antimicrob. Agents Chemother. **33**:1958–1963.
32. **Petit, A., D. L. Sirot, J. L. Chanal, R. L. Sirot, G. Gerbaud, and R. A. Cluzel.** 1989. Molecular epidemiology of TEM-3 (CTX-1) β-lactamase. Antimicrob. Agents Chemother. **32**:626–630.
33. **Richardson, J. S., and D. C. Richardson.** 1989. *In* Gerald D. Fasman (ed.), Prediction of protein structure and principles of protein conformation, p. 64. Plenum Press, New York.
34. **Richmond, M. H.** 1965. Wild type variants of exopenicillinase from *Staphylococcus aureus*. Biochem. J. **88**:452–459.
35. **Rosdahl, V. T.** 1973. Naturally occurring constitutive β-lactamase with novel serotype in *Staphylococcus aureus*. J. Gen. Microbiol. **77**:229–231.
36. **Rosdahl, V. T.** 1986. Penicillinase production in Staphylococcus aureus strains of clinical importance. Dan. Med. Bull. **33**:175–184.
37. **Ross, G. W., K. V. Chanter, A. M. Harris, S. M. Kirby, M. J. Marshall, and C. H. O'Callaghan.** 1974. Comparison of assay techniques for beta-lactamase activity. Anal. Biochem. **54**:9–16.
38. **Sanger, F., S. Nicklen, and A. R. Coulson.** 1977. DNA sequencing with chain-terminating inhibitors. Proc. Natl. Acad. Sci. USA **74**:5463–5467.
39. **Waley, S. G.** 1974. A spectrophotometric assay of beta-lactamase action on penicillins. Biochem. J. **139**:789–790.
40. **Wang, P., and R. P. Novick.** 1987. Nucleotide sequence and expression of the β-lactamase gene from *Staphylococcus aureus* plasmid pI258 in *Escherichia coli*, *Bacillus subtilis*, and *Staphylococcus aureus*. J. Bacteriol. **169**:1763–1766.
41. **Wong, J. T.** 1985. Kinetics of enzyme mechanisms. Academic Press, Inc., New York.
42. **Yanisch-Perron, C., J. Vieira, and J. Messing.** 1985. Improved M13 phage cloning vectors and host strains: nucleotide sequences of the M13mp18 and pUC19 vectors. Gene **33**:103–119.
43. **Zygmunt, D. J., C. W. Stratton, and D. S. Kernodle.** 1992. Characterization of four β-lactamases produced by *Staphylococcus aureus*. Antimicrob. Agents Chemother. **36**:440–445.

Proc. Natl. Acad. Sci. USA
Vol. 94, pp. 4504–4509, April 1997
Evolution

Directed evolution of a fucosidase from a galactosidase by DNA shuffling and screening

JI-HU ZHANG*, GLENN DAWES†, AND WILLEM P. C. STEMMER*‡

*Maxygen, Inc., and †Affymax Research Institute, 3410 Central Expressway, Santa Clara, CA 95051

Communicated by Charles Yanofsky, Stanford University, Stanford, CA, February 26, 1997 (received for review December 26, 1996)

ABSTRACT **An efficient β-fucosidase was evolved by DNA shuffling from the *Escherichia coli lacZ* β-galactosidase. Seven rounds of DNA shuffling and colony screening on chromogenic fucose substrates were performed, using 10,000 colonies per round. Compared with native β-galactosidase, the evolved enzyme purified from cells from the final round showed a 1,000-fold increased substrate specificity for *o*-nitrophenyl fucopyranoside versus *o*-nitrophenyl galactopyranoside and a 300-fold increased substrate specificity for *p*-nitrophenyl fucopyranoside versus *p*-nitrophenyl galactopyranoside. The evolved cell line showed a 66-fold increase in *p*-nitrophenyl fucosidase specific activity. The evolved fucosidase has a 10- to 20-fold increased k_{cat}/K_m for the fucose substrates compared with the native enzyme. The DNA sequence of the evolved fucosidase gene showed 13 base changes, resulting in six amino acid changes from the native enzyme. This effort shows that the library size that is required to obtain significant enhancements in specificity and activity by reiterative DNA shuffling and screening, even for an enzyme of 109 kDa, is within range of existing high-throughput technology. Reiterative generation of libraries and stepwise accumulation of improvements based on addition of beneficial mutations appears to be a promising alternative to rational design.**

Proteins and enzymes with novel functions and properties can be obtained either by searching the largely unknown natural species or by improving upon currently known natural proteins or enzymes. The latter approach may be more suitable for creating properties for which natural evolutionary processes are unlikely to have been selected.

One promising strategy to create such novel properties is by directed molecular evolution. Starting with known natural protein(s), multiple rounds of mutagenesis, functional screening, and amplification can be carried out. When the mutation rate, library size, and selection pressures are properly balanced, the desired phenotype of a protein generally increases with each round (1–8). The advantage of such a process is that it can be used to rapidly evolve any protein, without any knowledge of its structure.

A number of different mutagenesis strategies exist, such as oligonucleotide cassette mutagenesis, point mutagenesis by error-prone PCR or the use of mutator strains, as well as DNA shuffling (1–5, 8). A theoretical approach to choosing a preferred mutagenesis strategy would be to determine the target protein's fitness landscape (9), which is a plot of fitness (on the *y* axis) versus sequence space (on the *x* axis). However, because the sequence space of an average protein of 500 amino acids is 20^{500}, determination of even a fraction of the fitness landscape is a nearly impossible and impractical undertaking. Because there are just a few fundamental ways to search sequence space, it may be informative to compare the performance of these methods for specific model systems.

Natural genes are thought to have evolved by mutation and recombination within a population of diverse, but highly related, sequences. We suggest that a search algorithm similar to that which slowly created the fitness landscape of a natural protein in the first place is likely to also be the preferred method for further searching this natural sequence landscape (5, 10). This approach is supported by our demonstration of the advantage of recombining mutations (over introduction of point mutations alone) for increasing the activity of a natural β-lactamase protein (2). However, recombination may not always be the best search algorithm. For searching the fitness landscapes of nonnatural sequences under unusual conditions, it is conceivable that a different approach may be more optimal.

We obtain *in vitro* recombination of infrequent point mutations by a PCR-based technique called DNA shuffling (1–5). A pool of closely related sequences is fragmented randomly, and these fragments are reassembled into full-length genes via self-priming PCR and extension in a process we call reassembly PCR (4). This process yields crossovers between related sequences due to template switching. Shuffling allows rapid combination of positive-acting mutations and simultaneously flushes out negative-acting mutations from the sequence pool (Fig. 1). When coupled with effective selection and applied reiteratively, such that the output of one cycle is the input for the next cycle, reiterative DNA shuffling has been demonstrated to be an efficient process for directed molecular evolution (1–3).

In our previous shuffling studies we used selection and/or large libraries (1, 2). Our primary goal in this work was to determine whether detection by screening of libraries of 10,000 clones, a number that is within range of any high throughput screening procedure, would be sufficient to obtain significant enhancement of a minor activity of β-galactosidase, a highly specific and complex enzyme, and at 109 kDa, one of the largest single-chain proteins in *Escherichia coli*. If screening would detect significant improvement, we then would establish that improvements are obtainable by evolution with such small libraries.

E. coli β-galactosidase, encoded by *lacZ* (11), is widely used, and its biological function, catalytic mechanism, and molecular structures are well characterized (11–15). It is a tetramer of identical subunits of 1,023 amino acids (13, 16, 17). The crystal structure of β-galactosidase is solved and shows that each subunit forms five structural domains (14). Each active site resides mainly in one subunit, but part of another subunit also is involved (14). The native enzyme hydrolyzes β-galactosyl linkages, such as the β(1, 4)-linkage in its natural disaccharide

The publication costs of this article were defrayed in part by page charge payment. This article must therefore be hereby marked "*advertisement*" in accordance with 18 U.S.C. §1734 solely to indicate this fact.

0027-8424/97/944504-6$2.00/0
PNAS is available online at http://www.pnas.org.

Abbreviations: ONPG, *o*-nitrophenyl β-D-galactopyranoside; ONPF, *o*-nitrophenyl β-D-fucopyranoside; PNPG, *p*-nitrophenyl β-D-galactopyranoside; PNPF, *p*-nitrophenyl β-D-fucopyranoside; X-Fuc, 5-bromo-4-chloro-3-indolyl β-D-fucopyranoside.

‡To whom reprint requests should be addressed. e-mail: maxygen@maxygen.com.

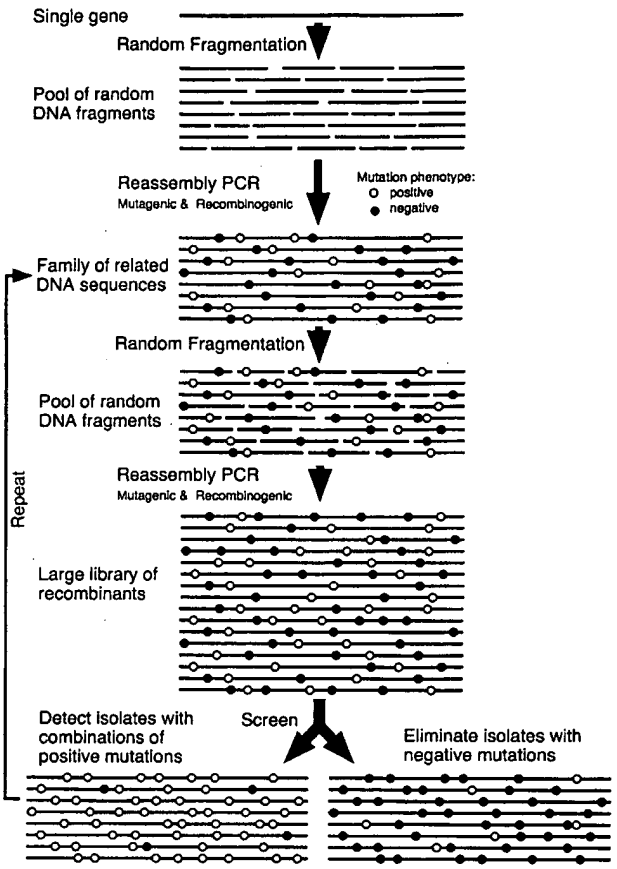

FIG. 1. Schematic illustration of the DNA shuffling process used in the present study.

substrate, lactose. The native β-galactosidase is known to be highly specific for β-D-galactosyl substrates. A multistep model of the reaction was proposed (18, 19) based on kinetic studies of the native enzyme for *o*-nitrophenyl β-D-galactopyranoside (ONPG), *p*-nitrophenyl β-D-galactopyranoside (PNPG), and other substrates and substrate analogs. The native β-galactosidase acts only weakly on β-D-fucosyl moieties (18–20) and does not act on most substrate analogs.

MATERIALS AND METHODS

E. coli β-galactosidase (EC 3.2.1.23) and the galactosyl and fucosyl substrates 5-bromo-4-chloro-3-indolyl β-galactopyranoside (X-Gal), PNPG, ONPG, 5-bromo-4-chloro-3-indolyl β-D-fucopyranoside (X-Fuc), *p*-nitrophenyl β-D-fucopyranoside (PNPF), and *o*-nitrophenyl β-D-fucopyranoside (ONPF) were purchased from Sigma. Plasmid pCH110 containing a *lacZ* gene was from Pharmacia. *E. coli* strain TB1 was a gift from Charles Roessner of Texas A&M University.

Construction of Plasmid p18lacZ. A 3.8-kb *Hin*dIII and *Bam*HI restriction nuclease fragment from pCH110 containing a *lacZ* gene (codon 8 fused to a short N-terminal peptide) and the *gpt* promoter region (21) was subcloned into the *Hin*dIII and *Bam*HI sites of vector p18-sfi-kan-sfi vector, a 2.3-kb pUC18 derivative in which the ampicillin gene is replaced by a kanamycin phosphotransferase gene (2). The resulting plasmid, named p18lacZ, was used for DNA shuffling. DNA fragments of 50–200 bp were used and reassembled as described previously (1, 2). The PCR primers for amplification of the reassembled genes were AGCGCCCAATACGCAAACCGCCTCTCCCCGCGCGTTGGCC (forward) and CTATGCGGCATCAGAGCAGATTGTACTGAGAGTGCACCAT (reverse), located on either side of the *Bam*HI and *Hin*dIII fragment. The reassembled gene was digested with restriction enzymes *Hin*dIII and *Bam*HI and ligated back into the P18-sfi-kan-sfi vector. The ligation mixture was electroporated into *E. coli* TB1 competent cells and plated out on Luria–Bertani plates (150 mm) with 40 μg/ml kanamycin and 2 mg/plate of the X-Fuc substrate (22). The plates were incubated 12 to 24 hr at 37°C. The resulting kanamycin-resistant transformants were visually screened for the intensity of the blue color. The 20–40 colonies with the most intense blue color were picked from about 10,000 transformants of each round and used for the next round of DNA shuffling. Seven rounds of DNA shuffling and screening were carried out. The best clone from the final screening round, called evolved β-fucosidase, was characterized in detail.

Enzyme Purification. For purification of the native β-galactosidase and the evolved β-fucosidase, a histidine tag (His_6) was fused to the N terminus of both enzymes by PCR with two primers [5′-(P)CATCACCATCACCACCATATCGTCACCTGGGACATGT and 5′-(P)GTATTTTTCGCTCATGTGAA] in a standard PCR. The histidine-tagged native and evolved enzymes were purified from overnight TB1 cell cultures harboring the corresponding plasmid (23). The crude cell extract, in 50 mM phosphate (pH 7.0) with 100 mM NaCl and 0.2 mM of phenylmethylsulfonyl fluoride protease inhibitor was passed through a 20-ml Ni-nitrilotriacetic acid agarose (Qiagen) column. The bound protein was stepwise-eluted with the same buffer containing 5 mM, 10 mM, 25 mM, and 100 mM imidazole. The active fractions from the metal affinity column were desalted and loaded on a DEAE column in 20 mM Tris (pH 7.5), followed by elution with a 0 to 1 M NaCl gradient. The active fractions were concentrated and loaded on a Superose 12 gel filtration column in an FPLC protein purification unit (Pharmacia). SDS/PAGE analysis (data not shown) showed that the native galactosidase and the evolved fucosidase were greater than 90% pure.

Enzyme Kinetics. β-Galactosidase activity was assayed using the synthetic chromogenic substrates ONPG and PNPG. β-Fucosidase activity was assayed using chromogenic fucosyl substrates ONPF and PNPF. Enzyme assays were performed at 25°C and pH 7.0 in 30 mM *N*-tris(hydroxymethyl)methylaminoethanesulfonic acid with 1 mM $MgCl_2$ and 150 mM NaCl. The absorbance change at 420 nm was recorded with time, and product formation was quantitated using the absorption extinction coefficient (2.65 $mM^{-1}\cdot cm^{-1}$ for *o*-nitrophenol and 6.7 $mM^{-1}\cdot cm^{-1}$ for *p*-nitrophenol). For kinetic parameter measurements, the initial velocity V_0 (when less than 10% of the substrate was converted into product) was determined with varied substrate concentrations. The values of V_{max} and K_m were calculated using the simple weighting method of Cornish-Bowden (24). The V_{max} values were converted to k_{cat} values, the turnover number per active site, by normalizing for the enzyme concentrations by the molecular mass of the monomer. The K_m and k_{cat} values of the wild-type β-galactosidase for ONPF could not be determined directly because of the low activity on this substrate. The k_{cat}/K_m value had to be estimated from the enzyme dilution factor required for the native enzyme to generate the same amount of *o*-nitrophenol product from ONPG after the same period of time (usually several hours) and from the k_{cat}/K_m value of the wild-type enzyme on ONPG.

Sequencing of the Evolved *lacZ* Gene. The 3.8-kb DNA fragment encoding the evolved β-galactosidase and its flanking regions was sequenced in both forward and reverse directions with 20 primers using an Applied Biosystems 391 DNA sequencer.

RESULTS AND DISCUSSION

Strategy for Evolving β-Galactosidase. The primary goal of the experiment was to determine if a substantial enhancement

in the specificity and/or activity of a large model enzyme could be obtained by reiterative screening of libraries of a size (10,000 clones) that is routinely accessible by high throughput detection assays. No structural information was used in the design of the experiment, but the structure of β-galactosidase is useful for interpretation of results.

Screening for Improved Fucosidase Activity. The 3.8-kb DNA fragment of p18LacZ containing the *lacZ* gene was shuffled as described previously (1–3), and the reassembled genes were digested with restriction enzymes (*Hin*dIII and *Bam*HI) and ligated back into the vector p18-sfi-kan-sfi. The initial diversity was introduced into the native *lacZ* gene by random point mutagenesis, which occurs by shuffling of small fragments (1, 2). We previously showed that shuffling with 10- to 50-bp fragments resulted in a 0.7% rate of point mutation. Here we used fragments of 50 to 200 bp, which results in a much lower rate of point mutation, resulting in inactivation of approximately 20% of the clones. X-Fuc was chosen as the indicator substrate for the plate assay because of the nondiffusable nature of the colored product and the high sensitivity (22). After each round of DNA shuffling, 10,000 kanamycin-resistant transformants, growing on plates supplemented with X-Fuc, were visually screened for enhanced blue color formation. About 2–5% of the transformant colonies in each round showed colonies that were more highly blue-colored than the bulk of the population. The 20–40 bluest colonies (0.2–0.4%) were picked at each round, individually verified to be more active than the pool from the previous round by plate assays, and then used as a pool for the source of DNA to initiate the next round of DNA shuffling. This number of colonies was chosen as a compromise between obtaining too little diversity (<10 colonies) and obtaining suboptimal selection pressure (≫100 colonies), which could limit the rate of improvement. In the seventh round of DNA shuffling some colonies developed a deep blue color after overnight growth (Fig. 2). One mutant from this seventh and final round of shuffling showed a 66-fold increase in fucosidase activity on 1 mM PNPF (Fig. 3).

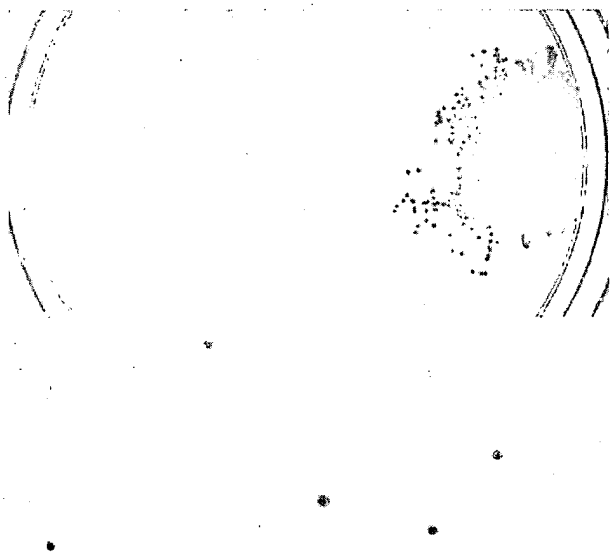

FIG. 2. *E. coli* TB1 cells expressing the native β-galactosidase (white colonies, *Upper Left*) and the evolved fucosidase of the seventh round (blue colonies, *Upper Right*) after overnight growth on an Luria–Bertani plus kanamycin plate supplemented with 0.1 mM X-Fuc. (*Lower*) The results of plating a deliberate mixture of the two types of colonies.

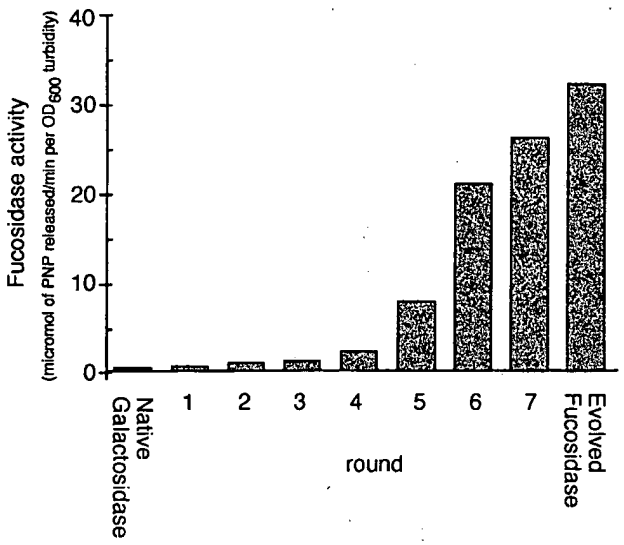

FIG. 3. Whole cell fucosidase activity on PNPF of the pool of colonies selected after each round of DNA shuffling. Rounds 1–7 are pools of colonies. Also shown are the activity of cells expressing the native β-galactosidase and cells expressing the evolved β-fucosidase, both measured as whole cell activity of single clones. The evolved fucosidase is the single-best colony selected after quantitative comparison of the 24 best colonies from the pool of colonies obtained after shuffling round 7. For assay conditions, see *Materials and Methods*.

Kinetics. After the final round of selection, $(His)_6$ tags were added to the foreign N terminus of the native β-galactosidase and the evolved β-fucosidase enzymes. Both enzymes were purified, and the kinetic constants of each enzyme on the synthetic chromogenic substrates ONPG, ONPF, PNPG, and PNPF were determined (Table 1). For PNPF, the K_m value of the evolved fucosidase is decreased by 20-fold from the K_m of wild-type β-galactosidase on the same substrate. The k_{cat} value is decreased about 2-fold. The k_{cat}/K_m values thus are increased about 10-fold in the evolved β-fucosidase. The activity of the wild-type enzyme on ONPF was very low and accurate K_m and k_{cat} values could not be obtained. By comparing the relative reaction rates of the

Table 1. Kinetic constants for the native and evolved enzymes

Substrate	Kinetic constant	Native galactosidase	Evolved fucosidase
PNPG	k_{cat}, s^{-1}	268	30.9
	K_m, mM	0.04	0.18
	k_{cat}/K_m, $mM^{-1}\cdot s^{-1}$	6,700	172
PNPF	k_{cat}, s^{-1}	209	96.6
	K_m, mM	31	1.5
	k_{cat}/K_m, $mM^{-1}\cdot s^{-1}$	6.7	64.4
Specificity	$\frac{(k_{cat}/K_m)_{PNPG}}{(k_{cat}/K_m)_{PNPF}}$	1,000	2.7
ONPG	k_{cat}, s^{-1}	765	14.5
	K_m, mM	0.11	0.11
	k_{cat}/K_m, $mM^{-1}\cdot s^{-1}$	6,950	132
ONPF	k_{cat}, s^{-1}	—	24.1
	K_m, mM	—	0.55
	k_{cat}/K_m, $mM^{-1}\cdot s^{-1}$	(2)*	43.9
Specificity	$\frac{(k_{cat}/K_m)_{ONPG}}{(k_{cat}/K_m)_{ONPF}}$	3,200	3.0

The native galactosidase and the evolved fucosidase were purified, and the enzymes were assayed on four different substrates.

*The k_{cat}/K_m value for the native galactosidase on ONPF was estimated to be about 2 $mM^{-1}\cdot s^{-1}$ by measuring the hydrolysis rate relative to that of ONPG.

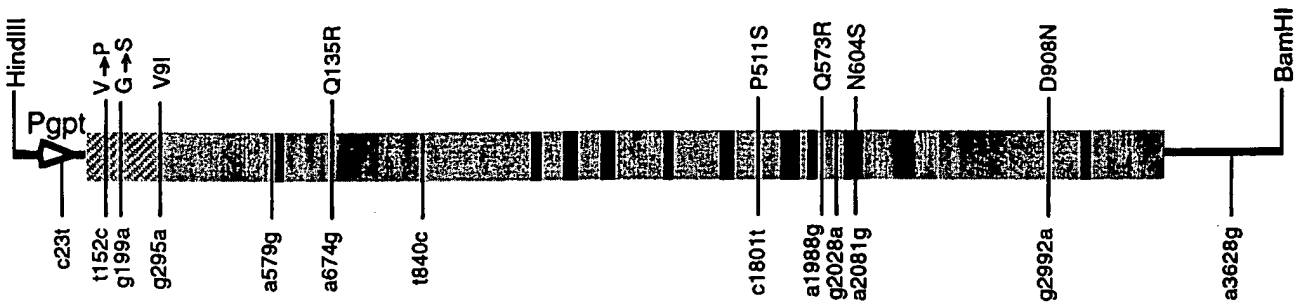

FIG. 4. Nucleotide substitutions in the evolved fucosidase gene. The predicted amino acid changes are shown above the gene by the single-letter denotation, numbered according to the wild-type β-galactosidase sequence (17). Amino acid changes in the N-terminally fused peptide region (hatched area) are indicated by small vertical arrows. Mutations that do not result in amino acid changes are shown below the gene, numbered starting at the *Hin*dIII site, as in the parental plasmid pCH110. The gpt promoter is indicated by a thick arrow. The positions of the known active site residues of the wild-type β-galactosidase are indicated by black bars.

wild-type enzyme on ONPF and ONPG (at the same enzyme and substrate concentrations), the k_{cat}/K_m for ONPF was estimated, assuming that the k_{cat}/K_m value is a second order rate constant. The k_{cat}/K_m values on ONPF were increased at least 20-fold in the evolved β-fucosidase. These increases in fucosidase activity were accompanied by decreases in galactosidase activity. For the substrates PNPG and ONPG, the k_{cat}/K_m is decreased 40-fold and 50-fold, respectively. These kinetic parameter changes suggest that the substrate binding pocket in the evolved β-fucosidase is different from that of the wild-type β-galactosidase.

The native enzyme is highly specific for hydrolyzing galactosyl rather than fucosyl substrates. The k_{cat}/K_m values we determined for PNPG and PNPF differ by about 1,000-fold, and for ONPG and ONPF the values differ by more than 3,000-fold (Table 1). The values we determined for the native β-galactosidase on ONPG, PNPG, and PNPF are in between the values reported previously (18, 20). The substrate specificity changed dramatically from the native β-galactosidase to the evolved β-fucosidase. For the evolved β-fucosidase the k_{cat}/K_m values for substrates PNPG and PNPF differ 2.7-fold and for substrates ONPG and ONPF the k_{cat}/K_m values differ 3-fold. Therefore, the relative substrate specificity for fucosyl substrates, from the native to the evolved enzyme, is increased 1,000-fold for the *o*-nitrophenyl substrates and 300-fold for the *p*-nitrophenyl substrates. The substrate specificity change was further supported by inhibition of the enzymatic activity by isopropyl β-D-thiogalactopyranoside, a β-galactosidase substrate analog and a competitive inhibitor of galactosyl substrates. The K_i values increased by one order of magnitude from the wild-type enzyme to the evolved β-fucosidase, from 0.1 mM to 0.9 mM. The changes in K_m values for the galactosyl substrates showed the same trend, because they either increased severalfold or stayed the same. These results imply that the substrate binding affinity of the evolved β-fucosidase is substantially increased for fucosyl substrates and decreased for galactosyl substrates, and hence the substrate binding pocket is likely to be significantly modified.

DNA Sequence. The DNA sequence of the evolved fucosidase gene showed 13 nucleotide substitutions of which 11 were in the coding region. Six of the mutations are predicted to cause amino acid changes in the translated β-galactosidase sequence. Two additional mutations are predicted to cause amino acid changes in the N-terminal fusion peptide (Fig. 4).

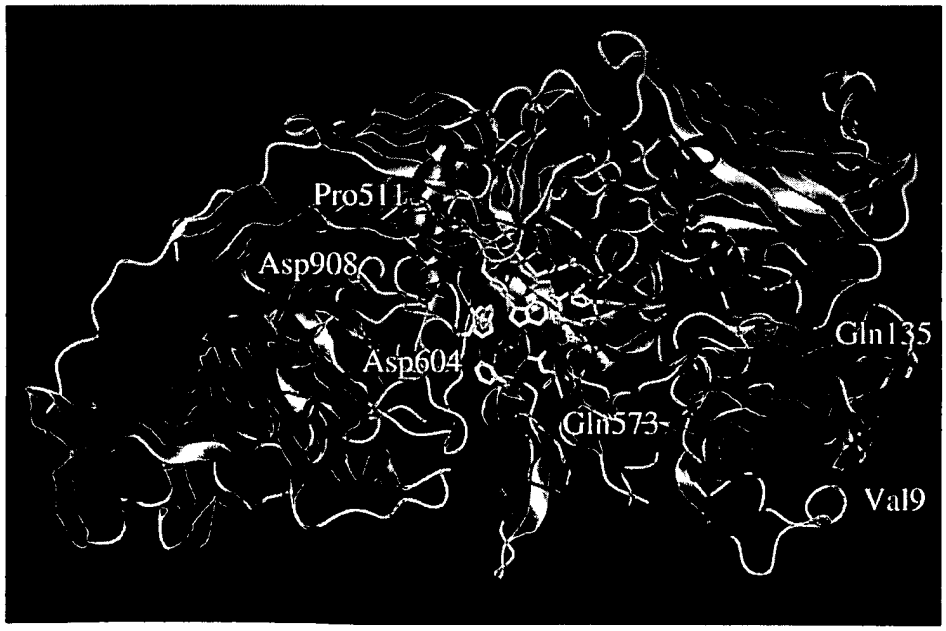

FIG. 5. Ribbon representation of the *E. coli* β-galactosidase subunit structure (14). The CNO atoms of the six amino acid mutations that conferred the fucosidase activity are shown with stick representation. Two mutations in the active site (Asp604 and Gln572) are shown in red. Two mutations in close proximity of the active site (Pro511 and Asp908) are shown in magenta. Two mutations far away from the active site and on the protein surface (Val9 and Gln135) are shown in green. The rest of the substrate binding and active site residues are shown in yellow.

All 13 nucleotide changes were base transitions between purines and/or between pyrimidines, which usually are more frequent than transversions.

One major advantage of *in vitro* evolution of enzymes over the structural modeling approach is that only minimal information is required for improving the desired phenotype. At each round of our experiment, only colonies with increased fucosidase activity were pooled and used for the next round of DNA shuffling and screening. Although both positive-acting mutations and neutral mutations may accumulate in the evolved fucosidase *lacZ* gene in each round, we expect that neutral mutations generally do not survive multiple rounds of shuffling and screening due to a backcrossing effect exerted by the consensus sequence (1, 2), combined with the lack of a selective advantage of the neutral mutations. Therefore, only mutations that somewhat contribute to the improved fucosidase activity are likely to accumulate in the evolved fucosidase. While we have not determined the effect of the separate mutations by site-specific mutational studies, we can predict what roles some of the mutations may play based on the three-dimensional structure of the parental β-galactosidase (ref. 14; Fig. 5) and the sophisticated kinetic models based on previous mutations and kinetic analysis of purified proteins (18, 20, 25, 26). Among the six amino acid changes in the β-galactosidase sequence, none appear directly involved in the inter-subunit contact. Three mutations (Pro511Ser, Gln573-Arg, and Asn604Ser) are located in domain 3 (residues 334–627) of the wild-type *E. coli* β-galactosidase (14). Domain 3 in the native protein contains most of the amino acids that form the substrate binding pocket (ref. 14; Fig. 5). Asn604 is one of the amino acids forming this substrate binding pocket in the protein (14), and this residue is conserved in several other known β-galactosidase sequences (25, 27–29), except the evolved galactosidase gene (*ebgA*) of *E. coli* (30). In our evolved fucosidase, Asn604 is replaced by Ser. This mutation presumably affects the enzyme's substrate specificity. All the other mutations found in the evolved β-fucosidase enzyme do not directly affect the active site and substrate binding pocket residues, and therefore they may have no effect or may only subtly change the conformation of the active site and substrate specificity. Gln573, substituted by Arg in the evolved fucosidase, is in close proximity to the substrate binding pocket (Fig. 5). The mutation Pro511Ser is also close to the active site and substrate binding pocket (Fig. 5). These two mutations are likely to affect the enzyme's active site. Asp908Asn is also close to the active site and may also affect the activity. Additional important catalytic residues of the active site, such as Glu461, Met502, Tyr503, and Glu537 (23, 26, 31), however, are unchanged in the evolved β-fucosidase, implying that the catalytic mechanism of the evolved enzyme remained the same. Therefore the evolved β-fucosidase seems to have only adjusted to fit the fucosyl substrate or its transition state better than the wild-type β-galactosidase does. In addition, one of the nucleotide mutations outside the structural gene (c23t) is very close to the gpt promoter region and could affect transcription (Fig. 4). This mutation, along with the two amino acid mutations in the N-terminal fusion peptide (Fig. 4), may influence the expression level of the protein. Indeed, we found that the evolved β-fucosidase enzyme was expressed at least 2- to 3-fold higher than the wild-type enzyme (data not shown). The mutations Val9Ile and Gln135Arg are far away from the active site and near the surface of the protein (Fig. 5), and may not have any significant effect on the enzymatic activity. The analysis of mutations obtained by molecular evolution of proteins provides a new tool for studying structure–function relationships. However, the real utility of DNA shuffling is the ability to rapidly improve enzyme functions without the need to delineate the myriads of complex molecular mechanisms.

There are several possible applications for the evolved β-fucosidase. One is as a novel reporter for β-D-fucosyl substrates, in addition to the widely used *lacZ* gene reporter. The advantage of using the novel enzyme is the low endogenous background of β-fucosidase activity because, unlike α-fucosidases, β-fucosidases are uncommon in nature. This well expressed fucosidase also could be used for the production of fucosyl adducts or for disaccharide synthesis by transglycosylation or reversal of the hydrolysis reactions, because analogous applications already have been demonstrated for the wild-type β-galactosidase (32, 33). Some of these applications may require further evolution of the fucosidase for the specific reaction. The present data suggests that it is reasonable to attempt to obtain such improvements by DNA shuffling and screening of libraries of modest size.

We thank A. Crameri for technical assistance and Drs. F. H. Arnold, R. E. Huber, and P. Schatz for useful discussions.

1. Stemmer, W. P. C. (1994) *Proc. Natl. Acad. Sci. USA* **91,** 10747–10751.
2. Stemmer, W. P. C. (1994) *Nature (London)* **370,** 389–391.
3. Crameri, A., Whitehorn, E. A., Tate, E. & Stemmer, W. P. C. (1996) *Nat. Biotechnol.* **14,** 315–319.
4. Stemmer, W. P. C. (1996) in *The Encyclopedia of Molecular Biology* (VCH, New York), pp. 447–457.
5. Stemmer, W. P. C. (1995) *Bio/Technology* **13,** 549–553.
6. You, L. & Arnold, F. H. (1995) *Protein Eng.* **9,** 77–83.
7. Chen, K. & Arnold, F. H. (1993) *Proc. Natl. Acad. Sci. USA* **90,** 5618–5622.
8. Moore, J. C. & Arnold, F. H. (1996) *Nat. Biotechnol.* **14,** 458–467.
9. Kauffman, S. A. (1993) *The Origins of Order* (Oxford Univ. Press, New York).
10. Stemmer, W. P. C. (1995) *Science* **270,** 1510.
11. Beckwith, J. (1996) in *Escherichia coli and Salmonella*, ed., Neidhardt, F. (Am. Soc. Microbiol., Washington, DC), pp. 1227–1231.
12. Zabin, I. & Fowler, A. V. (1980) in *The Operon*, eds. Miller, J. H. & Reznikoff, W. S. (Cold Spring Harbor Lab. Press, Plainview, NY), pp. 89–122.
13. Wallenfels, K. & Weil, R. (1972) in *The Enzymes*, ed. Boyer, P. D. (Academic, New York), pp. 618–663.
14. Jacobson, R. E., Zhang, X.-J., DuBose, R. F. & Matthews, B. W. (1994) *Nature (London)* **369,** 761–766.
15. Huber, R. E., Gupta, M. N. & Khare, S. K. (1994) *Int. J. Biochem.* **26,** 309–318.
16. Fowler, A. & Zabin, I. (1978) *J. Biol. Chem.* **253,** 5521–5525.
17. Kalnins, A., Otto, K., Ruther, U. & Muller-Hill, B. (1983) *EMBO J.* **2,** 593–597.
18. Roth, N. J. & Huber, R. E. (1996) *J. Biol. Chem.* **271,** 14296–14301.
19. Huber, R. E. & Gaunt, M. T. (1983) *Arch. Biochem. Biophys.* **220,** 263–271.
20. Wallenfels, K., Lehmann, J. & Malhotra, O. P. (1960) *Biochem. Z.* **333,** 209–215.
21. Hall, C. V., Jacob, P. E., Ringold, G. M. & Lee, F. (1983) *J. Mol. Appl. Genet.* **2,** 101–109.
22. Sambrook, J., Fritsch, E. F. & Maniatis, T. (1989) *Molecular Cloning: A Laboratory Manual* (Cold Spring Harbor Lab. Press, Plainview, NY), 2nd Ed.
23. Cupples, C. G., Miller, J. H. & Huber, R. E. (1990) *J. Biol. Chem.* **265,** 5512–5518.
24. Cornish-Bowden, A. (1976) *Principles of Enzyme Kinetics* (Butterworth, London), pp. 168–189.
25. Buvinger, W. E. & Riley, M. (1985) *J. Bact.* **163,** 850–857.
26. Gebler, J. C., Aebersold, R. & Withers, S. G. (1992) *J. Biol. Chem.* **267,** 11126–11130.
27. Schroeder, C. J., Robert, C., Lenzen, G., McKay, L. L. & Mercenier, A. (1991) *J. Gen. Microbiol.* **137,** 369–380.

28. Schmidt, B. F., Adams, R. M., Requadt, C., Power, S. & Mainzer, S. E. (1989) *J. Bacteriol.* **171**, 625–635.
29. Hancock, K. R., Rockman, E., Young, C. A., Pearce, L., Maddox, I. S. & Scott, D. B. (1991) *J. Bacteriol.* **173**, 3084–3095.
30. Stokes, H. W., Betts, P. W. & Hall, B. G. (1985) *Mol. Biol. Evol.* **2**, 469–477.
31. Ring, M. & Huber, R. E. (1990) *Arch. Biochem. Biophys.* **283**, 342–350.
32. Hedbys, L., Larsson, P. O., Mosbach K. & Svensson, S. (1984) *Biochem. Biophys. Res. Commun.* **123**, 8–15.
33. Huber, R. E. & Hurlburt, K. L. (1986) *Arch. Biochem. Biophys.* **246**, 411–418.

Complementary DNA Coding Click Beetle Luciferases Can Elicit Bioluminescence of Different Colors

KEITH V. WOOD,* Y. AMY LAM, HOWARD H. SELIGER, WILLIAM D. MCELROY

Eleven complementary DNA (cDNA) clones were generated from messenger RNA isolated from abdominal light organs of the bioluminescent click beetle, *Pyrophorus plagiophthalamus*. When expressed in *Escherichia coli*, these clones can elicit bioluminescence that is readily visible. The clones code for luciferases of four types, distinguished by the colors of bioluminescence they catalyze: green (546 nanometers), yellow-green (560 nanometers), yellow (578 nanometers), and orange (593 nanometers). The amino acid sequences of the different luciferases are 95 to 99 percent identical with each other, but are only 48 percent identical with the sequence of firefly luciferase (*Photinus pyralis*). Because of the different colors, these clones may be useful in experiments in which multiple reporter genes are needed.

NEARLY ALL OUR KNOWLEDGE OF beetle luciferases is derived from studies of a single species, the North American firefly *Photinus pyralis*. Comparative studies with other beetle luciferases have been hampered because of limited availability of the other species. Evolutionarily, beetle luciferases are unrelated to any of the other groups of luciferases that have been studied biochemically (*1*). Little is known about the luciferases from other beetles except that they all catalyze the production of various colors of light through the oxidative decarboxylation of beetle luciferin (*2*). Since the substrates of the luminescent reaction are the same in all these beetles, the different colors must be due to differences in the structure of the enzymes (*3*).

Recently we cloned a cDNA that codes for the luciferase of *P. pyralis*, and have shown that it can be used to express bioluminescence in *Escherichia coli*. We report here the cloning of cDNAs that code for several new luciferases from a bioluminescent click beetle, *Pyrophorus plagiophthalamus*. This beetle is unusual because it can emit bioluminescence of a wide range of colors from a single species. The expression products in *E. coli* of the cDNAs derived from this beetle are able to produce green, yellow-green, yellow, and orange light. As determined from the nucleotide sequences of the clones, the amino acid sequences of these click beetle luciferases are highly conserved among one another, but diverge from the sequence of the firefly luciferase. Taxonomy indicates that the click beetle luciferases probably are the most evolutionarily distant of the beetle luciferases from the firefly luciferase (*4*). This distance is reflected by differences in their chemical properties.

Pyrophorus plagiophthalamus is a large beetle with two sets of light organs. One set, on the dorsal surface of the head, emits light that is greenish but the exact color varies between individual beetles of the species, ranging from green (548 nm) to yellow-green (565 nm). The other set, at the anterior of the abdomen, generally emits light of a longer wavelength than the head organs but also varies between individuals ranging from green (547 nm) to orange (594 nm) (*5*). We converted mRNA isolated from the abdominal light organ of 60 beetles to cDNA and inserted this into a specialized lambda cloning vector, Lambda ZAP (*6*). The ability to convert this modified lambda vector into a bacterial expression plasmid (Bluescript) through an in vivo process allowed us to screen the cDNA library by two methods (*7*). In the phage form of the library, we screened with antibody to firefly luciferase that cross-reacts with the click beetle luciferases (*8*) and isolated four full-length clones that expressed bioluminescence in *E. coli*. A portion of the cDNA library was converted into the plasmid form, and we screened this for bioluminescence in the bacterial colonies. Bioluminescence can be initiated in colonies of *E. coli* expressing luciferase by adding luciferin to the media (*9*). Seven more cDNA clones were isolated by this method. It was determined visually that of the eleven clones, one produced green light, one produced yellow-green light, six produced yellow light, and three produced orange light.

Immunoblot analysis confirmed the production of full-length click beetle luciferase in *E. coli*. Despite some of these clones being detected with antibody to firefly luciferase during the library screening of plaques, we could not detect the gene products in blots made directly with *E. coli* lysates. The expression of bioluminescence was improved by transferring the cDNA clones into a plasmid vector incorporating the *tac* promoter (*10*). A lysate from *E. coli* expressing the green-emitting luciferase from this vector was partially purified. After gel electrophoresis and blotting, a single antigenic band was revealed that comigrated with the native click beetle luciferase. Subsequently one cDNA clone from each of the four color-emitting groups was sequenced. An open reading frame was revealed in each that could potentially code a protein, the sequence of which correlated with the entire length of the sequence for firefly luciferase. Thus the complete protein coding regions of the click beetle luciferases were apparently contained within their cDNA clones.

Expression of bioluminescence from the *tac* vector yielded sufficient intensity, upon addition of luciferin to the media, to allow measurement of the spectral distribution from intact cells (Fig. 1). This confirmed the visual assignment of the 11 cDNA clones into four color groups. For each of the four colors, the bioluminescence spectrum is a single peak qualitatively similar to the spectra of the native click beetle luciferases (*3*). The range of colors from the clones is representative of the full range measured from the abdominal light organs of living beetles. However, there are colors emitted by the beetles, within the extremes of this range, that do not correspond to any of the clones (*5*). Thus other luciferase genes may not have been isolated. Spectra of the luciferases were also measured from partially purified preparations obtained from lysates of the *E. coli* expressing the cDNA clones.

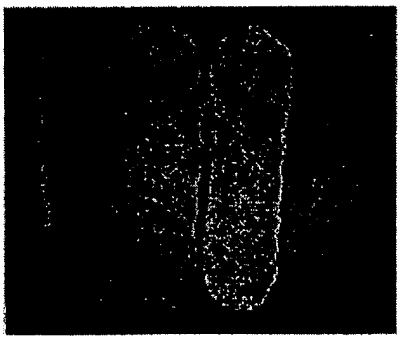

Fig. 1. Bioluminescence from colonies of *E. coli* expressing the click beetle luciferases. Four streaks of *E. coli*, each consisting of hundreds of colonies, show the four colors of bioluminescence emitted by the different luciferases. The colonies were grown on nitrocellulose filters layered on top of nutrient agar. To initiate the bioluminescent reaction, the filters were removed from the agar and soaked with 1 m*M* luciferin in 100 m*M* sodium citrate, *p*H 5.0. The photograph was produced from a 2-s contact exposure of the colonies onto Ektachrome 64.

K. V. Wood, Y. A. Lam, W. D. McElroy, Department of Chemistry, M-001, University of California, San Diego, La Jolla, CA 92093.
H. H. Seliger, Department of Biology, Johns Hopkins University, Baltimore, MD 21218.

*To whom correspondence should be addressed.

Between pH 6 to 7, the spectra of these preparations were indistinguishable from those of intact cells. At pH 8 there was a slight broadening of the spectra for the green- and yellow-emitting luciferases. The firefly luciferase shows a large spectral shift between pH 6 to 8. At pH 8 its spectral maximum is at 560 nm, which shifts to 615 nm (red) at pH 6 with a decrease in the quantum yield (*11*).

The sequences of the different click beetle luciferases are highly similar (Fig. 2). The open reading frame of each of the sequenced cDNA clones potentially codes a 543-residue polypeptide. Comparisons of the derived amino acid sequences show a 95 to 99% identity between the different color-emitting luciferases. Thus the number of amino acids that are responsible for the differences in the color is small. Because variation in color results directly from differences in the primary structures of the luciferases, specialized posttranslational modifications or unusual microenvironmental effects are not necessary to account for the color variation in the living beetles.

Comparison of the sequences of click beetle luciferases with that of firefly luciferase shows a low similarity. Alignment of their deduced amino acid sequences reveals that the various click beetle and the firefly luciferases are 48% identical (Fig. 3). Six gaps in the alignment of one to two amino acids in length account for most of a seven–amino acid difference in the lengths of the open reading frames between the firefly and click beetle luciferases. No regions in the alignment show especially high sequence similarity, thus giving little indication that particular regions have been conserved because of catalytic or structural constraints on the enzymes. An exception to this is in the last three amino acids which, for the firefly luciferase, have been shown to be necessary for translocation into peroxisomes (*12*). Given the close functional similarity of these enzymes, it is almost certain that the click beetle luciferases are also located in peroxisomes.

Firefly luciferase has historically been used as a bioluminescent reporter of chemical events associated with adenosine triphosphate (ATP) metabolism (*13*). With the cloning of its cDNA, this luciferase has also recently found application as an effective reporter of genetic events (*14, 15*). Its principal advantages are that (i) the initial polypeptide derived from the mRNA requires no posttranslational modifications for enzymatic activity; (ii) the luminescent reaction can be measured with high sensitivity; (iii) the assay of the gene product is rapid and does not use substrates requiring special precautions (such as radioactive isotopes or chemically unstable compounds); and (iv) gene expression may be detected without disruption of living tissue. Compared with the conventionally used assay of chloramphenicol acetyltransferase (CAT) for gene activity, firefly luciferase is assayed in minutes as opposed to hours, and is 100 to 1000 times more sensitive (*15*).

The cDNAs coding for the click beetle luciferases also have these features, and, as they can be distinguished by color, may be useful in situations where multiple reporters are desirable. Expression in exogenous hosts should differ little between these luciferases because of their sequence similarity. Also, since the colors do not shift near physiological pH, the different luciferases can be distinguished in vivo as well as in vitro. Thus the click beetle luciferases may provide a dual reporter system that can allow two different promoters to be monitored within a single host, or for different populations of

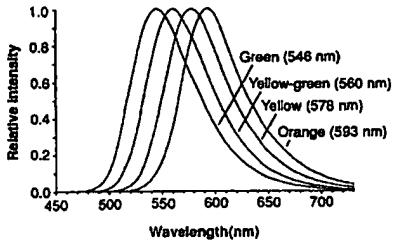

Fig. 2. Spectra of the click beetle luciferases, from intact *E. coli* immersed in luciferin, show four overlapping peaks of nearly even spacing. The maximum intensity of each spectrum has been normalized. The spectra were measured on a Fastie-Ebert–type grating spectrometer (*2*) and were corrected for the spectral sensitivity of the photomultiplier tube and for time-dependent variation in the intensity of the luminescent reactions. Wavelength positions were calibrated against the spectral lines of a mercury vapor lamp. Virtually identical spectra were obtained from lysates of these *E. coli* between pH 6 to 8. The lysates were prepared from cells grown to middle or late log-phase growth at 37°C, and then for 2 hours at 30°C with isopropylthiogalactoside (IPTG) added to 1 m*M*. The cells were washed and resuspended in approximately 1/150 volume of the culture with 100 m*M* potassium phosphate, pH 7.0, 2 m*M* EDTA, and 35% of saturation $(NH_4)_2SO_4$. After lysis by sonication and removal of the debris by centrifugation, $(NH_4)_2SO_4$ was added to 53% of saturation and the precipitate was dissolved in 1/15 volume of the lysate with 100 m*M* potassium phosphate, pH 7.0, 2 m*M* EDTA, and 50% glycerol. The spectra were measured from 10 μl of this solution diluted 100-fold with 50 m*M* 2-(*N*-morpholino)ethanesulfonic acid, 50 m*M* 2-(*N*-morpholino)propanesulfonic acid (MOPS), 50 m*M* tricine, 5 m*M* $MgSO_4$, 1 m*M* EDTA, 0.1 m*M* luciferin, 1.5 m*M* ATP, 1 m*M* NaF, 0.2 mg of bovine serum albumin per milliliter, and 10% glycerol. The spectra were measured at pH 6.0, 7.0, and 8.0.

```
FF  .EDA..IKK..A.FY....G....Q.HK.MKRYALV.GTI.FT.AHI.VN.T.A.Y..MSVR..EAMKRY.LNTNHRIVV.S..SLQ..M.   91
GR  MMKREKNVVVGPEPLHPLEDLTAGEMLFRALRKHSHLPQ--ALVDVVGEEWISYKEFPETTCLLAQSLHNCGYKMSDVVSICAENNKRFFVP  90
YG  .....I.....................................  .....F.D.SL.....A.............N.............I.  90
YE  .....I.....K...............  .I...F.D.SL.....A.............N.............  90
OR  .....I.....K...............  .I...F.D.SL.....A.............N.............I.  90

FF  VLG.LF..VA...A.DI.NER..LNS.N..Q.TV..VS.KG.Q.I.N..KKLPI.QK...M.SKTDYQ.FQ.MYT.VT.HLPP.F.EYD.V.  183
GR  IIAAWYIGMIVAPVNEGYIPDELCKVMGISRPQLVFCTKNILMKVLEVQSRTDFIKRIIILDAVENIHGCESLPNFI-SRYSDG-NIANFKP  180
YG  .....S.....K..I.....N.....T.....  180
YE  .....S.....K..I.....N.....T.....  180
OR  .....S.....K..I.....N.....T.....  180

FF  ESF.RDKTI.L.MN...S.....ALP..TA...FS..R..IF.N.I..DTAI.SVV..H.G..MFTT...LIC.F..VLMY..EE.L..R  275
GR  LHYDPVEQVAAILCSSGTTGLPKGVMQTHRNVCVRLIHALDPRVGTQLIPGVTVLVYLPFFHAFGFSINLGYFMVGLRVIMLRRFDQEAFLK  272
YG  .....Q.I.....A.....  272
YE  .....Q.I.....EA.....V.....E.....  272
OR  .....Q.I.....EA.....V.....G.....E.....  272

FF  SL...KIQ.ALL..TLFS.FA..T.I.....N.H.IAS.G...S...G.AVA..FH.....Q.Y....T...ILITPEGDD.P.AV.K.V.  367
GR  AIQDYEVRSVINVPAIILFLSKSPLVDKYDLSSLRELCCGAAPLAKEVAEIAVKRLNLPGIRCGFGLTESTSANIHSLRDEFKSGSLGRVTP  364
YG  .....V.....G.....  364
YE  .....IV.....G.....  364
OR  .....IV.....G.....  364

FF  FFE..VV.LD...T..V...R....VR...IMS.....P...NAL..K.....IA.W.....FI...L.S.....Y.....S...  459
GR  LMAAKIADRETGKALGPNQVGELCIKGPMVSKGYVNNVEATKEAIDDDGWLHSGDFGYYDEDEHFYVVDRYKELIKYKGSQVAPAELEEILL  456
YG  .....V.....  456
YE  .....  456
OR  .....K.....  456

FF  QH.N.F.AG.A.L..DD.....A.V..LEH..TN.E..IV..V.SQ.TTA.K.....V...EV.KGL...LDA..IR.I.I.AK.GGK...  550
GR  KNPCIRDVAVVGIPDLEAGELPSAFVVIQPGKEITAKEVYDYLAERVSHTKYLRGGVRFVDSIPRNVTGKI-TRK--E-LLKQLLEKESKL  543
YG  .....K.....  543
YE  .....  543
OR  .....  543
```

Fig. 3. Alignment of the amino acid sequences of the click beetle and the firefly luciferases is shown to emphasize sequence differences. The sequence information is derived from the open reading frames of the corresponding cDNA clones. The identity of each luciferase sequence is indicated at the right of each line by a two letter code: FF, firefly; GR, green-emitting click beetle; YG, yellow-green–emitting click beetle; YE, yellow-emitting click beetle; and OR, orange-emitting click beetle. Only the sequence for the green-emitting click beetle luciferase is shown in entirety. Gaps in the alignment of this sequence are indicated by hyphens. Other luciferase sequences have letter designations only at sites where they differ from the green-emitting luciferase; where the sequences are the same there is a period. Numbers on the right indicate the position of the amino acid at the end of each line. Abbreviations for the amino acid residues are A, Ala; C, Cys; D, Asp; E, Glu; F, Phe; G, Gly; H, His; I, Ile; K, Lys; L, Leu; M, Met; N, Asn; P, Pro; Q, Gln; R, Arg; S, Ser; T, Thr; V, Val; W, Trp; and Y, Tyr.

Protein Engineering vol.12 no.4 pp.313–318, 1999

Site-directed mutagenesis of residues 164, 170, 171, 179, 220, 237 and 242 in PER-1 β-lactamase hydrolysing expanded-spectrum cephalosporins

Anne-Typhaine Bouthors[1], Jean Delettre[2], Pierre Mugnier[1,3], Vincent Jarlier[1] and Wladimir Sougakoff[1,4]

[1]Laboratoire de Recherche Moleculaire sur les Antibiotiques, Universite Pierre et Marie Curie (Paris VI), Faculte de Medecine Pitie-Salpetriere and Faculte de Medecine Broussais-Hotel Dieu, F-75634 Paris cedex 13 and, [2]Laboratoire de Mineralogie-Cristallographie, CNRS URA 09, Universite Pierre et Marie Curie (Paris VI), F-75252 Paris cedex 05, France

[3]Present address: Department of Biosciences, University of Kent, Canterbury, Kent CT2 7NJ, UK

[4]To whom correspondence should be addressed. E-mail: sougakof@lmcp.jussieu.fr

The class A β-lactamase PER-1, which displays 26% identity with the TEM-type extended-spectrum β-lactamases (ESBLs), is characterized by a substrate profile similar to that conferred by these latter enzymes. The role of residues Ala164, His170, Ala171, Asn179, Arg220, Thr237 and Lys242, found in PER-1, was assessed by site-directed mutagenesis. Replacement of Ala164 by Arg yielded an enzyme with no detectable β-lactamase activity. Two other mutants, N179D and A164R+N179D, were also inactive. Conversely, a mutant with the A171E substitution displayed a substrate profile very similar to that of the wild-type enzyme. Moreover, the replacement of Ala171 by Glu in the A164R enzyme yielded a double mutant which was active, suggesting that Glu171 could compensate for the deleterious effect of Arg164 in the A164R+A171E enzyme. A specific increase in k_{cat} for cefotaxime was observed with H170N, whereas R220L and T237A displayed a specific decrease in activity towards the same drug and a general increase in affinity towards cephalosporins. Finally, the K242E mutant displayed a kinetic behaviour very similar to that of PER-1. Based on three-dimensional models generated by homology modelling and molecular dynamics, these results suggest novel structure–activity relationships in PER-1, when compared with those previously described for the TEM-type ESBLs.
Keywords: β-lactamase/expanded-spectrum cephalosporins/homology modelling/PER-1/serine enzyme

Introduction

PER-1 is a class A β-lactamase characterized by a high catalytic activity against expanded-spectrum cephalosporins [e.g. cefotaxime (CTX) and ceftazidime (CAZ)] and monobactams [e.g. aztreonam (AZT)]. The enzyme, which was first identified in *Pseudomonas aeruginosa* (Nordmann *et al.*, 1993), displays a kinetic behaviour very similar to that of various extended-spectrum β-lactamases (ESBLs) belonging to the TEM and SHV families (Jacoby and Medeiros, 1991). In contrast, PER-1 shares a relatively low amino acid identity with these latter enzymes, e.g. 26% with TEM-3 (Nordmann and Naas, 1994).

Recently, we have undertaken biochemical studies in order to elucidate the molecular basis of PER-1 activity against expanded-spectrum cephalosporins (Bouthors *et al.*, 1998). Molecular modelling and site-directed mutagenesis were used to investigate in this enzyme the role played by the amino acid residues corresponding to those found at positions 104, 164, 238 and 240 in the TEM-type ESBLs. In brief, two residues, Asn104 and Ala164, were shown to be important for the activity of PER-1. Asn104, which corresponds to the lysine residue found at the same position in various TEM-type ESBLs, would be connected to the key catalytic residue Glu166 via a hydrogen bond network, whereas Ala164, which corresponds to a highly conserved arginine in the Ω-loop of class A β-lactamases described so far (Ambler *et al.*, 1991), could play an important structural role. By contrast, modification of the serine residue found at position 238 in PER-1, which is an amino acid found specifically in a large number of TEM-type ESBLs (Bush and Jacoby, 1997), resulted in no significant modification of the activity of PER-1 against expanded-spectrum cephalosporins. Similarly, Gly240 in PER-1 was shown to have no essential role in the substrate profile of the enzyme. Finally, the catalytic residue Glu166, found in all class A β-lactamases, appeared to be essential to the β-lactamase activity of PER-1. However, an unexpected residual activity against CAZ and AZT was observed for a mutant in which Glu166 was replaced by Ala, suggesting that other residues in PER-1 could contribute to the high activity of the enzyme against expanded-spectrum cephalosporins.

In this work, we investigated other amino acid residues found either within or at the vicinity of the PER-1 active site: Ala164, His170, Ala171 and Asn179 which are located within the putative Ω-loop of PER-1, Thr237 which is found at the end of the β3 strand and is likely to participate in the formation of the oxyanion hole (Herzberg and Moult, 1987; Strynadka *et al.*, 1992), Arg220 which is located in a position similar to that of Arg244 found on strand β4 in TEM-1 and which could contribute to the stabilization of the oxyanion pocket via hydrogen bonding interactions with strand β3 (Moews *et al.*, 1990; Jacob-Dubuisson *et al.*, 1991) and Lys242 found in the loop connecting strands β3 and β4. All these residues were modified by site-directed mutagenesis and the kinetic properties of the resulting mutants were characterized. By using homology modelling and molecular dynamics simulations, we have attempted to interpret at the structural level the kinetic data obtained for some of the Ω-loop mutants.

Materials and methods

Chemicals

Antibiotic powders were provided by the following manufacturers: penicillin G, Laboratoires de Therapeutique Moderne (Suresnes, France); ampicillin, cephalothin and kanamycin, Sigma Chemical (St Louis, MO, USA); cefotaxime, Laboratoires Roussel (Paris, France); nitrocefin and ceftazidime, Glaxo (Paris, France); and aztreonam, Bristol Myers Squibb (Paris-La Defense, France).

Table I. Nucleotide sequence of the oligonucleotides used in site-directed mutagenesis

Amino acid modification	Oligonucleotide sequence[a]
Ala164 → Arg	5′-CATCTGCGCTTCATTTCGGACCACAGCGGTCTC-3′
His170 → Asn	5′-CACCTGATCATCGGCGTTCATCTGCGCTTCATT-3′
Ala171 → Glu	5′-CTGCACCTGATCATCTTCGTGCATCTGCGCTTC-3′
Asn179 → Asp	5′-TTTCATCGAGGTCCAGTCTTGATACTGCACCTG-3′
Arg220 → Leu	5′-TAACAAACCTTTTAACAGCTCTGGTCCTGTGGT-3′
Thr237 → Ala	5′-GGCTTTGATACCCGAAGCACCAGTTTTATGTG-3′
Lys242 → Glu	5′-CGCAGTTTTTCCGGCTTCGATACCCGAAGTACC-3′

[a]Specific base changes are underlined.

The restriction enzymes used in this study were obtained from Boehringer Mannheim (Meylan, France) and T4 DNA ligase from Promega (Madison, WI, USA). [^{33}P]dCTP was purchased from Isotopchim (Ganagobie, France).

Escherichia coli strains, plasmids and growth conditions

E.coli CJ236 (Kunkel *et al.*, 1987) and MV1190 (McClary *et al.*, 1989) were used as hosts for phages in site-directed mutagenesis experiments. *E.coli* JM109 (Promega) was used for DNA cloning experiments and for expression of bla_{PER-1} and the corresponding mutant genes.

The recombinant plasmid pRAZ1, encoding bla_{PER-1}, has been described by Nordmann *et al.* (1993). Bacteriophage M13mp19 (Messing, 1983) was used as a vector in site-directed mutagenesis experiments. Plasmid pK19 (kanamycin®) (Pridmore, 1987) was used in cloning experiments.

E.coli MV1190 and JM109 were grown at 37°C in Lurian–Bertani (LB) (Difco, Detroit, MI, USA) and brain-heart infusion (BHI) (Difco), respectively. Solid media were obtained by the addition of 2% Bacto-Agar (Difco). Kanamycin (25 μg/ml) and ampicillin (100 μg/ml) were added when necessary. Competent *E.coli* cells were prepared and transformed as described by Chung *et al.* (1989).

Nucleic acid techniques

Plasmid DNA was purified using either the alkaline lysis for mini-preparations (Birnboim and Doly, 1979) or the Qiagen plasmid kit for maxi-preparations (Qiagen, Hilden, Germany). Isolation of single-stranded DNA and other standard DNA manipulations were carried out according to Sambrook *et al.* (1989). Double- and single-stranded DNA sequencing were carried out by the dideoxynucleotide chain termination method (Sanger *et al.*, 1977) using the T7 Sequencing kit (Pharmacia Biotech, Saint Quentin en Yvelines, France).

Site-directed mutagenesis

Site-directed mutagenesis experiments were performed as described previously (Bouthors *et al.*, 1998). In brief, the bla_{PER-1} gene was excised from pRAZ1 (1.3 kb) and introduced into M13mp19 RF. Site-directed mutagenesis was performed using the uracil template procedure of Kunkel *et al.* (1987). The sequences of the synthetic phosphorylated oligonucleotides (Eurogentec, Liege, Belgium) used to introduce the different mutations in the bla_{PER-1} gene are listed in Table I. After mutagenesis, each mutant gene was cloned into plasmid pK19 and the recombinant plasmids thus obtained were introduced by transformation into *E.coli* JM109. The mutant genes were all sequenced in their entirety and on both strands.

Expression and purification of the wild-type and mutant β-lactamases

The wild-type and mutant enzymes were purified from 1 l cultures by a two-step procedure based on an anion-exchange column followed by a gel filtration, as described previously (Bouthors *et al.*, 1998). The mutant β-lactamases displaying significant activity were detected using the chromogenic cephalosporin nitrocefin (O'Callaghan *et al.*, 1972), while the almost inactive enzymes A164R, N179D and A164R+N179D were identified by electrophoresis on 12% SDS–polyacrylamide gels (Laemmli, 1970), with the wild-type PER-1 β-lactamase as a molecular mass reference. In order to avoid concerns about enzyme stability, kinetic studies were performed shortly after purification. The purity of the different enzymes was assessed by Coomassie Blue staining of SDS–polyacrylamide gels after electrophoresis. Protein concentration was determined by measuring the absorbance at 280 nm (Lorber and Giege, 1992) with an ε value of 34 850 $M^{-1}.cm^{-1}$ (Bouthors *et al.*, 1998). For mutants exhibiting more than one protein band on SDS–PAGE analysis, the intensity of the β-lactamase band was measured with a computerized densitometer (Densylab, Bioprobe) and the enzyme concentration was determined with reference to a standard BSA scale analyzed in the same conditions.

Isoelectric focusing

Isoelectric focusing was performed with a LKB Multiphor apparatus with pH 3.5–9.5 PAG plates (Pharmacia Biotech). Gels were focused at 30 W for 90 min at 10°C. β-Lactamase activity was revealed by staining with the nitrocefin assay.

Determination of the kinetic parameters of the wild-type and mutant enzymes

Kinetic assays were performed spectrophotometrically in 0.1 M sodium phosphate buffer (pH 7.0) at 30°C on a Uvikon 940 spectrophotometer. The wavelengths and the extinction coefficients used were as follows: penicillin G, 232 nm, $\Delta\varepsilon = -1100\ M^{-1}.cm^{-1}$; cephalothin, 262 nm, $\Delta\varepsilon = -7960\ M^{-1}.cm^{-1}$; cefotaxime, 260 nm, $\Delta\varepsilon = -6710\ M^{-1}.cm^{-1}$; ceftazidime, 260 nm, $\Delta\varepsilon = -8660\ M^{-1}.cm^{-1}$; and aztreonam, 318 nm, $\Delta\varepsilon = -650\ M^{-1}.cm^{-1}$. For each antibiotic, initial rates were measured at six different substrate concentrations. Kinetic parameters were determined by fitting the Michaelis–Menten equation to the experimental data using the regression analysis program LEONORA written by Cornish-Bowden (1995). The values for k_{cat} and K_m were estimated using a non-linear least-sqares regression method with dynamic weights (Cornish-Bowden, 1995).

Molecular modelling

The refined theoretical three-dimensional structures of PER-1 and the mutant enzymes were constructed by homology modelling using the computer program Swiss-Model (Peitsch, 1996), as described previously (Bouthors *et al.*, 1998). The models were then subjected to 5000 steps of energy minimization using the Powell minimizer of X-PLOR (Brunger, 1988). The Ω-loop region in the resulting minimized structures was subjected to molecular dynamic simulations in vacuum. The molecular dynamics were initially performed on the 150–190 region of PER-1 containing the Ω-loop (residues 161–179) and the two α-helix regions enclosing the loop (residues 150–160 and 180– 190, respectively). The results obtained from this large segment indicated that the two α-helix regions enclosing the loop were very stable (r.m.s.d. = 0.2 Å).

Therefore, the molecular dynamic simulations were subsequently confined to the region encompassing residues 160–180, using the following simulation procedure: the target temperature started at 0 K to reach the final temperature, 300 K, within 18 ps. After 30 ps of stabilization at 300 K, the molecular dynamic phase lasted 100 ps at 300 K, with a time step of 0.001 ps and a dielectric constant (ε) of 4.0. The conformations trapped at 300 K were visualized by using the VMD (Visual Molecular Dynamics) program (Humphrey *et al.*, 1996). The mean of the conformations, which was subjected to 500 steps of energy minimization, was used in structure comparison.

Results

Production and purification of the mutant enzymes

Site-directed mutagenesis was used to replace the amino acid residues located at positions 164, 170, 171, 179 and 237 in PER-1 by those found at the same positions in TEM-1 having no significant activity against expanded-spectrum cephalosporins. Thus, the single mutants A164R, H170N, A171E, N179D and T237A, and also two double mutants, A164R+A171E and A164R+N179D, were constructed. In addition, Lys242 in PER-1, which could be the counterpart of the lysine residue found at position 240 in various TEM-ESBLs (Bush and Jacoby, 1997), was replaced by a glutamic acid residue, as found in TEM-1 at position 240 (Sutcliffe, 1978). Finally, Arg220 in PER-1, which is equivalent to Arg244 located on the β4 strand in TEM-1, was replaced by a leucine. SDS–PAGE analysis of crude extracts showed that all the mutant β-lactamases except three, were expressed in normal amounts (data not shown). Indeed, when compared with the wild-type enzyme, the A164R, N179D and A164R+N179D mutants were expressed at very low levels and the various purification attempts carried out in order to determine the kinetic features of the three mutants remained unsuccessful. Production and purification of the other enzymes, which were all active, were performed as described previously (Bouthors *et al.*, 1998).

Isoelectric focusing, carried out on the purified enzymes, indicated that three mutants, A164R+A171E, H170N and T237A, displayed p*I* values indistinguishable from that of the wild-type protein (p*I* = 5.4). Conversely, the p*I* values found for the R220L, A171E and K242E mutants were shifted towards more acidic values (p*I* = 5.2, 5.0 and 4.9, respectively) (data not shown). Finally, the isoelectric points of the three mutants A164R, N179D and A164R+N179D could not be determined since the corresponding crude extracts contained no significant β-lactamase activity.

Kinetic analysis

The steady-state kinetic parameters k_{cat} and K_m for penicillin G, cephalothin, cefotaxime (CTX), ceftazidime (CAZ) and aztreonam (AZT) were determined from the purified active β-lactamases. The values obtained are shown in Table II.

Wild-type β-lactamase. As expected, the values of the rate constants obtained for the wild-type PER-1 β-lactamase were similar to those reported previously (Bouthors *et al.*, 1998). The enzyme was characterized by a high apparent affinity for penicillin G, cephalothin and AZT (K_m values ranging from 23 to 147 μM), but a poor apparent affinity for the expanded-spectrum cephalosporins CTX and CAZ (441 and 4150 μM, respectively). Conversely, the k_{cat} values for the last two drugs (41 and 109 s^{-1}, respectively) were markedly higher than those found for the other β-lactam antibiotics (k_{cat} values ranging between 8 and 11 s^{-1}) (Table II).

Mutants of residues located in the Ω-loop. Four positions were investigated at the level of the Ω-loop region of the protein: 164, 170, 171 and 179. Four single mutants (A164R, H170N, A171E and N179D) and two double mutants (A164R + A171E and A164R + N179D) were analyzed, as described below.

Mutants A164R, A171E and A164R+A171E. As observed previously (Bouthors *et al.*, 1998), no significant enzymatic activity was detected with the A164R mutant. By contrast, the substitution of the alanine residue found at position 171 in PER-1 by a glutamate resulted in no significant modifications of the k_{cat} and K_m values, when compared with the wild-type enzyme (Table II). Similarly, the double mutant A164R+A171E yielded an active enzyme which showed k_{cat} and K_m values similar to those of PER-1, but the k_{cat}/K_m ratios for CTX, CAZ and AZT were increased by at least an order of magnitude (Table II).

Mutants N179D and A164R+N179D. Position 179 is well conserved in class A β-lactamases, where an aspartate residue is generally found (Table III). The mutation Asn179 → Asp in PER-1, either in the N179D mutant or in the double mutant A164R + N179D, resulted in a complete loss of activity and the corresponding enzymes could not be purified.

Mutant H170N. A histidine residue is found at position 170 in PER-1, instead of the highly conserved Asn170 found in most of the class A β-lactamases described so far (Ambler *et al.*, 1991) (Table III). For penicillin G, cephalothin, CAZ and AZT, the H170N mutant displayed k_{cat} and K_m values similar to those of PER-1 (Table II). By contrast, a marked increase in k_{cat} was observed for CTX (5.5-fold) with a concomittant decrease in the apparent affinity (~3-fold), thus resulting in a 2-fold increase in k_{cat}/K_m.

Mutants of residues located in the α/β domain. Three positions were studied in the α/β domain: position 220, position 237 on strand β3 and position 242 on the loop connecting β3 and β4 (Bouthors *et al.*, 1998).

Mutant R220L. An arginine is found at position 220 in PER-1 (Table III). This residue might be the equivalent of Arg244 in the TEM enzymes, as previously suggested (Matagne and Frere, 1995). Replacement of Arg220 by a leucine yielded a mutant (R220L) displaying no significant modifications of the kinetic parameters for penicillin G and cephalothin. For the other drugs (CTX, CAZ and AZT), a general increase in apparent affinity was observed. In addition, a significant decrease in k_{cat} for CTX was noticed (3.2-fold) (Table II).

Mutant T237A. As in the ESBLs TEM-5 and TEM-24 (Sougakoff *et al.*, 1989; Chanal *et al.*, 1992), position 237, which contibutes to the oxyanion pocket and corresponds to an alanine in TEM-1, is occupied by a threonine in PER-1 (Table III). The replacement of Thr237 by Ala yielded an enzyme which exhibited a higher apparent affinity for most of the substrates tested, particularly for CTX and AZT (K_m values lowered by 40- and 10-fold, respectively). By contrast, specific and divergent variations of k_{cat} were observed for CAZ (6-fold increase) and CTX (4-fold decrease), but, overall, the k_{cat}/K_m ratio for all the substrates tested was markedly increased.

Mutant K242E. Lysine 242, which would be located in PER-1 on a large loop connecting strands β3 and β4 (Bouthors *et al.*, 1998), could be the counterpart of Lys240 found in

Table II. Kinetic parameters[a] for hydrolysis of β-lactam antibiotics by PER-1 and the corresponding mutants

Enzyme	Penicillin G			Cephalothin			Cefotaxime			Ceftazidime			Aztreonam		
	K_m	k_{cat}	k_{cat}/K_m	K_m	k_{cat}	k_{cat}/K_m	K_m	k_{cat}	k_{cat}/K_m	K_m	k_{cat}	k_{cat}/K_m	K_m	k_{cat}	k_{cat}/K_m
PER-1	27 ± 3	8 ± 0.2	296 ± 22	23 ± 1	8 ± 0.1	348 ± 17	441 ± 42	41 ± 2	93 ± 8	4150 ± 611	109 ± 15	26 ± 8	147 ± 15	11 ± 0.7	75 ± 15
A164R	ND[b]	ND	ND	ND	ND	ND	ND	ND	ND	ND	ND	ND	ND	ND	ND
A171E	49 ± 2	9 ± 0.2	184 ± 13	47 ± 2	14 ± 0.2	298 ± 20	284 ± 6	39 ± 0.4	137 ± 4	4309 ± 95	134 ± 3	31 ± 1	42 ± 1	5 ± 0.1	119 ± 5
N179D	ND	ND	ND	ND	ND	ND	ND	ND	ND	ND	ND	ND	ND	ND	ND
A164R+A171E	23 ± 0.01	9 ± 0.01	391 ± 0.2	27 ± 1	12 ± 0.2	444 ± 25	300 ± 19	61 ± 2	203 ± 20	2087 ± 207	123 ± 10	59 ± 11	45 ± 4	15 ± 0.5	333 ±39
A164R+N179D	ND	ND	ND	ND	ND	ND	ND	ND	ND	ND	ND	ND	ND	ND	ND
H170N	15 ± 0.7	4 ± 0.04	266 ± 15	10 ± 0.4	4 ± 0.05	400 ± 9	1286 ± 85	225 ± 11	175 ± 8	4051 ± 616	150 ±19	37 ± 10	78 ± 9	14 ± 1	179 ±19
R220L	15 ± 0.4	10 ± 0.06	666 ± 47	10 ± 0.3	4 ± 0.03	400 ± 14	167 ± 8	13 ± 0.3	78 ± 5	1329 ± 33	83 ± 1	62 ±3	39 ± 3	6 ± 0.1	154 ±14
T237A	22 ± 0.4	11 ± 0.05	500 ± 11	7 ± 0.3	15 ± 0.1	2143 ± 117	10 ± 0.7	10 ± 0.2	1000 ± 94	2181 ± 232	678 ± 56	311 ± 59	14 ± 1	18 ± 0.2	1286 ± 110
K242E	34 ± 0.5	8 ± 0.03	235 ± 4	36 ± 0.6	12 ± 0.06	333 ± 7	873 ± 0.7	94 ± 0.05	108 ± 0.1	3672 ± 31	147 ± 1	40 ± 0.6	104 ± 5	16 ± 0.4	154 ± 11

[a]Units for K_m, k_{cat} and k_{cat}/K_m are μM, s^{-1} and $s^{-1}.mM^{-1}$, respectively. Values of standard errors are indicated below the kinetic values.
[b]ND, not detectable ($k_{cat} < 0.05\ s^{-1}$).

Table III. Multiple sequence alignment of β-lactamases PER-1, TEM-1, TEM-5, SHV-8, *Streptomyces albus* G and *Staphylococcus aureus* PC1

β-Lactamase	Amino acid at position[a]							Reference
	164	170	171	179	220	237	240	
PER-1	A	H	A	N[b]	**R**	**T**	**K**[c]	Nordmann and Naas (1994)
TEM-1	R	N	E	D	L	A	E	Sutcliffe (1978)
TEM-5	S	N	E	D	L	**T**	**K**	Sougakoff *et al.* (1989)
SHV-8	R	N	E	N	L	A	E	Rasheed *et al.* (1997)
S.albus G	R	N	S	D	**R**	Q	R	Dehottay *et al.* (1987)
S.aureus PC1	R	N	Y	D	L	A	I	East and Dyke (1989)

[a]Numbering according to Ambler *et al.* (1991).
[b]Boldface letters indicate the amino acids shared by PER-1 and other enzymes.
[c]Residue number 242 in PER-1.

various ESBLs displaying a high activity against CAZ and AZT (Bush and Jacoby, 1997) (Table III). This residue was replaced by a glutamic acid, which is the residue found at position 240 in TEM-1 (Table III). As shown in Table II, the steady-state kinetic parameters determined from the K242E mutant were nearly identical with those measured from PER-1.

Discussion

We have described the catalytic behaviour of various PER-1 mutants in which residues 164, 170, 171, 179, 220, 237 and 242 were modified.

In PER-1, an alanine residue is found at position 164 instead of the highly conserved arginine identified in the other class A β-lactamases (Ambler *et al.*, 1991). As reported above and as observed previously (Bouthors *et al.*, 1998), replacement of Ala164 by Arg in PER-1 resulted in a mutant protein which could not be detected on SDS–PAGE analysis and which displayed no detectable β-lactamase activity. In order to explain such a result, theoretical three-dimensional models of the class A β-lactamase PER-1 and the corresponding mutant A164R were constructed and compared with each other (Figure 1A). Despite the relatively low degree of identity found at the amino acid level between PER-1 and the other class A β-lactamases, homology modelling was used to generate the model structures of PER-1 and the A164R enzyme because it is now well established that class A β-lactamases form a super family of enzymes that are all characterized by a very similar structural organization, particularly at the level of the active site (Joris *et al.*, 1991). Molecular dynamic simulations were then performed from the models in order to assess the extent of the conformational modifications that could occur in the Ω-loop region of the mutant by comparison with that of the wild-type enzyme. Based on the results obtained, the Ω-loop region in PER-1 appears to be characterized by fairly high flexibility (data not shown). Such a result could be related to the fact that the PER-1 Ω-loop is not stabilized by several ionic-bonding interactions, thus contrasting with the four salt bridges found in TEM-1 between the Ω-loop residues Arg161 and Asp163, Arg164 and Glu171, Arg164 and Asp179, and Asp176 and Arg178 (Jelsch *et al.*, 1993). Therefore, it is likely that the Ala164 → Arg substitution induces in PER-1 significant conformational modifications at the level of the Ω-loop. Accordingly, the topology of the main-chain atoms between residues 171–179 is significantly different in the A164R mutant, when compared with PER-1 (r.m.s.d. = 0.6 Å) (Figure 1A). In the the wild-type enzyme model, the Ω-loop conformation is generally wider than in the mutant structure, the side chain of Asp172 being oriented outwards the loop. By contrast, in the A164R enzyme, the bulky side chain of Arg164 would point inwards the Ω-loop and, due to a putative salt bridge bonding interaction, the Asp172 side chain would be reoriented towards that of Arg164 (Figure 1A). Such a salt bridge cannot be established without a significant conformational modification of the 172 region (Figure 1A), which accounts for the instability and the loss of activity of the mutant enzyme.

Contrasting with the behaviour of the A164R mutant, the substitution in PER-1 of Ala171 by a glutamic acid yielded an enzyme characterized by kinetic parameters very similar to

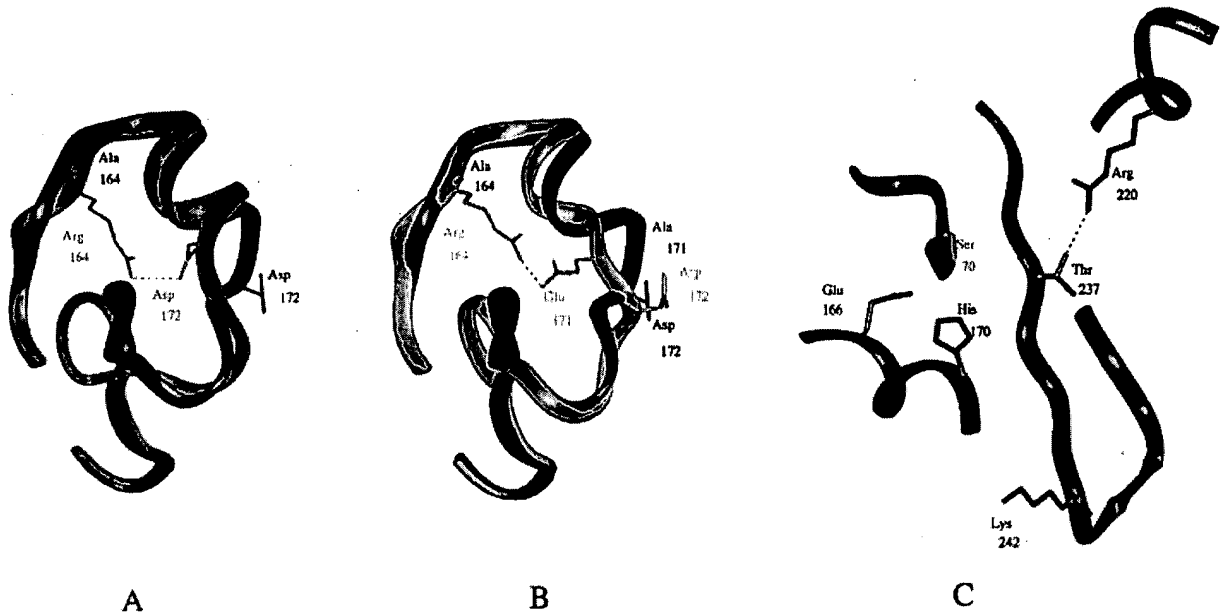

Fig. 1. Ribbon models of PER-1 (blue) and the two mutants A164R (red) and A164R+A171E (yellow). (**A**) Superposition of PER-1 and A164R; (**B**) superposition of PER-1 and A164R+A171E; (**C**) model of strands β3 and β4 in wild-type PER-1. In (A) and (B), the models represent the mean of the conformations obtained by dynamic simulations of the 160–180 region encompassing the Ω-loop (residues 161–179). Model (C) was obtained by homology modelling and energy minimization, as decribed in the Materials and methods section. Thin colour sticks: side chains of residues 70, 164, 166, 170, 171, 172, 220 and 237. Green dotted lines: hydrogen bonds. The figures were generated by using the program InsightII from Molecular Simulations.

those obtained from the wild-type enzyme. Moreover, it is noteworthy that introduction of the Ala171 → Glu mutation in the inactive mutant A164R yielded a double mutant, A164R+A171E, which was fully active and exhibited k_{cat} and K_m values nearly identical with those of PER-1 and A171E (Table II). Strikingly, in the minimized mean of the A164R+A171E structure model obtained by molecular dynamic simulations, the side chain of Glu171 could be adequately oriented to be hydrogen bonded and/or to form a strong ionic bond with the side chain of Arg164, while that of Asp172 would be consequently oriented outwards the Ω-loop, i.e. in a position nearly identical with that found in the wild-type PER-1 enzyme (Figure 1B), explaining why the double mutant remained fully active despite the presence of Arg164.

Two other amino acids (Asn179 and His170) were investigated in the Ω-loop of PER-1. The asparagine residue, found at position 179 in PER-1 as in the ESBL SHV-8 (Rasheed *et al.*, 1997) (Table III), was initially thought to play a specific role in the activity of PER-1 against expanded-spectrum cephalosporins. Unexpectedly, replacement of Asn179 by an aspartate, which is a residue conserved in a large number of class A β-lactamases, was highly deleterious for the overall β-lactamase activity of the two PER mutants N179D and A164R+N179D (Table II). It must be pointed out that the interaction between residues 164 and 179, which links the two ends of the Ω-loop region in class A β-lactamases, is important for a suitable positioning of the key catalytic residue Glu166 (Knox, 1995; Matagne *et al.*, 1998). Therefore, it is tempting to speculate that the presence of an aspartate residue at position 179 in the inactive mutants N179D and A164R+N179D could alter significantly the position of Glu166 and, thereby, the β-lactamase activity.

The histidine found at position 170 in PER-1 corresponds to a highly conserved asparagine residue in the other class A β-lactamases (Ambler *et al.*, 1991) (Table III). Unexpectedly, the kinetic parameters exhibited by the H170N mutant were similar to those obtained from PER-1, except for a 5.5-fold increase in the k_{cat} value for CTX with a concomitant decrease in the apparent affinity for this antibiotic. Palzkill *et al.* (1994) have reported that the replacement of the highly conserved Asn170 by a histidine in TEM-1 yielded an active enzyme showing unmodified catalytic constants. Taken altogether, these data suggest that His170 is not a key residue for the substrate profile of PER-1 and one can hypothesize that this residue was present in the ancestor of the PER-1 β-lactamase and has been conserved during the evolution process leading to PER-1.

Three positions in PER-1 were investigated in the region of the α/β domain forming one of the two edges of the active site. Residue 237, located on the β3 strand, belongs to the so-called oxyanion pocket and is involved in the binding of β-lactams (Ghuysen, 1994; Matagne *et al.*, 1998). In PER-1, a threonine is found at position 237 (Figure 1C), which is located between the KTG triad and Ser238. Strikingly, it has been previously reported that various TEM-type ESBLs harbour a A237T substitution (Bush and Jacoby, 1997). Moreover, another hydroxylated residue (a serine) is found naturally at position 237 in the class A β-lactamase from *Proteus vulgaris* which displays a high catalytic activity against CTX and it has been shown that the substitution Ser237 → Ala in this enzyme leads to a decrease in the catalytic efficiency against this drug (Tamaki *et al.*, 1994). Therefore, the decrease in k_{cat} observed for CTX with the T237A mutant of PER-1 confirms that Thr237 is important for the catalytic activity of PER-1 towards this drug. However, the general increase in k_{cat}/K_m observed for the T237A mutant of PER-1 against CTX, CAZ and AZT, which is due to a general increase in apparent affinity towards cephalosporins, was rather unexpected (Table II). Nonetheless, these results were confirmed by modifying the arginine found at position 220 in PER-1. Indeed,

according to the hypothetical model of PER-1 shown in Figure 1C, the side chain of Arg220 would point towards the active site cavity and could be hydrogen-bonded to that of Thr237. As a consequence of this structural organization, it is likely that both residues contribute to adjusting the topology of the oxyanion pocket, as previously suggested for other class A β-lactamases (Matagne and Frere, 1995). In accordance with such a model, the replacement of Arg220 by Leu in PER-1, which leads to the loss of the hydrogen-bonding interactions between residues 220 and 237, yielded a mutant enzyme (R220L) showing kinetic properties similar to those exhibited by the T237A mutant, i.e. a significant decrease in the catalytic activity against CTX associated with a better apparent affinity for expanded-spectrum cephalosporins and AZT (see Table II).

Finally, we also studied the lysine residue found at position 242 at the end of the β3 strand in PER-1 (Figure 1C), which might be the counterpart of Lys240 found in various TEM-type ESBLs (Bush and Jacoby, 1997). The replacement of Lys242 in PER-1 by a glutamic acid residue, which is the residue found at position 240 in TEM-1 (Table III), yielded a mutant enzyme with kinetic properties very similar to those of PER-1. This result indicates that Lys242 does not play in PER-1 a role equivalent to that of the lysine found at position 240 in the TEM-type ESBLs.

In conclusion, PER-1 is a class A ESBL which illustrates well the fact that enzymes showing a high level of divergence in their amino acid sequences can share very similar substrate profiles. Furthermore, our results indicate that, in contrast to the TEM-type ESBLs, the PER-1 activity towards expanded-spectrum cephalosporins does not stem from the presence in the active site of a limited number of residues having a specific role in the hydrolysis of these drugs. The X-ray structure determination of PER-1, which is in progress, will aid further understanding of the structure–activity relationships of this peculiar class A β-lactamase.

Acknowledgements

We thank N.Dagoneau-Blanchard for technical assistance. We are indebted to Professor P.Nordmann and to Dr T.Naas for the gift of the recombinant plasmid pRAZ1 encoding bla_{PER-1}. This work was supported by the Institut National de la Sante et de la Recherche Medicale (INSERM, grant CR1950601). A.T.Bouthors is a Fellow of the Institut SmithKline-Beecham (SmithKline-Beecham Pharmaceuticals, Nanterre, France).

References

Ambler,R.P., Coulson,F.W., Frere,J.M., Ghuysen,J.M., Joris,B., Forsman,M., Levesque,R.C., Tiraby,G. and Waley,S.G. (1991) *Biochem. J.*, **276**, 269–272.

Birnboim,H.C. and Doly,J. (1979) *Nucleic Acids Res.*, **7**, 1513.

Bouthors,A.T., Dagoneau-Blanchard,N., Naas,T., Nordmann,P., Jarlier,V. and Sougakoff,W. (1998) *Biochem. J.*, **330**, 1443–1449.

Brunger,A.T., (1988) In Isaac,N.W. and Taylor,M.R. (eds), *Crystallographic Computing 4: Techniques and Technologies.* Clarendon Press, Oxford, pp. 126–140.

Bush,K. and Jacoby,G.A. (1997) *J. Antimicrob. Chemother.*, **39**, 1–3.

Chanal,C., Poupart,M.C., Sirot,D., Labia,R., Sirot,J. and Cluzel,R. (1992) *Antimicrob. Agents Chemother.*, **36**, 1817–1820.

Chung,C.T., Niemela,S.L. and Miller,R.H. (1989) *Proc. Natl Acad. Sci. USA*, **86**, 2172–2175.

Cornish-Bowden,A. (1995) *Analysis of Enzyme Kinetic Data.* Oxford University Press, Oxford.

Dehottay,P., Dusart,J., De Meester,F., Joris,B., Van Beeumen,J., Erpicum,T., Frere,J.M. and Ghuysen,J.M. (1987) *Eur. J. Biochem.* **166**, 345–350.

East,A.K. and Dyke, G.H. (1989) *J. Gen. Microbiol.* **135**, 1001–1015.

Ghuysen,J.M. (1994) *Trends Microbiol.*, **2**, 327–380.

Herzberg,O. and Moult,J. (1987) *Science*, **236**, 694–701.

Humphrey,W., Dalke,A. and Schulten,K. (1996) *J. Mol. Graphics*, **14**, 33–38.

Jacob-Dubuisson,F., Lamotte-Brasseur, J., Dideberg,O., Joris,B. and Frere,J.M. (1991) *Protein Engng*, **4**, 811–819.

Jacoby,J.A. and Medeiros,A.A. (1991) *Antimicrob. Agents Chemother.*, **35**, 1697–1704.

Jelsch,C., Mourey,L., Masson,J.M. and Samama,J.P. (1993) *Proteins: Struct. Funct. Genet.*, **16**, 364–383.

Jonis,B., Ledent,P., Dideberg,O., Fonze,E., Lamotte-Brasseur,J., Kelly,J.A., Ghuysen,J.M. and Frere,J.M. (1991) *Antimicrob. Agents Chemother.*, **35**, 2294–2301.

Knox,J.R. (1995) *Antimicrob. Agents Chemother.*, **39**, 2593–2601.

Kunkel,T.A., Roberts,J.D. and Zakow,R.A. (1987) *Methods Enzymol.*, **154**, 367–382.

Laemmli,U.K. (1970) *Nature*, **227**, 680–685.

Lorber, B. and Giege, R. (1992) In Ducruix, A. and Giege, R. (eds), *Crystallization of Nucleic Acids and proteins: a Practical Approach.* IRL Press, Oxford, p. 29.

Matagne,A. and Frere,J.M. (1995) *Biochim. Biophys. Acta*, **1246**, 109–127.

Matagne,A., Lamotte-Brasseur,J. and Frere,J.M. (1998) *Biochem. J.*, **330**, 581–598.

McClary,J.A., Witney,F. and Geisselsoder,J. (1989) *BioTechniques*, **3**, 282–289.

Messing,J. (1983) *Methods Enzymol.*, **101**, 20–78.

Moews,P.C., Knox,J.R., Dideberg,O., Charlier,P. and Frere,J.M. (1990) *Proteins: Struct. Funct. Genet.*, **7**, 156–171.

Nordmann,P. and Naas,T. (1994) *Antimicrob. Agents Chemother.*, **38**, 104–114.

Nordmann,P., Ronco,E., Naas,T., Duport,C., Michel-Briand,Y. and Labia,R. (1993) *Antimicrob. Agents Chemother.*, **37**, 962–969.

O'Callaghan,C.H., Morris,A., Kirby,S.M. and Shingler,A.M. (1972) *Antimicrob. Agents Chemother.*, **1**, 283–288.

Palzkill,T., Quyen-Quyen,L., Venkatachalam,K.V., LaRocco,M. and Ocera,H. (1994) *Mol. Microbiol.*, **12**, 217–229.

Peitsch,M.C. (1996) *Biochem. Soc. Trans.*, **24**, 274–279.

Pridmore,R.D. (1987) *Gene*, **56**, 309–312.

Rasheed,J.K., Jay,C., Metchock,B., Berkowitz,F., Weigel,L., Crellin,J., Steward,C., Hill,B., Medeiros,A.A. and Tenover,F.C. (1997) *Antimicrob. Agents Chemother.*, **41**, 647–653.

Sambrook,J., Fritsch,E.F. and Maniatis,T. (1989) *Molecular Cloning. A Laboratory Manual.* 2nd edn. Cold Spring Harbor Laboratory Press, Cold Spring Harbor, NY.

Sanger,F., Nicklen,S. and Coulson,A.R. (1977) *Proc. Natl Acad. Sci. USA*, **74**, 5463–5467.

Sougakoff,W., Petit,A., Goussard,S., Sirot,D., Bure,A. and Courvalin,P. (1989) *Gene*, **78**, 339–348.

Strynadka,N.C.J., Adachi,H., Jensen,S.E., Johns,K., Sielecki,A., Betzel,C., Suton,K. and James,M.N.J. (1992) *Nature*, **359**, 700–705.

Sutcliffe,J.G. (1978) *Proc. Natl Acad. Sci. USA*, **75**, 3737–3741.

Tamaki,M., Nukaga, M. and Sawai,T. (1994) *Biochemistry*, **33**, 10200–10206.

Received July 23, 1998; revised January 4, 1999, accepted January 21, 1999

Proc. Natl. Acad. Sci. USA
Vol. 88, pp. 4438–4442, May 1991
Biochemistry

Isolation and expression of a cDNA encoding *Renilla reniformis* luciferase

(bioluminescence/*Renilla* luciferase/green fluorescent protein/gene expression)

W. WALTER LORENZ*, RICHARD O. MCCANN*, MATHEW LONGIARU†, AND MILTON J. CORMIER*‡

*Department of Biochemistry, University of Georgia, Athens, GA 30602; and †Hoffman-La Roche, Nutley, NJ 07110

Communicated by W. D. McElroy, December 26, 1990 (received for review, October 12, 1990)

ABSTRACT **_Renilla reniformis_ is an anthozoan coelenterate capable of exhibiting bioluminescence. Bioluminescence in _Renilla_ results from the oxidation of coelenterate luciferin (coelenterazine) by luciferase [_Renilla_-luciferin:oxygen 2-oxidoreductase (decarboxylating), EC 1.13.12.5]. _In vivo_, the excited state luciferin–luciferase complex undergoes the process of nonradiative energy transfer to an accessory protein, green fluorescent protein, which results in green bioluminescence. _In vitro_, _Renilla_ luciferase emits blue light in the absence of any green fluorescent protein. A _Renilla_ cDNA library has been constructed in λgt11 and screened by plaque hybridization with two oligonucleotide probes. We report here the isolation and characterization of a luciferase cDNA and its gene product. The recombinant luciferase expressed in _Escherichia coli_ is identical to native luciferase as determined by SDS/PAGE, immunoblot analysis, and bioluminescence emission characteristics.**

Renilla reniformis (class Anthozoa) is a bioluminescent soft coral found in shallow coastal waters of North America, which displays blue-green bioluminescence upon mechanical stimulation (1, 2). The components involved in *Renilla* bioluminescence have been described in detail (3). *Renilla* luciferase [*Renilla*-luciferin:oxygen 2-oxidoreductase (decarboxylating), EC 1.13.12.5] catalyzes the oxidative decarboxylation of coelenterazine in the presence of dissolved oxygen to yield oxyluciferin, CO_2, and blue light (λ_{max} = 480 nm) (4). This reaction has a bioluminescence quantum yield of ≈7%. The stoichiometry of this reaction and the detailed mechanism leading to excited-state formation have been described (4, 5).

The color of *in vitro*-catalyzed bioluminescence changes from blue to green upon addition of submicromolar amounts of an energy-transfer acceptor green fluorescent protein (GFP), which has been purified from *Renilla* and characterized (6). This green fluorescence (λ_{max} = 509 nm) is identical to the *in vivo* emission in *Renilla*. The energy-transfer process is nonradiative; an increase in both the quantum yield (6) and calculated lifetimes has been determined for this process (7). Luciferase and GFP form a specific 1:1 rapid equilibrium complex in solution (8).

The elucidation of mechanisms involved in nonradiative energy transfer processes as well as determination of detailed structural information on both luciferase and GFP have been hindered by a lack of material. To overcome this, we have cloned, sequenced, and expressed in *Escherichia coli* a cDNA encoding *Renilla* luciferase.§

MATERIALS AND METHODS

Amino Acid Sequence Determination of *Renilla* Luciferase. Native *Renilla* luciferase was isolated as described (4). Purified luciferase was digested with *Staphlococcal* protease V-8 (9). The resulting peptides were purified by HPLC and subjected to NH_2-terminal Edman sequencing as described (10). Based on these peptide sequences two 17-base oligonucleotide probes were synthesized with an Applied Biosystems DNA synthesizer at the Molecular Genetics Instrumentation Facility at the University of Georgia.

Construction of a cDNA Library in λgt11. Live *R. reniformis* were collected at the University of Georgia Marine Institute located at Sapelo Island. The animals were frozen immediately in liquid N_2 and stored at −80°C. Frozen tissue was ground to a fine powder in liquid N_2 with mortar and pestle. Total RNA was isolated from the frozen powder by the guanidine thiocyanate method (11), and poly(A)$^+$ RNA was isolated by oligo(dT)-cellulose chromatography (12). cDNA was synthesized by the method of Gubler and Hoffman (13). Phosphorylated *Eco*RI linkers (Collaborative Research) were ligated to the cDNAs, which were then digested with *Eco*RI. Separation of cDNA from free linkers after *Eco*RI digestion as well as size selection of cDNAs were accomplished by electrophoresis in low-melting-temperature agarose (NuSieve, FMC) (14). cDNAs were ligated into the *Eco*RI site of λgt11 (15). The library was amplified in Y1088 cells (16) by a plate method (17).

Isolation and DNA Sequence Determination of a Luciferase cDNA. Oligonucleotide probes were 5′ end-labeled with T4 polynucleotide kinase (Bethesda Research Laboratories) and [γ-^{32}P]ATP (3000 Ci/mmol; 1 Ci = 37 GBq; ICN) to specific activities ≥1 × 10^8 cpm/μg (18). A total of 6 × 10^5 recombinant plaque-forming units were screened by plaque hybridization (19). Phage DNA was isolated as described (20). A luciferase cDNA, isolated from the clone λRLuc-6, was subcloned into the M13 sequencing vectors mp18 and mp19, and sequencing templates were prepared (21). The DNA sequence of both strands was determined by the dideoxynucleotide chain-termination technique by using a Sequenase kit (United States Biochemical) and [α-^{35}S]dATP (400 Ci/mmol; Amersham) (22). The M13 universal primer and a λgt11 sequencing primer (Amersham) were used to prime the sequencing reactions.

Expression of Recombinant Luciferase (r-luciferase). Positive clones were converted to lysogens in *E. coli* Y1089 cells (16). Lysogens were grown at permissive temperatures and induced with 1 mM isopropyl β-D-thiogalactopyranoside (IPTG). Crude cell extracts were prepared and assayed for luciferase activity as described below. The plasmid pTZR-Luc-1 was constructed by ligation of a 2.2-kilobase-pair (kbp) *Eco*RI/*Sst* I λRLuc-6 restriction fragment into the plasmid pTZ18R (Pharmacia), which contains the *lacZ′* gene. *E. coli* TG-1 cells (23) were transformed with pTZRLuc-1 (24). Single colonies were isolated and grown at 37°C in LB

Abbreviations: GFP, green fluorescent protein; IPTG, isopropyl β-D-thiogalactopyranoside; r-luciferase, recombinant luciferase; ORF, open reading frame.

The publication costs of this article were defrayed in part by page charge payment. This article must therefore be hereby marked "*advertisement*" in accordance with 18 U.S.C. §1734 solely to indicate this fact.

‡To whom reprint requests should be addressed.

§The sequence reported in this paper has been deposited in the GenBank data base (accession no. M63501).

medium containing ampicillin (100 μg/ml) to an OD_{600} = 0.6–0.8 unit and induced with 1 mM IPTG for 4 hr. The cells were centrifuged at 10,000 × *g* and frozen solid at −20°C. The pellets were thawed and resuspended 1:5 in 10 mM EDTA, pH 8, and lysozyme at 4 mg/ml (Sigma). After 20-min incubation at 25°C, the cells were placed on ice for 1 hr and then sonicated for 30 sec with a Branson cell disrupter. The cell lysate was clarified by centrifugation at 30,000 × *g*. The clarified lysate was used in subsequent bioluminescence assays and emission studies.

Assay for *Renilla* Luciferase Activity and Determination of Emission Spectra. Bioluminescence assays (4) were done with a Turner model TD-20e luminometer, and peak light intensities were determined. Bioluminescence intensity was converted to quanta per second by calibrating the instrument relative to a radioactive ^{63}Ni light standard that emits in the 460- to 480-nm region (25). Corrected emission spectra were collected on an on-line computerized fluorimeter (26). A 100-μl sample of a clarified pTZRLuc-1 cell extract was added to 1 ml of luciferase assay buffer (4) or to 1 ml of "energy-transfer buffer" containing 1×10^{-6} M GFP (8). An excess of coelenterazine (0.47 mM) dissolved in MeOH was added to maintain a strong emission signal.

Genomic Southern Blot Analyses. A 790-bp *Eco*RI/*Bam*HI cDNA restriction fragment was labeled to specific activities $\geq 1 \times 10^9$ cpm/μg with both [α-^{32}P]dATP and dCTP (4000 Ci/mmol, ICN) by the random hexamer-priming method (27). Genomic DNA was isolated from *Renilla* by a guanidine thiocyanate method developed for coelenterate DNA isolation (D. Prasher, personal communication). DNA samples were digested with the appropriate enzymes and resolved in a 0.8% agarose gel, followed by transfer to nitrocellulose filters (Schleicher & Schuell) (28). Aqueous hybridizations and washes were done at high stringencies as described for a homologous probe (17).

Electrophoretic Analysis of Protein. Protein samples were analyzed on 12.5% SDS/PAGE gels that were fixed and stained with Coomassie blue as described (29). Immunoblots were done as described (30). Proteins were transferred to nitrocellulose (Schleicher & Schuell) and incubated in a 1:50 dilution of rabbit anti-native luciferase antibody. Detection of the secondary antibody (horseradish peroxidase-conjugated goat anti-rabbit IgG) signal was determined according to the vendor's instructions (Bio-Rad).

Computer-Facilitated DNA and Amino Acid Sequence Analyses. The DNA sequence was compiled and manipulated using MicroGenie sequence software (Beckman).

RESULTS

Synthesis of Luciferase Oligonucleotides. Seven luciferase peptides (V8-1–V8-7) were purified by HPLC, and their amino acid sequences were determined. Two of the peptides contained regions of relatively low codon degeneracy. Amino acid sequence from these regions was used to synthesize two mixed-sequence 17-base oligonucleotide hybridization probes with the following sequences; RLP-1 {GAR-AAYAAY-TTY-TTY-GT} and RLP-2 {AAR-AAR-TTY-CCN-AAY AT}, which are 32- and 64-fold degenerate, respectively.

Nucleotide and Deduced Amino Acid Sequence Analyses of *Renilla* Luciferase. Six clones were isolated from the *Renilla* cDNA library. One clone, λRLuc-6, hybridized to both oligonucleotide probes. The cDNA insert could not be isolated after *Eco*RI digestion, as one of the linker sites was lost during cloning. A double digest with *Eco*RI and *Sst* I produced a 2.2-kbp fragment that contained a 1.2-kbp cDNA with 1 kbp of λgt11 DNA at the 3′ end. This fragment was subcloned into the M13 vectors mp18 and mp19. DNA sequencing provided the locations of six base restriction sites (Fig. 1), which were used to generate specific sequencing subclones. The entire 1.2-kbp luciferase cDNA was sequenced on both strands.

The cDNA, excluding the *Eco*RI linkers, is 1196 nucleotides long and encodes an open reading frame (ORF) of 314 amino acids (Fig. 2). Although an ATG in-frame codon is found at the 5′ end of the cDNA, the intrinsic mRNA may contain additional 5′ coding nucleotides. If the first ATG codon in the ORF is designated as the initiation codon, the predicted 311 amino acid sequence is essentially identical in size (34 kDa) and composition to native *Renilla* luciferase (4).

Comparison of the deduced amino acid sequence with the native peptides reveals that λRLuc-6 encodes a luciferase cDNA (Fig. 2). One discrepancy lies at amino acid residue 222, which is leucine in the peptide sequence but tryptophan in the deduced sequence. Sequencing autoradiograms from this region of the clone have been examined carefully and found free of any irregularities. The protein sequence also contains a consensus N-linked glycosylation site (Asn-Xaa-Ser) beginning at residue 92.

Genomic Southern Analysis. A *Renilla* genomic Southern blot was probed with a 790-base-pair (bp) *Eco*RI/*Bam*HI luciferase cDNA restriction fragment (Fig. 3). The *Bam*HI digest, lane A, contains two hybridizing bands as does the *Sma* I digest, lane B. The *Bgl* II digest, lane C, contains four bands. If luciferase is encoded by a single gene containing no introns, a single band would be expected in the *Bam*HI and *Sma* I digests, as these two sites are not spanned by the hybridization probe. Similarly, two bands would be expected in the *Bgl* II digest. That the *Bam*HI and *Sma* I digests contain two hybridizing bands shows either that there is more than one luciferase gene or that the luciferase gene(s) has introns containing *Bam*HI and *Sma* I sites. The four bands seen in the *Bgl* II could be explained by two very large introns containing *Bgl* II sites. When genomic DNA was digested with restriction enzymes having no sites within the cDNA sequence, there were always at least two or more hybridizing bands (data not shown). These results suggest that luciferase is encoded for by more than one gene, which may or may not contain introns.

Luciferase Expression in *E. coli*. The λRLuc-6 lysogen is capable of low-level r-luciferase expression as determined by light emission from clarified, crude extracts (5×10^{10} hv·sec^{-1}·ml^{-1}). When these cells are induced with 1 mM IPTG, light emission decreases by 2-fold; this happens because the cDNA is reversely oriented with respect to the λgt11 *lacZ* promoter. Presumably, when IPTG is absent, the luciferase gene is transcribed from a promoter in the right end of λgt11, as reported (31).

The 2.2-kbp *Eco*RI/*Sst* I fragment was subcloned into the plasmid pTZ18R, which uses the *lacZ* promoter. The ORF of

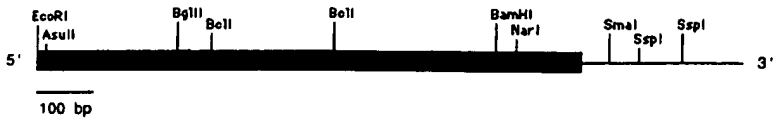

FIG. 1. Location of six base restriction enzyme sites within the luciferase cDNA. The boxed region defines the ORF. The *Eco*RI site at the 5′ end is a synthetic linker site.

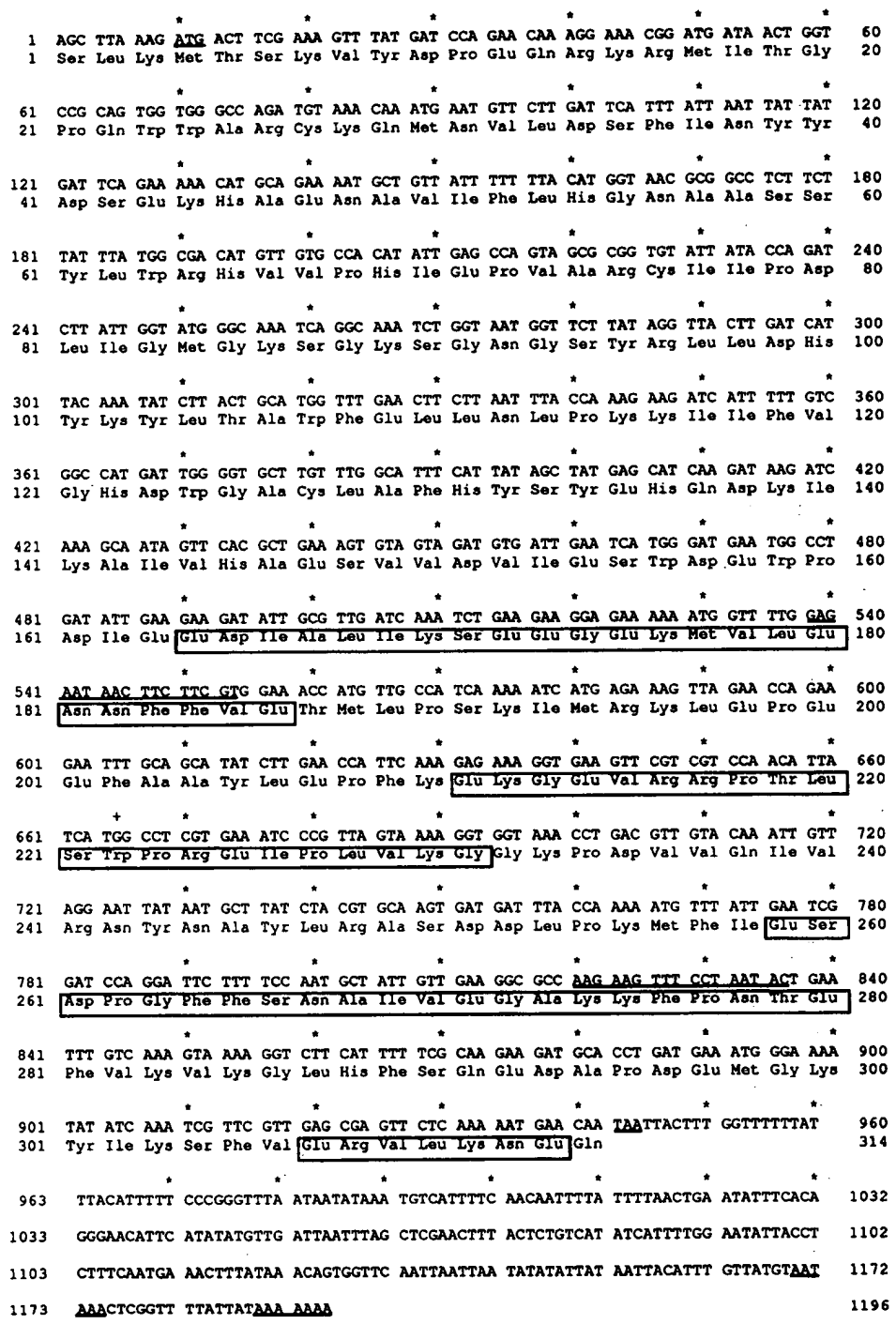

FIG. 2. Nucleotide sequence and translated amino acid sequence of the *Renilla* luciferase cDNA. Putative and known translation control elements, as well as oligonucleotide hybridization sites, are underlined. Positions of native luciferase peptide sequences are boxed and, except at one residue (+), are identical to the deduced amino acid sequence obtained from the luciferase cDNA. Some of the native luciferase peptide sequences overlap at glutamic acid residues.

the cDNA is not in frame with the *lacZ'* gene ORF of pTZ18R. Supernatants were prepared from IPTG-induced pTZRLuc-1 cells, as described, and the level of luciferase expression was measured by the standard luciferase assay. A high level of r-luciferase activity, 2×10^{15} hv·sec^{-1}·ml^{-1}, is detected in clarified crude extracts of pTZRLuc-1 cells. This level of activity is 7-fold greater than in uninduced pTZR-Luc-1 cells.

A prominent protein band (M_r = 34,000) migrating to the position of native luciferase is seen after SDS/PAGE of pTZR-Luc-1 crude extracts (Fig. 4). Crude extracts of IPTG-induced pTZRLuc-1 cells were analyzed by immunoblotting (Fig. 5). The protein band that reacts with antiluciferase antibody, lane B, corresponds to the same band seen in the Coomassie-stained gel (Fig. 4). Native luciferase was used as a positive control, lane A. No signal is detectable in the crude extract of pTZ18R cells, lane C. A duplicate filter incubated with preimmune serum showed no detectable signal.

Bioluminescence Emission Spectra. The r-luciferase-catalyzed bioluminescence emission spectrum (Fig. 6*a*) is

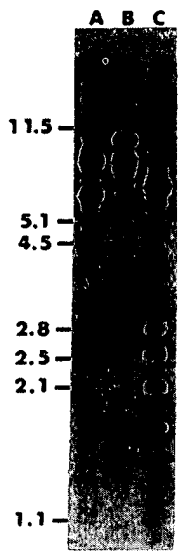

FIG. 3. Genomic Southern blot of *R. reniformis* DNA hybridized to a 790-bp *Eco*RI/*Bam*HI luciferase cDNA fragment. Genomic DNA had been digested with the following restriction enzymes: *Bam*HI (lane A); *Sma* I (lane B); and *Bgl* II (lane C). Samples were resolved in a 0.8% agarose gel and transferred to nitrocellulose. Each lane contains 20 μg of digested genomic DNA. Molecular size markers are in kbp.

very similar to that seen with native luciferase (32). The r-luciferase emission spectrum has a λ_{max} = 480 nm and a slight shoulder at 400 nm, which correspond to emission from the excited-state oxyluciferin monoanion and neutral species, respectively. Disproportionation between these species is sensitive to environmental factors (7); thus, this spectrum indicates the strong similarity of the active-site environment between r-luciferase and the native enzyme. Although an increase in quantum yield has yet to be determined, r-luciferase can clearly transfer energy in the presence of *Renilla* GFP (Fig. 6*b*). The emission spectrum dramatically shifted

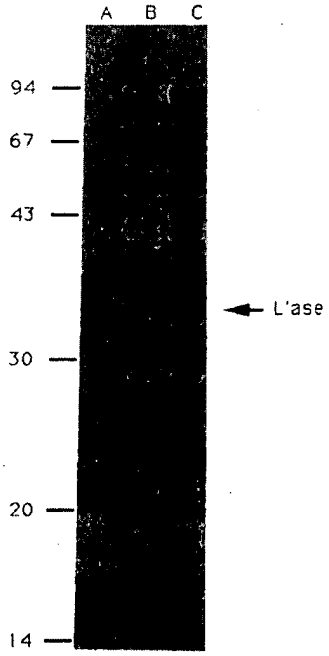

FIG. 4. SDS/PAGE analysis of total protein from IPTG-induced *E. coli* cells transformed with either pTZRLuc-1 or pTZ18R. Ten-milliliter cultures were grown to an OD_{600} = 0.8 and induced with 1 mM IPTG for 4 hr. One-milliliter of cell culture, OD_{600} = 5.0, was pelleted and resuspended in 0.5 ml of SDS sample buffer. Samples were boiled for 5 min, and 20 μl was loaded per lane: native luciferase (10 μg) (lane A); pTZRLuc-1 cells (lane B); and pTZ18R cells (lane C). Molecular weight ($M_r \times 10^{-3}$) standard positions are indicated. Arrow shows position of native luciferase (L'ase).

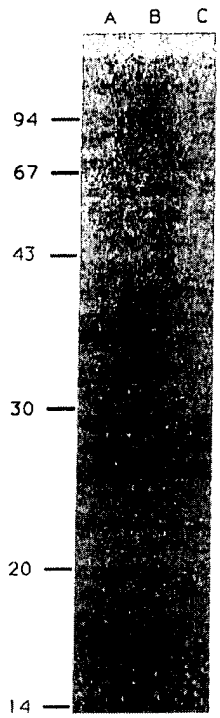

FIG. 5. Immunoblot analysis of total protein. Sample preparation and electrophoresis were the same as in Fig. 4. Native luciferase (2 μg) (lane A); 10 μl of pTZRLuc-1 cell extract (lane B); and 10 μl of pTZ18R cell extract (lane C). Molecular weight ($M_r \times 10^{-3}$) standard positions are indicated.

from the broad emission band generated by r-luciferase to the narrow, structured emission band (λ_{max} = 509) seen when GFP is present. The emission spectrum generated with r-luciferase and GFP is very similar to the same spectrum generated with native luciferase and GFP (33).

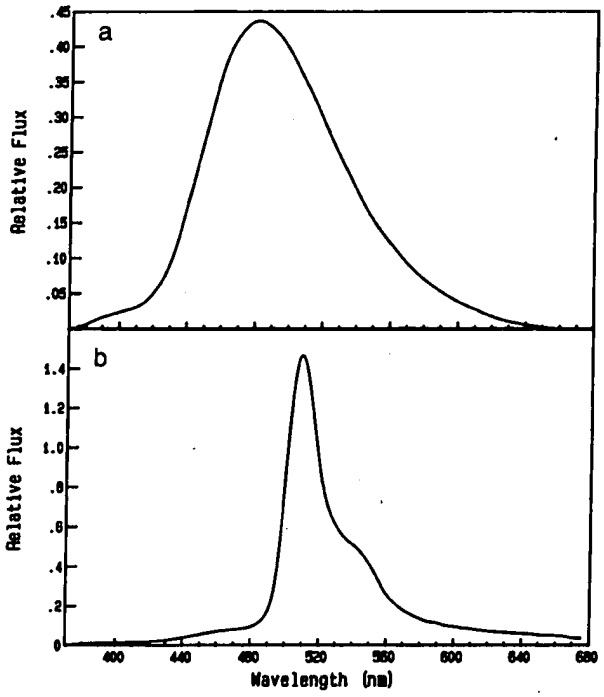

FIG. 6. Bioluminescence emission spectra generated with crude r-luciferase and r-luciferase plus GFP. Crude pTZRLuc-1 cell extracts were prepared, as described, and 100 μl, $\approx 1 \times 10^{-6}$ M r-luciferase, as determined by peak light emission, was used to generate each spectrum. (*a*) Emission spectrum of crude r-luciferase. (*b*) Spectrum that results when 1×10^{-6} M *Renilla* GFP is added to crude r-luciferase in energy-transfer buffer.

DISCUSSION

This work describes the isolation of a 1.2-kbp *R. reniformis* luciferase cDNA capable of directing the expression of r-luciferase. The cDNA contains an ORF encoding a 314-amino acid sequence in which all of the native luciferase peptide sequences obtained from V8-protease digestion are found. Rescreening the cDNA library with a 790-bp luciferase cDNA fragment as a hybridization probe has failed to produce other clones that contain the 5′ noncoding region; therefore, whether the luciferase cDNA is full-length is not known. This uncertainty can be resolved by sequencing genomic clones corresponding to the 5′ end of the luciferase gene.

The genomic Southern hybridization data indicates that *Renilla* luciferase is probably encoded by more than one gene, which may or may not contain intervening sequences. Further characterization of luciferase genomic clones will be required before the genetic organization of the luciferase gene(s) can be defined.

A putative initiation codon located at triplet position 4 of the ORF may be the translation initiation site for *Renilla* luciferase; the 311-amino acid sequence is essentially identical to native luciferase with respect to its composition and predicted molecular weight. Irrespective of whether this cDNA is full length, the luciferase that it encodes is expressed in pTZRLuc-1 cells and is catalytically active. The expression data demonstrate that r-luciferase is the same size as native luciferase on SDS/PAGE gels and is reactive with polyclonal rabbit antibodies raised against native *Renilla* luciferase. Expression of r-luciferase from the plasmid pTZRLuc-1 is "leaky" because activity can be detected from uninduced cell cultures. The luciferase cDNA ORF is not in frame with the short *lacZ′* ORF contained in this construct. Any translation product initiating at the β-galactosidase sequence of pTZRLuc-1 would be terminated at a stop codon immediately adjacent to the putative initiation codon in the luciferase cDNA. Thus, the r-luciferase seen in SDS/PAGE gels does not contain any β-galactosidase sequence. We propose that expression of r-luciferase by pTZRLuc-1 is due to a translation coupling mechanism (34).

r-luciferase displays two very important characteristics of native luciferase: the ability to catalyze coelenterazine oxidation with the concomitant emission of blue light (λ_{max} = 480 nm) and the ability to transfer energy to *Renilla* GFP with the production of green light (λ_{max} = 509 nm). The two emission bands at 400 nm and 480 nm in the r-luciferase spectrum verify the strong similarity between the native and recombinant proteins and suggest that the integrity of the luciferase active site has been maintained. Furthermore, that energy transfer occurs in the presence of GFP shows that the luciferase domain(s) required for the interaction between luciferase and GFP is present in r-luciferase. Once pure r-luciferase is available, energy transfer quantum yield measurements will offer a more quantitative determination of the efficiency of the nonradiative energy-transfer process. Finally, the data demonstrate that N-linked glycosylation is not required for luciferase activity because *E. coli* do not perform this modification (35). r-luciferase in *E. coli* crude extracts behaves like the native enzyme by every criterion examined thus far.

We thank Yu-Ching Pan and Jeffery Hulmes (Roche Diagnostic Systems) for the partial amino acid sequence data on native luciferase; John Wunderlich for the synthesis of oligonucleotide probes; Dennis O'Kane and John Wampler for help in obtaining bioluminescence emission spectral data; Leon Dure, Claiborne Glover, and Douglas Prasher for their critical comments; and Judy Gray for technical assistance. This is contribution number 659 from the University of Georgia Marine Institute, Sapelo Island, GA. This work was funded, in part, by a grant from ELA Technologies Inc.

1. Harvey, E. N. (1952) in *Bioluminescence*, ed. Harvey, E. N. (Academic, New York), pp. 148–194.
2. Morin, J. G. (1974) in *Coelenterate Biology: Reviews and Perspectives*, eds. Muscatine, L. & Lenhoff, H. M. (Academic, New York), pp. 397–438.
3. Cormier, M. J. (1978) in *Bioluminescence in Action*, ed. Herring, P. J. (Academic, New York), pp. 75–108.
4. Matthews, J. C., Hori, K. & Cormier, M. J. (1977) *Biochemistry* **16**, 85–91.
5. Hart, R. C., Stempel, K. E., Boyer, P. D. & Cormier, M. J. (1978) *Biochem. Biophys. Res. Commun.* **81**, 980–986.
6. Ward, W. W. & Cormier, M. J. (1979) *J. Biol. Chem.* **254**, 781–788.
7. Hart, R. C., Matthews, J. C., Hori, K. & Cormier, M. J. (1979) *Biochemistry* **18**, 2204–2210.
8. Ward, W. W. & Cormier, M. J. (1978) *Photochem. Photobiol.* **27**, 389–396.
9. Houmard, J. & Drapeau, G. R. (1972) *Proc. Natl. Acad. Sci. USA* **69**, 3506–3509.
10. Charbonneau, H., Walsh, K. A., McCann, R. O., Prendergast, F. G., Cormier, M. J. & Vanaman, T. C. (1985) *Biochemistry* **24**, 6762–6771.
11. Chirgwin, J. M., Przybyla, A. E., MacDonald, R. J. & Rutter, W. J. (1979) *Biochemistry* **18**, 5294–5299.
12. Aviv, H. & Leder, P. (1972) *Proc. Natl. Acad. Sci. USA* **69**, 1408–1412.
13. Gubler, U. & Hoffman, B. J. (1983) *Gene* **25**, 263–269.
14. Weislander, L. (1979) *Anal. Biochem.* **98**, 305–309.
15. Young, R. A. & Davis, R. W. (1983) *Proc. Natl. Acad. Sci. USA* **80**, 1194–1198.
16. Ausubel, F. M., Brert, R., Kingston, R. E., Morre, D. D., Seidmon, J. G., Smith, J. A. & Struhl, K. (1987) *Current Protocols in Molecular Biology* (Wiley, New York).
17. Maniatis, T., Fritsch, E. F. & Sambrook, J. (1982) *Molecular Cloning: A Laboratory Manual* (Cold Spring Harbor Lab., Cold Spring Harbor, NY).
18. Chaconas, G. & van de Sande, J. H. (1980) *Methods Enzymol.* **68**, 75–88.
19. Wood, W. I., Gitschier, J., Lasky, L. A. & Lawn, R. M. (1985) *Proc. Natl. Acad. Sci. USA* **82**, 1585–1588.
20. Grossberger, D. (1987) *Nucleic Acids Res.* **15**, 6737.
21. Yanisch-Perron, C., Vieria, J. & Messing, J. (1985) *Gene* **33**, 103–119.
22. Sanger, F., Nicklen, S. & Coulson, A. R. (1977) *Proc. Natl. Acad. Sci. USA* **74**, 5463–5467.
23. Gay, N. J. & Walker, J. E. (1985) *Biochem. J.* **225**, 707–712.
24. Kushner, S. R. (1978) in *Genetic Engineering*, eds. Boyer, H. W. & Nicosia, S. (Elsevier Biomed., Amsterdam), pp. 17–23.
25. O'Kane, D. J. & Lee, J. (1990) *Photochem. Photobiol.* **52**, 723–734.
26. Mulkerrin, M. G. & Wampler, J. E. (1982) *Anal. Chem.* **54**, 1778–1782.
27. Feinberg, A. P. & Vogelstein, B. (1983) *Anal. Biochem.* **132**, 6–13.
28. Southern, E. M. (1975) *J. Mol. Biol.* **98**, 503–517.
29. Laemmli, U. K. (1970) *Nature (London)* **277**, 680–685.
30. Burnett, W. H. (1981) *Anal. Biochem.* **112**, 195–203.
31. Chirala, S. S. (1986) *Nucleic Acids Res.* **14**, 5935.
32. Matthews, J. C., Hori, K. & Cormier, M. J. (1977) *Biochemistry* **16**, 5217–5220.
33. Ward, W. W. & Cormier, M. J. (1978) *Methods Enzymol.* **57**, 257–267.
34. Stormo, G. D. (1986) in *Maximizing Gene Expression*, eds. Rezinikoff, W. & Gold, L. (Butterworths, Boston), pp. 195–224.
35. Kornfeld, R. & Kornfeld, S. (1985) *Annu. Rev. Biochem.* **54**, 631–664.

Directed evolution of the surface chemistry of the reporter enzyme β-glucuronidase

Ichiro Matsumura[1], John B. Wallingford[2,3], Neeraj K. Surana[1,4], Peter D. Vize[2], and Andrew D. Ellington[1]*

[1]Institute of Cellular and Molecular Biology, ICMB A4800/MBB 3.424, 26th and Speedway, University of Texas, Austin, TX 78712. [2]Center for Developmental Biology, Department of Zoology, University of Texas, Austin, TX 78712. [3]Present address: Department of Molecular and Cell Biology, University of California, Berkeley, Berkeley, CA 94720. [4]Present address: Division of Biology and Biomedical Sciences, Washington University, St. Louis, MO 63108. *Corresponding author (e-mail: andy.ellington@mail.utexas.edu).

Received 29 December 1999; accepted 4 May 1999

The use of the *Escherichia coli* enzyme β-glucuronidase (GUS) as a reporter in gene expression studies is limited due to loss of activity during tissue fixation by glutaraldehyde or formaldehyde. We have directed the evolution of a GUS variant that is significantly more resistant to both glutaraldehyde and formaldehyde than the wild-type enzyme. A variant with eight amino acid changes was isolated after three rounds of mutation, DNA shuffling, and screening. Surprisingly, although glutaraldehyde is known to modify and cross-link free amines, only one lysine residue was mutated. Instead, amino acid changes generally occurred near conserved lysines, implying that the surface chemistry of the enzyme was selected to either accept or avoid glutaraldehyde modifications that would normally have inhibited function. We have shown that the GUS variant can be used to trace cell lineages in *Xenopus* embryos under standard fixation conditions, allowing double staining when used in conjunction with other reporters.

Keywords: β-glucuronidase, reporter gene, in vitro evolution, directed evolution, DNA shuffling, *Xenopus laevis*

Since plants express endogenous β-galactosidase activity, *lacZ* cannot be employed as a reporter gene[1]. Instead, the *Escherichia coli* β-glucuronidase gene (*gusA*, formerly *uidA*) has been developed as a reporter gene for plants, and has been widely used for over a decade[2]. Both chromogenic and fluorogenic GUS substrates have been synthesized[3], allowing rapid nonradioactive assays. The GUS enzyme is stable and active under a variety of conditions[1], even when fused to other sequences[4].

The utility of GUS as a reporter, however, has been constrained in three ways. First, many animal systems, and some plants and plant-associated bacteria express endogenous glucuronidase activities[2,3]. Second, GUS activity is greatly reduced during tissue fixation by glutaraldehyde or formaldehyde, making it necessary to trade off retention of activity for preservation of tissue structure[5]. Third, both of these considerations drastically restrict the use of GUS as a reporter gene in vertebrate systems[6].

Enzymatic inactivation by aldehydes is largely due to the formation of Schiff bases with surface-accessible lysine residues[7]. While the removal of lysine residues by directed mutation might render an enzyme more resistant to fixatives, many surface lysines are critical for function and cannot be readily changed. The sequences of the *E. coli* [8], human[9], mouse[10], rat[11], and dog[12] homologs are known. Six of the 27 lysine residues in the *E. coli* protein are conserved in the other species and thus are likely essential. Moreover, to find what combination of the 27 lysine residues could be changed in order to increase resistance to fixatives without abrogating enzyme activity would require constructing and assaying a dauntingly large number of mutant enzymes. Therefore, in order to alter the surface chemistry of GUS, either to avoid or to accommodate aldehyde modifications without loss of enzyme activity, we employed a random mutational approach similar to those previously proven useful for altering enzyme substrate specificity[13] or thermostability[14].

Results

Directed evolution of glutaraldehyde-resistant variants. Random mutations were initially introduced into the *gusA* structural gene by mutagenic PCR[15]. Mutated PCR products were ligated into the expression vector *gusA*-pBSΔ and transformed into *E. coli*. When the library was induced on plates containing the chromogenic GUS substrate, 5-bromo-4-chloro-3-indolyl-β-D-glucuronide (X-gluc), approximately 80% of the colonies were visibly less green than control colonies expressing only the chromosomal gene (see Experimental protocol). β-Glucuronidase functions as a tetramer[16], so it was likely that many of the mutations in the highly expressed, plasmid-borne library had a dominant negative effect on the function of the chromosomal gene. This did not deter us from utilizing this library for screening experiments, since successive rounds of DNA shuffling should efficiently select against neutral or deleterious mutations[13].

Nine thousand replica-plated colonies, each expressing a randomly mutated *gusA* gene, were exposed to buffer containing 0.2% glutaraldehyde for 20 min. The colony remnants were then incubated in buffer containing X-gluc and the histochemical indicator, nitroblue tetrazolium (NBT) (Fig. 1). The catalytic activity of the wild-type enzyme is greatly diminished under those conditions, indicating that the glutaraldehyde disrupts the cell membranes and covalently modifies many intracellular proteins, including GUS (cf. Figs 2A and B). Of all the variants examined, only 10 colonies reproducibly exhibited greater catalytic activity than control colonies expressing wild-type *gusA* (Fig. 2B). The corresponding colonies on master plates were isolated, and their expression vectors purified

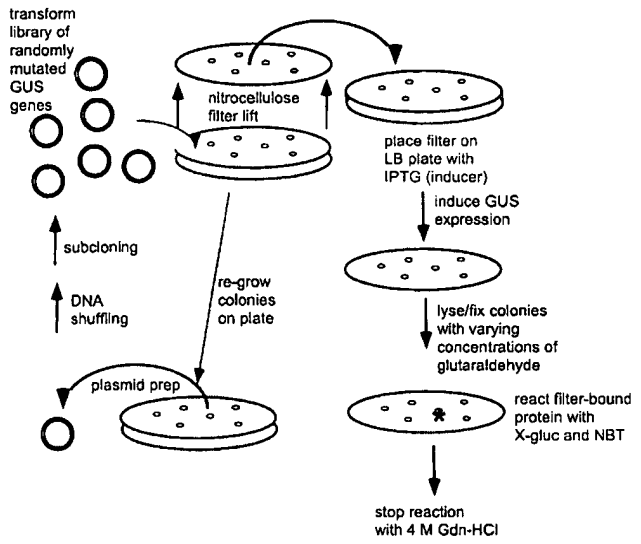

Figure 1. Screen for glutaraldehyde-resistant β-glucuronidase (GUS) function (sequence from top left). A library of randomly mutated β-glucuronidase genes (*gusA*) is subcloned into an inducible expression vector and transformed into *Escherichia coli*. The resulting colonies are transferred to a nitrocellulose filter, which is overlaid upon an agarose plate containing an inducer and incubated for 12–24 h at 37°C. The filter-bound colonies are incubated in buffer containing glutaraldehyde, then transferred to buffer containing the histochemical indicators of β-glucuronidase, X-gluc and NBT. The brief incubation in 4 M guanidine HCl (Gdn-HCl) arrests color development. Colonies that retain GUS activity are isolated from the original plate and randomly recombined by DNA shuffling for the next round of screening.

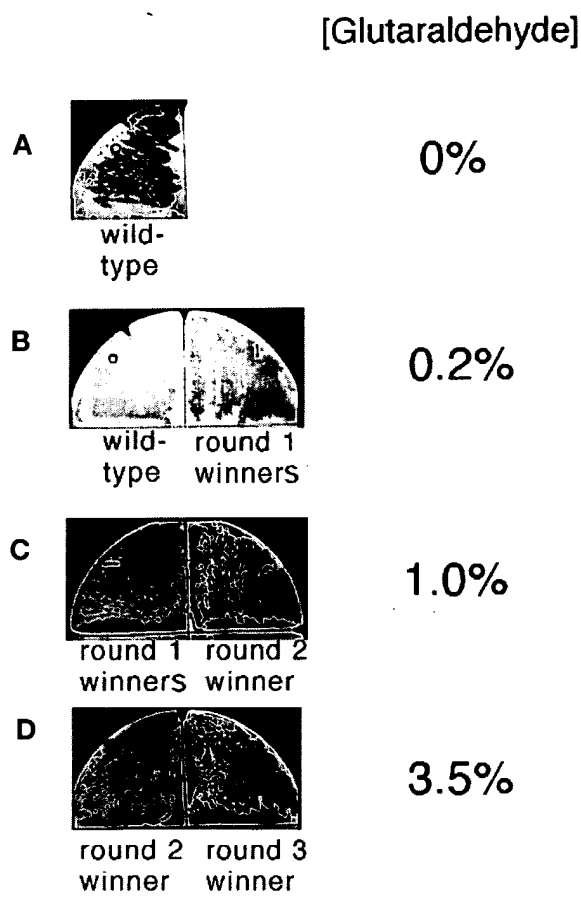

Figure 2. Detection of glutaraldehyde-resistant GUS activity. *Escherichia coli* cells transformed with vectors expressing the wild-type (A, B left), a pool of the ten glutaraldehyde-resistant variants from round 1 (B right, C left) or the most resistant variants from rounds 2 (C right, D left), or 3 (D right) were streaked onto noninducing plates. The colonies were propagated, induced, and treated for 20 min with the indicated concentrations of glutaraldehyde, then reacted with X-gluc and NBT, as described in the legend to Figure 1.

and pooled. The variant *gusA* genes were amplified using the PCR and randomly recombined by DNA shuffling[17]. We then screened 6,000 random recombinants in a second round for variants that retained catalytic activity after a 20 min incubation in 1.0% glutaraldehyde. Nine colonies contained variants that exhibited greater residual catalytic activity than the most resistant clone isolated in the first round of screening (Fig. 2C). These variants were again pooled, amplified, and randomly recombined. Then, 6,000 recombinants were screened in a third round for variants that retained catalytic activity after a 20 min incubation in 3.5% glutaraldehyde. Again, nine improved clones were isolated, one of which (GUS^{AR}) reproducibly showed the greatest activity under the most stringent conditions (Fig. 2D).

In vitro characterization of GUS^{AR}. To determine whether the colony-lift assay significantly influenced the apparent fixative-resistant phenotype of GUS^{AR}, activity assays were also carried out in cell extracts. The GUS-deficient strain, pREP4/GMS407, was transformed with vectors that expressed either wild-type *gusA*, the *GUS^{AR}* variant, or the *lacZ* α-fragment. Cell extracts from induced cultures were treated with glutaraldehyde or formaldehyde for 20 min at 23°C, and diluted 100-fold in buffer containing saturating concentrations of a GUS substrate, p-nitrophenyl β-D-glucuronide (PNPG). The extracts containing wild type or GUS^{AR} catalyzed the hydrolysis of PNPG; no hydrolysis was detected in the negative control extracts, in which only the *lacZ* α-fragment was expressed (data not shown). Treatment of the extract containing wild-type GUS with only 0.04% glutaraldehyde for 20 min at 23°C reduced catalytic activity by 99.6 ± 0.24%. In sharp contrast, the GUS^{AR} extract retained 78.1 ± 0.69% of its activity after treatment with a fivefold higher (0.2%) concentration of glutaraldehyde (Fig. 3A).

Extracts were also separately treated with formaldehyde to assess whether the fixative-resistant phenotype was specific to glutaraldehyde. Again, the GUS^{AR} variant exhibited much greater resistance to the fixative than did the wild-type GUS. The wild-type extract retained only 4.6 ± 0.05% of its catalytic activity after treatment with 0.08% formaldehyde; the GUS^{AR} extract retained 62.4 ± 0.40% activity after incubation with 0.4% formaldehyde (Fig. 3B). To determine how sequence and chemical modifications may have influenced GUS activity, we conducted kinetic studies of the mutant enzyme (Fig. 3C). The wild-type and evolved *gus* genes were subcloned, expressed as fusion proteins with N-terminal hexahistidine tags, and purified by immobilized metal ion adsorption chromatography. Purified enzymes were assayed with varying concentrations of PNPG (Fig. 3C). The kinetic parameters of the wild-type enzyme (K_M for the complex with PNPG = 110 ± 2.9 μM; k_{cat} = 920 ± 7.3 s^{-1}) were very similar to those of the GUS^{AR} variant (K_M = 150 ± 3.9 μM; k_{cat} = 750 ± 5.8 s^{-1}). The kinetic parameters of wild-type and evolved enzymes were also determined following reaction with a sublethal concentration (0.04%) of formaldehyde for 20 min at 23°C. Formaldehyde had a larger effect on the turnover number (250 ± 17 s^{-1} for the partially modified wild type, 650 ± 4.7 s^{-1} for the modified GUS^{AR} variant), than on the Michaelis constants (99 ± 6.7 μM and 170 ± 3.7 μM for the modified wild-type and GUS^{AR} enzymes,

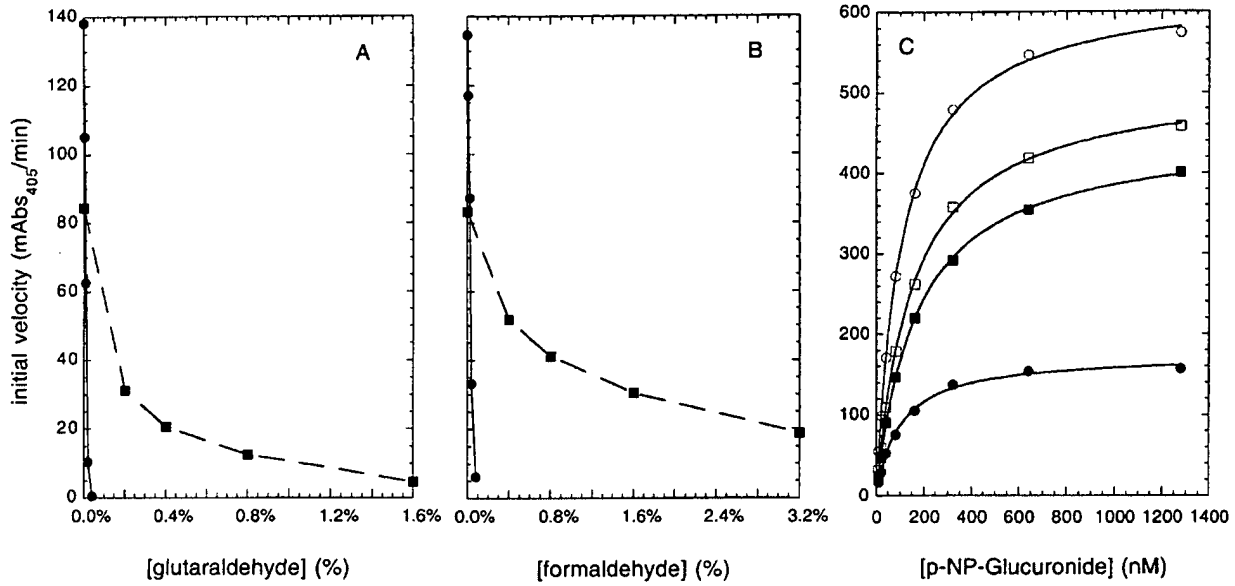

Figure 3. GUS catalytic activity as a function of aldehyde concentration. ***Escherichia coli*** **cell extracts containing the wild-type (circles) or evolved GUS^{AR} (squares) β-glucuronidase were incubated for 20 min at 23°C in buffer containing the indicated concentrations of glutaraldehyde (A) or formaldehyde (B). The protein was then diluted 100-fold into buffer containing the chromogenic GUS substrate, p-nitrophenyl-β-D-glucuronide (PNPG). Hydrolysis of the substrate was followed at 405 nm using a spectrophotometer (see Experimental Protocol). Each point represents the average of three initial velocity values; the points subsume the error bars. The control extract from an isogenic strain not expressing GUS does not have detectable activity (not shown). (C) Purified wild-type (circles) or evolved GUS^{AR} (squares) enzymes were incubated for 20 min at 23° C in buffer containing 0% (empty symbols) or 0.04% (filled symbols) formaldehyde, then reacted with the indicated concentrations of PNPG. The initial velocity values were fitted to the Michaelis–Menten equation (lines); the derived kinetic parameters are presented in the text.**

respectively). These results in conjunction with the cell extract data show that GUS^{AR} is expressed at lower levels than the wild type, but is inherently more aldehyde resistant.

Sequence and structural mapping of the evolved GUS^{AR} variant. Upon sequencing, the evolved *gusA* gene was found to contain the following amino acid substitutions: N66D, D151N, A219V, I396T, T480A, Q498R, D508E and K567R, as well as six silent mutations. Only one of these changes, the D508E mutation, results from a transversion, indicating a strong transition bias in our random mutagenesis methods. The amino acid sequences of the *E. coli* and human GUS proteins are 50% identical[18] and could be readily aligned by the algorithm devised by Needleman and Wunsch[19] using the program GAP 4.0 (Genetics Computing Group, Madison, WI). Both proteins are tetramers[16,18] and are virtually identical in substrate specificity[1]. The positions of the loci that were altered in the evolved *E. coli* enzyme could thus be tentatively mapped onto the crystal structure of the human GUS protein[18] (Fig. 4).

The 10 *gusA* mutants isolated in the first round of screening were sequenced; mutations were found at a frequency of three per 1.8 kb. Seven of the first-round variants contained amino acid substitutions (K567R, T480A, D508E or N66D/D151N) that were subsequently found in the most active third-round GUS^{AR} variant. It is instructive that many of the single substitutions that confer modest resistance to aldehyde modification can interact additively or synergistically to confer robust resistance to aldehyde modification.

GUS^{AR} as a lineage tracer in *Xenopus* embryos. The N358S mutant of GUS is a commercially available and commonly used reporter gene in plants[4]. The N358S mutation eliminates a cryptic glycosylation site, and should not affect its function in the cytoplasm; we chose this construct because it also contained the upstream sequences necessary for expression in eukaryotic cells[20]. In order to determine if the fixative-resistant GUS might also prove useful in other model organisms, transcripts encoding GUS^{AR} and N358S GUS were microinjected into 16- to 32-cell stage *Xenopus* embryos. Two days later, the embryos were fixed in 3.7% formaldehyde for 20 min and stained using a standard protocol for the detection of *lacZ* expression, except that X-gluc was substituted for X-gal. The descendants of cells injected with the wild-type-like N358S GUS mRNA did not change color (Fig. 5A). Endogenous GUS activity was apparently also abrogated by the 20 min incubation in 3.7% formaldehyde. In contrast, the descendents of cells injected with the GUS^{AR} mRNA turned bright blue-green (Fig. 5B).

In order to determine if multiple reporters might be used in tandem for lineage analysis, mRNAs encoding either N358S or the GUS^{AR} were co-injected into embryonic cells along with mRNA encoding *lacZ*. When the embryos were first stained with X-gluc, again only the cells that inherited the GUS^{AR} mRNA turned blue-green (Fig. 6A and B). The embryos were subsequently stained with rose-gal, a β-galactosidase substrate that forms a red precipitate. In embryos that received either the N358S or GUS^{AR}, some cells were colored red, indicating the inheritance of *lacZ*. However, in embryos that received GUS^{AR} some cells or patches were also purple, indicating the co-inheritance of the GUS^{AR} and *lacZ* (Fig. 6C and D). The *lacZ* mRNA in this experiment also served as an internal control that demonstrated that RNAs were entering cells and surviving until fixation.

Discussion

Mechanisms of aldehyde resistance. The *E. coli* GUS protein contains 27 lysine residues, six of which are conserved among the sequenced GUS genes. Although the fraction of lysine residues that are modified by aldehydes is unknown, wild-type GUS activity is quite susceptible to even low levels of fixatives. For example, the catalytic activities of the wild-type (Fig. 3B) and N358S GUS (Figs 5A and 6A) are inactivated by <3.7% formaldehyde, while β-galactosidase, which contains 20 lysine residues, is not (Fig. 6). Taken together, these results suggest that one or more of the GUS

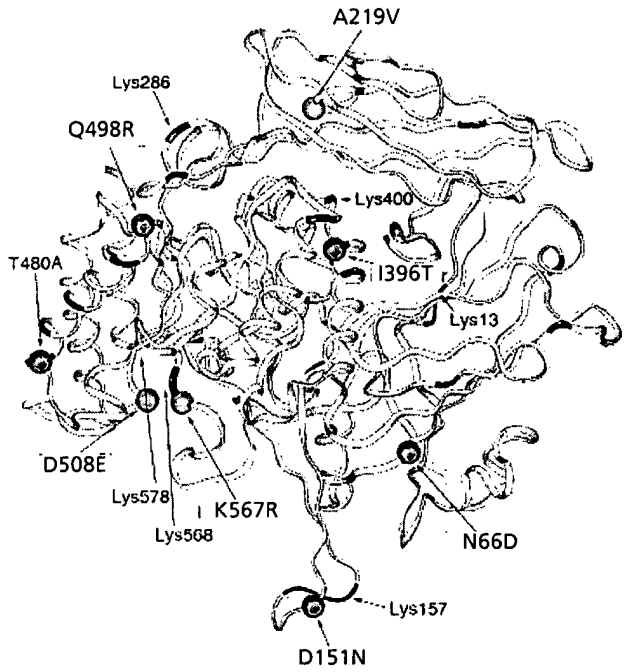

Figure 4. Homology mapping of amino acid substitutions that confer aldehyde resistance. The crystal structure of a subunit of the Cα trace of human GUS[18] is shown. The amino acid sequences of the *E. coli* and human GUS proteins were aligned using the application GAP 4.0 (Genetics Computer Group) and were found to be 48.5% identical. The positions of lysine residues are darkened, and the conserved lysines are labeled. The positions of amino acid substitutions in the evolved GUS^{AR} *E. coli* protein are shown as balls.

lysine residues is either itself critical for activity or presents a conjugation site that leads to functional disruption. However, identifying which of the many lysine residues in GUS were responsible for inhibition by fixatives would have been a daunting task. Instead, we relied on a random mutagenesis to identify GUS variants with catalytic activity resistant to aldehydes. Following three rounds of screening and amplification, we isolated an octuple-mutant GUS^{AR} with catalytic activity resistant to roughly 80-fold higher levels of glutaraldehyde than the wild-type activity (Fig. 3A).

Surprisingly, only one of the amino acid substitutions, K567R, in the evolved GUS^{AR} occurred at a lysine residue. Since AAA or AAG encodes lysine, the apparent transition bias in our random-mutagenesis method and the size of our initial library provided ample opportunities for each lysine to conservatively mutate into arginine (AGA or AGG). While it is possible that mutation of this single lysine was largely responsible for protection against aldehydes, this explanation is unlikely. Three of the 10 clones isolated in the first round of screening contain the K567R sequence substitution, but none of these first-round isolates are as resistant as any of the second-round isolates (Fig. 2C). The aldehyde resistance of GUS progressively increased over three rounds of screening and selection, and the final product had accumulated seven additional amino acid substitutions. The finding that amino acid substitutions that modulate protein function are dispersed in the primary and tertiary structure of GUS is congruent with previous attempts to evolutionarily engineer the physical and kinetic parameters of enzymes. Experiments that directed an increase in the catalytic activity of a p-nitrobenzyl esterase in organic enzymes yielded multiple sequence substitutions scattered throughout the tertiary structure[21]. Site-directed mutation studies of T4 lysozyme have shown that stabilizing amino acid changes, which occur in the core of that enzyme, are additive in effect[22].

Interestingly, the seven non-lysine amino acid substitutions mapped onto the surface of the protein near lysine residues (Fig. 4). Protein structure is more highly conserved than protein sequence[23], and since the primary sequences of the *E. coli* and human GUS enzymes are quite similar (48.5% identity[8]), it can be conservatively assumed that their tertiary structures also align well. Based on this assumption, we can advance hypotheses regarding the contributions of individual amino acid substitutions to aldehyde resistance. For example, Lys568 (*E. coli* numbering) is conserved among the sequenced GUS genes, and is in the active-site[18]. The Cα–Cα distance from Lys568 to the D508E substitution is 3.97 Å (Fig. 4). Since the lysine side chain is 7 Å in length, this adjacent sequence substitution might raise the pK_a of the epsilon amino group of Lys568, thereby reducing its reactivity with aldehydes. Similarly, the K567R substitutions already mentioned is within 3.81 Å of the active-site lysine, and mutation to arginine may prevent modification that could sterically interfere with substrate binding or catalysis.

Similarly, β-glucuronidase is active only as a tetramer[16,18], and lysines play a key role in its quaternary structure. To the extent that modifications of interfacial lysines disrupt quaternary structure and enzymatic function, adjacent amino acid substitutions could render these lysines less reactive. In this regard, the loop containing D151N and three lysines is <5 Å away from the α-helix of the adjacent subunit containing T480A and three other lysines. These amino acid substitutions could also prevent structural and functional disruption by independently increasing the affinity between the subunits. For example, the A219V substitution also maps to the other interface, although it is not immediately adjacent to any lysines.

Overall, it appears the surface chemistry of the enzyme has coordinately evolved either to cause lysines to be less reactive or to functionally accommodate covalent modification of lysines. Our results suggest that there may be multiple possible routes by which proteins could be adapted to function in a wide variety of fixatives or solvent systems. More importantly, they suggest a way of augmenting protein chemistry by introducing amino acids with novel surface conjugates.

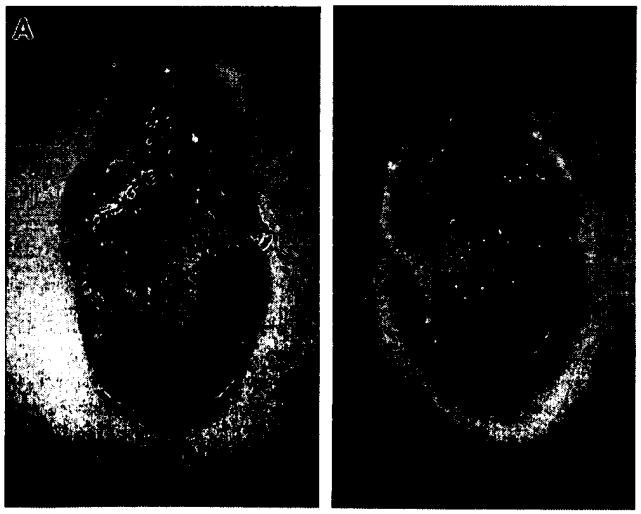

Figure 5. Expression of GUS^{AR} in *Xenopus* embryos. Embryos at the 16- to 32-cell stage were injected with 1 ng of mRNA encoding N358S (A) or GUS^{AR} (B) and fixed two days later in 3.7% formaldehyde for 20 min. GUS activity was detected using the chromogenic substrate X-gluc (light blue/green). The reddish-purple color of the cement gland of the embryo shown in (A) is from a natural pigment, and the blue color of the embryo shown in (B) is from GUS^{AR} activity.

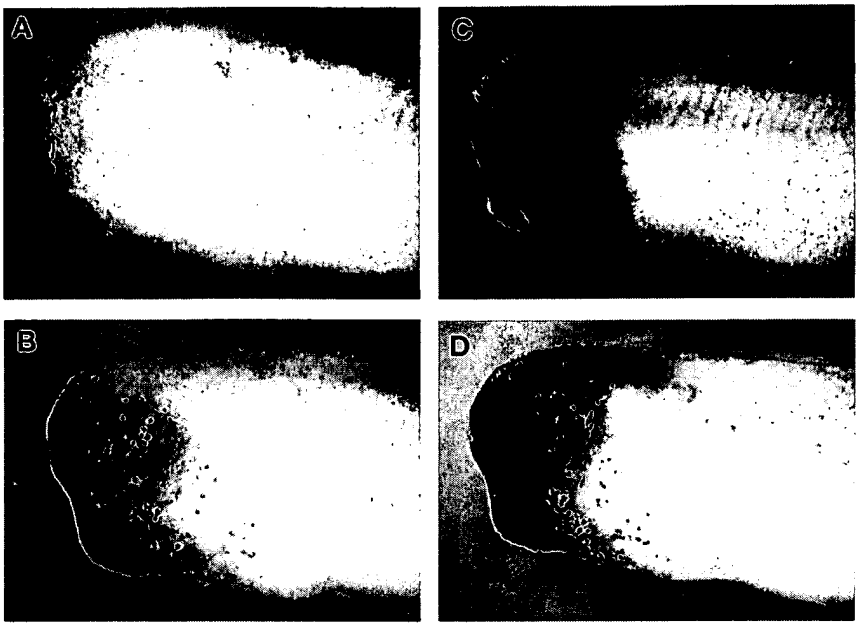

Figure 6. Multiple marker staining of *Xenopus* embryos. Embryos were co-injected with 0.5 ng of *lacZ* mRNA and 1 ng of either N358S GUS (A, C) or GUS^{AR} (B, D), and subsequently fixed in 3.7% formaldehyde for 20 min. Following fixation, embryos were reacted with X-gluc (light blue/green in all frames). As in Figure 5, embryos injected with mRNA encoding GUS^{AR} (B) stained much more intensely than those injected with N358S GUS mRNA (A). All embryos were subsequently rinsed free of X-gluc and stained with the chromogenic substrate for β-galactosidase, rose-gal (red in C and D).

GUS^{AR} as a universal reporter gene. Since most naturally occurring β-glucuronidases are likely to be fixative-labile, the fixative-resistant GUS^{AR} we have isolated should prove useful for expanding the range and power of GUS staining techniques. In addition, it should be possible to develop methods for following multiple genes or cell lineages in parallel. Such methods generally rely on protocols in which fixed tissues are reacted with antibodies conjugated to dyes or reporter enzymes (for example, see ref. 24).

Reporter genes are very commonly used in *Xenopus* as cell lineage tracers, and have proved important for gene expression studies in developing embryos[25,26]. Following mRNA microinjection, the fixative-resistant GUS could be specifically followed in *Xenopus* relative to both background activity and the wild-type reporter. Moreover, a lineage trace in tandem with β-galactosidase demonstrated the use of GUS in a multiple-reporter format. These experiments pave the way for the practical development of two-enzyme reporter systems, and could potentially be combined with a β-lactamase reporter system developed by Raz *et al.*[27] to create three-enzyme reporter systems.

The results in *Xenopus* embryos are notable in that that no special precautions were taken to enhance gene expression or enzymatic activity. In contrast to the transformation of reporter constructs, microinjected reporter mRNAs do not replicate and their dosage progressively decreases as messages are segregated or broken down. Further, no attempt was made to increase the signal intensity of GUS^{AR} by fusing it to a nuclear localization signal, as was the case for the *lacZ* control. Nor were fluorescent or other highly sensitive commercially available GUS substrates[3] utilized. In short, the evolved enzyme is itself robust enough so that new staining techniques can easily be adapted from extant methods.

Experimental protocol

Materials. DNA-modifying enzymes, including restriction enzymes and Vent polymerase, were purchased from New England Biolabs (Beverly, MA). Deoxyribonuclease I was from GIBCO-BRL (Gaithersburg, MD). Taq polymerase was expressed and purified as described by Grimm and Arbuthnot[28]. DNA sequencing kits were from Perkin-Elmer/Applied Biosystems (Foster City, CA). Cloning vector pGEM-5 was from Promega (Madison, WI), pBluescript II SK(+) was from Stratagene (La Jolla, CA), and the regulatory vector pREP4 was from Qiagen (Chatsworth, CA). pGUS N358S was from Clontech (Palo Alto, CA), and pET28a(+) from Novagen (Madison, WI). DNA purification columns were purchased from Qiagen (Chatsworth, CA). X-gluc was from Gold Biotechnology (St. Louis, MO) and Butterfly nitrocellulose membranes from Schleicher and Schuell (Keene, NH). The mMessage mMachine SP6 in vitro mRNA transcription kit was from Ambion (Austin, TX). MicroSpin G-25 Sephadex spin columns were from Pharmacia Biotech (Piscataway, NJ). *Escherichia coli* strain InvαF' was from Invitrogen (Carlsbad, CA), W3110 (ATCC No. 27325) from the ATCC (Rockville, MD), GMS407 from the *E. coli* Genetic Stock Center (New Haven, CT), and BL21(DE3)pLysS from Novagen. Other chemicals, including glutaraldehyde, PNPG and NBT, were from Sigma Chemicals (St. Louis, MO).

Cloning of *gusA*. The *E. coli gusA* gene was amplified from W3110 cells using Vent polymerase and the primers 5'-CCGGATCCTCTAGAGATGTTACGTCCTGTAGAAACC-3' and 5'-GCGAATTCTGCAGTCATTGTTTGCCTCCCTGCT-3' (*Xba*I and *Eco*RI sites underlined). The PCR product was blunt-end ligated into the *Eco*RV site of pGEM-5 by standard methods[29]. *Escherichia coli* InvαF' cells were transformed by the method described by Inoue *et al.*[30]. The *gusA* gene was subcloned into pBluescript II SK(+) using restriction endonucleases *Xba*I and *Eco*RI. The nucleotides encoding the *lacZ* α-fragment that would normally have been located between the ribosome binding site and the *gusA* start codon were deleted by amplifying the remainder of the plasmid using primers 5'-CCGGATCCTCTAGAGATGTTACGTCCTGTAGAAACC-3' and 5'-CGTCTAGAAGCTGTTTCCTGTGTGAAATTG-3', digesting with *Xba*I, ligating, and transforming pREP4/InvαF' (see below). The resultant construct placed the *gusA* gene under direct control of the lac promoter. The GUS expression vector was named *gusA*-pBSΔ.

Library construction and screening. For the first round of screening, random mutations were introduced into the cDNA by mutagenic PCR[15] using primers 5'-CCCAGTCACGACGTTGTAAAA CGACG-3' and 5'-ATGCTTCCGGCTCGTATGTTGTGTGG-3', which anneal to the pBluescript II SK(+) vector outside of the boundaries of the *gusA* insert. The amplification reaction was carried out with 100 nM primers, 60 mM Tris-HCl pH 8.5, 15 mM $(NH_4)SO_4$, 3.2 mM $MgCl_2$, 0.125 mM $MnCl_2$, 0.2 mM dGTP, 0.2 mM dATP, 0.4 mM dTTP, 0.4 mM dCTP, for 35 cycles of 94°C × 30 s, 72°C × 2 min. The *gusA*-pBSΔ plasmid library was transformed into *E. coli* InvαF' cells harboring the *lacI* expression vector pREP4. The plasmid was unstable when propagated in *E. coli* InvαF' without pREP4, probably because the lac repressor is not present at high enough levels to limit expression of the *gusA*. For colony-lift assays, *gusA*-pBSΔ/pREP4/InvαF' colonies were propagated on liquid Luria Broth supplemented with 25 μg/ml kanamycin and 100 μg/mL ampicillin (LB-kan/amp) + 0.4% glucose plates for 12 h at 37°C. The colonies adsorbed to a nitrocellulose filter and were transferred colony side up to LB-kan/amp plates containing 0.5 mM isopropyl β-D-thiogalactopyranoside (IPTG), and induced at 37°C for 12–24 h. The nitrocellulose-bound colonies were transferred to GUS buffer (50 mM sodium phosphate pH 7.0, 0.1% Triton X-100, 1 mM EDTA) containing 0.2% glutaraldehyde and incubated for 20 min at 23°C. The filters were then transferred to buffer containing 165 μg/ml X-gluc and 330 μg/ml NBT and incubated for 10–30 min. The filters were incubated briefly in 4 M guanidine hydrochloride to arrest color development. Those colonies on the master plate corresponding to the darkest colony remnants on the filter were isolated and amplified.

For subsequent rounds of screening, the alleles were randomly recombined and mutated by DNA shuffling as described by Stemmer[17]. In short, the *gusA* variants were PCR amplified using the same primers as in the

mutagenic PCR reactions already described, partially digested with DNase I, and reassembled in a PCR reaction without primers. The products were amplified in a PCR with primers, then subcloned back into *gusA*-pBSΔ for screening. The second and third rounds were carried out in the same way, except that 1.0% and 3.5% glutaraldehyde was used to fix the colonies before the incubation in X-gluc and NBT. The most resistant round 3 clone was isolated and sequenced at the University of Texas, Institute of Cellular and Molecular Biology Core Facility using the Applied Biosystems protocol, via the primers originally used for mutagenic PCR and two additional internal primers: 5′-CGCCGGGAATGGTGATTACC-3′ and 5′-CTGATGGTATCGGTGTGAGCG-3′.

In vitro characterization of enzyme activity. For the preparation of lysates, *gusA*-pBSΔ/pREP4/GMS407 cells were propagated at 37°C in LB-kan/amp. The *gusA* gene was induced by the addition of 0.5 mM IPTG to mid-log (OD_{600} = 0.3) cultures, and the induced cultures were grown overnight. Cells were centrifuged, resuspended in distilled water, centrifuged again, and resuspended in GUS buffer. Cells were lysed with the addition of 10 mM EDTA and 1 mg/ml chicken lysozyme. The insoluble fraction was centrifuged down, and the aldehyde resistance of the GUS in the supernatant was determined as follows. Glutaraldehyde or formaldehyde was added to an aliquot of supernatant and the mixture was incubated at 23°C for exactly 20 min. The mixture was then diluted 1/100 into GUS buffer containing 0.5 mM PNPG. The hydrolysis of the substrate was followed for 1 min at 23°C at 405 nm in a Shimadzu UV-1601 spectrophotometer. The absorption extinction coefficient of p-nitrophenol under these conditions was 11.50 mM^{-1} cm^{-1}. The initial rates of hydrolysis were linear (data not shown).

To generate purified GUS enzymes, the wild-type and evolved *gusA* genes were amplified by PCR with the primers: 5′-GCTCTAGACATATGTTACGTCCTGTAGAAACC-3′ and 5′-GCGAATTCTGCAGTCATTGTTTGCCTCCCTGCT-3′ and subcloned into the expression vector pET28a(+) using the restriction enzymes *Nde*I and *Eco*RI (sites underlined in primers). The resultant genes were sequenced as described already to confirm that no additional mutations had been introduced during amplification or cloning. The expression constructs were transformed into BL21(DE3)/pLysS. The transformed strains were propagated and induced, and the proteins purified by nickel chelate chromatography, as suggested by Novagen (Madison, WI). The protein preparations were judged to be >99% pure following SDS–PAGE and Coomassie Blue staining (data not shown). Purified protein concentrations were determined via Bradford protein assays (Bio-Rad, Hercules, CA).

A 10 pmol quantity of purified GUS protein was preincubated for 20 min at 23°C in 10 μl of GUS buffer (1 μM) containing 0% or 0.04% formaldehyde. Then, 5 μl of protein solution were added to 1 ml of buffer (5 nM) containing varying concentrations of PNPG, and the initial velocity of each reaction was determined as already described. The kinetic parameters of the wild-type and mutant enzymes were calculated by fitting the initial velocity values to the Michaelis–Menten equation using the application Kaleidagraph 3.0.5 (Adelbeck Software, Reading, PA).

Expression of *gusA* in *Xenopus* embryos. The GUS^{AR} gene was subcloned into pGUS N358S; this placed the gene downstream of a Kozak sequence[20], so that its transcript could be recognized by eukaryotic translation systems. N358S GUS and GUS^{AR} were subcloned into the *Xenopus* expression vector p64TS. This plasmid provides in vitro-transcribed mRNAs with *Xenopus* globin 5′- and 3′-untranslated regions and greatly increases the amount of protein translated from the mRNA[31]. Capped mRNA was produced by *in vitro* transcription[32] of the clones already described using the Ambion mMessage mMaker SP6 protocol. In vitro transcriptions were also treated with DNase I, and the mRNA was purified using a Sephadex G-25 spin column to minimize nonspecific toxicity effects. Purified mRNAs were resuspended in sterile water for injections.

Female adult *Xenopus* were induced to ovulate with human chorionic gonadotropin, and eggs were fertilized in vitro. Embryos were dejellied in 3% cysteine solution and washed in 0.2× MMR[33]. Embryos were then reared at 13–18°C in 0.2× MMR. Microinjections were performed as described[34]. Embryos were fixed in MEMFA (0.1 M MOPS, pH 7.4 / 2 mM EGTA/1 mM $MgSO_4$ / 3.7% formaldehyde) for 20 min, and embryos were washed 5 × 5 min in 1× PBS. GUS activity was detected using 1 mg/ml X-gluc in a solution of 1× PBS / 20 mM potassium ferricyanide / 20 mM potassium ferrocyanide / 2 mM $MgCl_2$ / 0.02% NP-40 at 37°C for 2 h. β-Galactosidase was detected using the same buffer but substituting rose-gal for X-gluc. Injection experiments repeated on different days with different preparations of mRNA gave similar results (data not shown).

Acknowledgments

We thank the Office of Naval Research for funding. I.M. was supported by a National Science Foundation/Alfred P. Sloan Postdoctoral Research Fellowship in Molecular Evolution (DBI-9750002). We thank Dr. Mary Berlyn of the E. coli Genetic Stock Center for sending us strain GMS407 and Ms. Sabine Bell for synthesizing oligonucleotides. Finally, we thank members of the Ellington group and Dr. William Wu of Ambion for helpful discussion.

1. Jefferson, R.A., Burgess, S.M. & Hirsh, D. Beta-glucuronidase from *Escherichia coli* as a gene-fusion marker. *Proc. Natl. Acad. Sci. USA* **83**, 8447–8451 (1986).
2. Martin, T., Woehner, R-V., Hummel, S., Willmitzer, L. & Frommer, W.B. in *GUS Protocols: using the GUS gene as a reporter of gene expression.* (ed. Gallagher, S.R.). 23–43 Academic Press, New York; 1992).
3. Naleway, J.J. in *GUS Protocols: using the GUS gene as a reporter of gene expression.* (ed. Gallagher, S.R.). 61–76 (Academic Press, New York; 1992).
4. Farrell, L.B. & Beachy, R.N. Manipulation of beta-glucuronidase for use as a reporter in vacuolar targeting studies. *Plant Mol. Biol.* **15**, 821–825 (1990).
5. Craig, S., in *GUS Protocols: using the GUS gene as a reporter of gene expression* (ed. Gallagher, S.R.) 115–124 (Academic Press, New York; 1992).
6. Jefferson, R.A. The GUS reporter gene system. *Nature* **342**, 837–838 (1989).
7. Habeeb, A.F.S.A. & Hiramoto, R. Reactions of proteins with glutaraldehyde. *Arch. Biochem. Biophys.* 126:16–26 (1968).
8. Schlaman, H.R., Risseeuw, E., Franke-van Dijk, M.E. & Hooykaas, P.J. Nucleotide sequence corrections of the uidA open reading frame encoding beta-glucuronidase. *Gene* **138**, 259–260 (1994).
9. Oshima, A. *et al.* Cloning, sequencing, and expression of cDNA for human beta-glucuronidase. *Proc. Natl. Acad. Sci. USA* **84**, 685–689 (1987).
10. D'Amore, M.A., Gallagher, P.M., Korfhagen, T.R. & Ganschow, R.E. The complete sequence and organization of the murine beta-glucuronidase gene. *Biochemistry* **27**, 7131–7140 (1988).
11. Nishimura, Y. *et al.* Nucleotide sequence of rat preputial gland beta-glucuronidase cDNA and *in vitro* insertion of its encoded polypeptide into microsomal membranes. *Proc. Natl. Acad. Sci. USA* **83**, 7292–7296 (1986).
12. Ray, J. *et al.* Cloning of canine beta-glucuronidase cDNA, mutation identification in canine MPS VII, and retroviral vector-mediated correction of MPS VII cells. *Genomics* **48**, 248–253 (1988).
13. Zhang, J.H., Dawes, G. & Stemmer, W.P. Directed evolution of a fucosidase from a galactosidase by DNA shuffling and screening. *Proc Natl Acad Sci USA* **94**, 4504–4509 (1997).
14. Giver, L., Gershenson, A., Freskgard, P.O. & Arnold, F.H. Directed evolution of a thermostable esterase. *Proc. Natl. Acad. Sci. USA* **95**, 12809–12813 (1998).
15. Cadwell, R.C. & Joyce, G.F. Randomization of genes by PCR mutagenesis. *PCR Methods Appl.* **2**, 28–33 (1992).
16. Blanco, C. & Nemoz, G. One step purification of *Escherichia coli* beta-glucuronidase. *Biochimie* **69**, 157–161 (1987).
17. Stemmer, W.P.C. DNA shuffling by random fragmentation and reassembly: *in vitro* recombination for molecular evolution. *Proc. Natl. Acad. Sci. USA* 91:10747–10751 (1994).
18. Jain, S., Drendel, W.B., Chen, Z.W., Mathews, F.S., Sly, W.S. & Grubb, J.H. Structure of human beta-glucuronidase reveals candidate lysosomal targeting and active-site motifs. *Nat. Struct. Biol.* **3**, 375–381 (1996).
19. Needleman, S.B. & Wunsch, C.D. A general method applicable to the search for similarities in the amino acid sequence of two proteins. *J. Mol. Biol.* **48**, 443–453 (1970).
20. Kozak, M. An analysis of 5′-noncoding sequences from 699 vertebrate messenger RNAs. *Nucleic Acids Res.* **15**, 8125–8148 (1987).
21. Moore, J.C. & Arnold, F.H. Directed evolution of a para-nitrobenzyl esterase for aqueous-organic solvents. *Nat. Biotechnol.* **14**, 458–467 (1996).
22. Zhang, X.J., Baase, W.A., Shoichet, B.K., Wilson, K.P. & Matthews, B.W. Enhancement of protein stability by the combination of point mutations in T4 lysozyme is additive. *Protein Eng.* **8**, 1017–1022 (1995).
23. Holm, L. & Sander, C. Mapping the protein universe. *Science* **273**, 595–603 (1996).
24. van der Loos, C.M., Becker, A.E. & van den Oord, J.J. Practical suggestions for successful immunoenzyme double-staining experiments. *Histochem. J.* **25**, 1–13 (1993).
25. Wallingford, J., Seufert, D., Virta, V. & Vize, P. p53 Activity is essential for normal development in *Xenopus laevis*. *Curr. Biol.* **7**, 747–757 (1997).
26. Wallingford, J., Carroll, T. & Vize, P. Precocious expression of the Wilms' tumor gene xWT1 inhibits embryonic kidney development in *Xenopus laevis*. *Dev. Biol.* **202**, 103–112 (1998).
27. Raz, E., Zlokarnik, G., Tsien, R.Y. & Driever, W. Beta-lactamase as a marker for gene expression in live zebrafish embryos. *Dev. Biol.* **203**, 290–294 (1998).
28. Grimm, E. & Arbuthnot, P. Rapid purification of recombinant Taq DNA polymerase by freezing and high temperature thawing of bacterial expression cultures. *Nucleic Acids Res.* **23**, 4518–4519 (1995).
29. King, P.V. & Blakesley, R.W. Optimizing DNA ligations for transformations. *FOCUS* **8**, 30–32 (1986).
30. Inoue, H., Nojima, H. & Okayama, H. High efficiency transformation of *Escherichia coli* with plasmids. *Gene* **96**, 23–28 (1990).
31. Krieg, P.A. & Melton, D.A. Functional messenger RNAs are produced by SP6 *in vitro* transcription of cloned cDNAs. *Nucleic Acids Res.* **12**, 7057–7070 (1984).
32. Krieg, P. & Johnson, A. in *A laboratory guide to RNA: isolation, analysis, and synthesis.* (ed. Krieg, P.) 141–153 (Wiley-Liss, New York; 1996).
33. Peng, H.B. Solutions and protocols. *Methods Cell Biology* **36**, 657–662 (1991).
34. Vize, P., Melton, D., Hemmati-Brivanlou, A. & Harland, R. Asssays for gene function in developing *Xenopus* embryos. **36**, 367–387 (1991).